

LOW TEMPERATURE SYNTHESIS OF THE MICROWAVE DIELECTRIC MATERIAL, BARIUM
MAGNESIUM TANTALATE (BMT)

by

Heather Marie Shirey

B.S. in Chemistry, Chatham College, 1999

Submitted to the Graduate Faculty of

School of Engineering in partial fulfillment

of the requirements for the degree of

Master of Science

University of Pittsburgh

2002

UNIVERSITY OF PITTSBURGH

SCHOOL OF ENGINEERING

This thesis was presented

by

Heather Marie Shirey

It was defended on

July 05, 2002

and approved by

Pradeep P. Phule', PhD, Professor, Materials Science and Engineering

Nicholas G. Eror, PhD, Professor, Materials Science and Engineering

Thesis Advisor: Ian Nettleship, PhD, Associate Professor, Materials Science and Engineering

Low Temperature Synthesis of the Microwave Dielectric Material, Barium Magnesium Tantalate (BMT)

Heather Marie Shirey, MS

University of Pittsburgh, 2002

Wireless communication systems utilize microwave dielectrics for coupling, selecting and filtering microwaves. Over the past several years there has been an increased demand for smaller, lighter and temperature stable devices. An important material that has been studied extensively for these applications is barium magnesium tantalate (BMT). Although BMT has very good dielectric properties: relatively high dielectric constant (25), temperature stability and low dielectric loss in the microwave region ($Q_d * f_o \approx 150,000$ GHz at 4.9 GHz), it can be expensive to produce because of the high sintering temperatures ($>1600^\circ\text{C}$) required to obtain the desired properties.

The objective of this study was to dope BMT with ZnGa_2O_4 , Ga_2O_3 , and ZnO to try and lower the sintering temperature without severe degradation of the microwave dielectric properties. The study showed that the BMT co-doped with both Ga_2O_3 and ZnO gave the best properties at the lowest sintering temperatures. BMT co-doped with 4mol% Ga_2O_3 and ZnO has been successfully sintered at 1400°C for 2 hours had an average density of 95% with a dielectric constant of 24 and a $Q_d * f_o$ of 130,000 at 4.9 GHz. BMT co-doped with 8mol% Ga_2O_3 and ZnO and sintered at 1450°C for 2 hours had an average density of 94%, a dielectric constant of 24 and a $Q_d * f_o$ of 135,000 at 4.9GHz. The BMT materials doped with ZnGa_2O_4 and Ga_2O_3 both had average densities of over 95% and dielectric constants of approximately 24 but high dielectric

loss. The BMT doped with Ga_2O_3 had a $Q_d^*f_o$ of only 84,000 at 4.9 GHz and the BMT doped with ZnGa_2O_4 had a $Q_d^*f_o$ of 93,000 at 4.9 GHz. Phase evolution and densification behavior of these materials are described.

DESCRIPTORS

Barium Magnesium Tantalate	BMT
Cellular Phones	Dielectric Constant
Dielectric Resonator	Dopants
Liquid Phase Sintering	Microwaves
Ordering	Q-factor
Resonator	Solid State Sintering
Temperature Coefficient of Resonant Frequency	Zinc Gallate

ACKNOWLEDGEMENTS

I wish to express my sincere gratitude to my thesis advisor, Dr. Ian Nettleship, for his patience, understanding and guidance throughout my graduate studies. I would also like to thank my committee members, Dr. P.P. Phule , for his guidance and support and Dr. N. Eror for his interest and discussion.

I would like to extend my appreciation to George McManus, Seval Genc, and S. Ra for their support and friendship.

I also want to thank my family for their love and support. I want to thank my parents for always believing that I could accomplish anything and encouraging me to work hard to achieve my goals.

And finally I would like to thank Dr. John Hagen for sparking my interest in research and materials science and engineering. I would also like to thank him for believing in me and always pushing me to do my best.

TABLE OF CONTENTS

1.0	INTRODUCTION.....	1
2.0	BACKGROUND.....	3
2.1	Microwave Communications.....	3
2.1.1	Dielectric Resonators.....	4
2.1.2	Microwave Dielectric Properties.....	6
2.1.3	Microwave Dielectric Property Measurements.....	12
2.2	High Q Perovskite Ceramics.....	14
2.2.1	Barium Magnesium Tantalate (BMT).....	15
3.0	OBJECTIVES.....	32
4.0	EXPERIMENTAL PROCEEDURE.....	33
4.1	Synthesis of BMT Powders.....	33
4.2	Powder Processing.....	34
4.3	Microstructural Characterizations.....	35
4.3.1	X-ray Diffraction (XRD) Analysis.....	35
4.3.2	Scanning Electron Microscopy (SEM) Characterization.....	36
4.3.3	Density Measurements.....	36
4.4	Microwave Dielectric Property Measurements.....	37
4.4.1	Measurement of the Dielectric Constant.....	37
4.4.2	Measurement of the Quality Factor.....	38

5.0	RESULTS.....	47
5.1	BMT Doped with 8mol% ZnO and Ga ₂ O ₃	47
5.1.1	Powder Development.....	47
5.1.2	Ceramics Sintered at a Constant Heating Rate.....	47
5.1.3	Ceramics Sintered Isothermally at 1350oC.....	49
5.1.4	Ceramics Sintered at Various Temperatures for 2 hours.....	51
5.2	Comparing the Concentration of ZnO and Ga ₂ O ₃ on the Sintering and Microwave Dielectric Properties of BMT.....	52
5.3	Comparing the Effect of Several Similar Dopants (ZnO and Ga ₂ O ₃ ; Ga ₂ O ₃ ; ZnO and ZnGa ₂ O ₄) on BMT Sintered at 1450oC for 2hours.....	54
5.4	Overall Effect of Density on the Q-factor.....	56
5.5	Effect of Additives and Process Condition of Ordering.....	57
5.6	The Effect of additives and Processing Condition on the Dielectric Constant.....	57
6.0	DISCUSSION.....	89
6.1	Phase Evolution.....	89
6.1.1	BMT Doped with ZnO & Ga ₂ O ₃ and ZnGa ₂ O ₄	89
6.1.2	BMT Doped with Ga ₂ O ₃ , ZnO and MgO.....	90
6.2	Densification Behavior.....	91
6.2.1	BMT Doped with ZnO & Ga ₂ O ₃ and ZnGa ₂ O ₄	91
6.2.2	BMT Doped with Ga ₂ O ₃ , ZnO and MgO.....	92
6.3	Q-factors.....	94
6.3.1	BMT Doped with ZnO & Ga ₂ O ₃ and ZnGa ₂ O ₄	94
6.3.2	BMT Doped with each of the following Ga ₂ O ₃ , ZnO and MgO.....	94
7.0	CONCLUSION.....	97

8.0	SUGGESTIONS FOR FUTURE WORK.....	98
Appendix A.....		100
Chemical Analysis of Starting Materials.....		100
Appendix B.....		102
Procedure for the Synthesis of BMT Ceramics.....		102
Appendix C.....		105
Procedure for the Network Analyzer.....		105
BIBLIOGRAPHY.....		121

LIST OF TABLES

Table 1 Starting Materials for Various Compositions of BMT.....	46
Table 2 Ionic Radii of BMT and Other Relevant Ions	96

LIST OF FIGURES

Figure 1	Microwaves are electromagnetic radiation. They lie in the region of 10^{-1} to 10^{-3} m	23
Figure 2	The microwave spectrum and some of the current applications utilizing microwaves.[64]	24
Figure 3	Fields in a microwave dielectric resonator in the simplest standing wave mode (TE _{01d}): (a) magnetic field, H; (b) electric field, E; (c) variation in E_r and H_z with r at $Z=0$ with reference to cylindrical coordinates.	25
Figure 4	Mechanisms of dielectric polarization.	26
Figure 5	A sample resonance curve that is produced when a DR is coupled to a microwave circuit.	27
Figure 6	The parameter used describes the signals that the network analyzer is measuring. The dielectric constant is measured by the S_{21} parameter and the Q-factor is measured using the S_{11} parameter.	28
Figure 7	The Q-factor of a microwave ceramic can be measured by using the single port reflection technique. The DR is placed on a piece of Styrofoam in the center of a silver cavity. Microwaves are sent from the network analyzer into the cavity. The signal bounces around the cavity and exits through the same port as it entered.	29
Figure 8	The Courtney method can be used to measure the dielectric constant of a microwave ceramic. The ceramic is placed between two metal plates. The signal comes from the network analyzer into the cavity and leaves the opposite side back into the network analyzer.	30
Figure 9	The perovskite structure of BMT. The barium ions occupy the corner positions of the cube. The magnesium and tantalum ions occupy the body-centered positions. And the oxygen anions occupy the face-centered positions.	31
Figure 10	The procedure for the synthesis of BMT. When BMT was doped with ZnO, Ga ₂ O ₃ , and MgO, the dopant(s) was added before the first ballmilling. When the BMT was doped with ZnGa ₂ O ₄ , the dopant was added before the second ballmilling.	40
Figure 11	The JCPDS X-ray diffraction pattern for BMT (18-176).	41

Figure 12	The JCPDS X-ray diffraction pattern for ZnGa_2O_4 (3-1155).....	42
Figure 13	Courtney method set-up for the measurement of the dielectric constant.....	43
Figure 14	Single port reflection technique set-up for the measurement of the quality factor.	44
Figure 15	A smith chart showing critical, over and under coupling.....	45
Figure 16	X-ray diffraction pattern of calcined BMT powder doped with 8mol% ZnO and Ga_2O_3 . This pattern shows only BMT peaks and no superlattice peaks.....	58
Figure 17	SEM micrograph of calcined BMT powder doped with 8mol% ZnO and Ga_2O_3 . There is no evidence of any second phases.....	59
Figure 18	The density Vs sintering temperature for BMT co-doped with 8mol% ZnO and Ga_2O_3 and sintered at a constant heating rate of $10^\circ\text{C}/\text{min}$	60
Figure 19	The Q^*f vs sintering temperature for BMT doped with 8mol% ZnO and Ga_2O_3 and sintered at a constant heating rate of $10^\circ\text{C}/\text{min}$. The largest increase in Q-factor was between the temperatures of 1400°C and 1450°C ; this corresponds to densities where the pores would be closing off. (The resonant frequency for these pellets was approximately 4.9 GHz.).....	61
Figure 20	Selected SEM micrographs of BMT doped with 8mol% ZnO and Ga_2O_3 and sintered at a constant heating rate of $10^\circ\text{C}/\text{min}$. Some of the zinc and gallium rich second phase has been circled. The only pellet shown that did not show any evidence of Zn and Ga rich second phase is shown in figure (a) and was sintered at 1300°C for 0 hours. The pellets were also sintered at 1400°C for 0 hours (b), 1450°C for 0 hours (c), 1500°C for 0 hours (d), and 1600°C for 0 hours(e).....	62
Figure 21	An XRD pattern of BMT doped with 8mol% ZnO and Ga_2O_3 and sintered at a constant heating rate of 10°C per minute increasing to 1500°C and then immediately decreasing at 10° per minute to room temperature.....	63
Figure 22	The density vs. sintering time for BMT doped with 8mol% ZnO and Ga_2O_3 and sintered at 1350°C	64
Figure 23	The Q^*f vs. sintering time for BMT doped with 8mol% ZnO and Ga_2O_3 and sintered at 1350°C (The resonant frequency for these pellets was approximately 4.9 GHz.).....	65
Figure 24	Selected SEM micrographs of sintered surfaces of BMT doped with 8mol% ZnO and Ga_2O_3 and sintered isothermally at 1350°C . Some of the zinc and gallium rich second phase has been circled. The pellet shown in micrograph (a) has been sintered at 1350°C for 0 hours and shows no evidence of any Zn and Ga rich second phase. The pellet shown in micrograph (b) has been sintered at 1350°C for 2 hours, (c) has been sintered at 1350°C for	

6 hours. Micrograph (c) was taken using the backscattered electrons and therefore the Zn and Ga rich crystals appear darker than the BMT grains. And the pellet shown in micrograph (d) has been sintered at 1350°C for 24 hours.....66

Figure 25 A SEM micrograph of a fracture surface of BMT doped with 8mol% ZnO and Ga₂O₃ and sintered at 1350°C for 1 hour. Some of the Zn and Ga rich second phase has been circled.....67

Figure 26 A typical pattern from BMT doped with 8mol% ZnO and Ga₂O₃. This particular pattern came from a sample sintered at 1350°C/24hr. The circles peak has been identified as the start of barium tantalite. All other peaks have been identified as BMT peaks.....68

Figure 27 A graph of Density vs. Sintering Temperature (time=2 hrs) for BMT Doped with 8mol% ZnO and Ga₂O₃.....69

Figure 28 The Q*f vs. sintering temperature (time=2 hrs) for BMT doped with 8mol% ZnO and Ga₂O₃. (The resonant frequency was approximately 4.9 GHz.).....70

Figure 29 Selected SEM micrographs of BMT doped with 8mol% ZnO and Ga₂O₃ and sintered at various temperatures for 2 hours. Some of the zinc and gallium rich second phase has been circled. Micrograph a) has been sintered for 1450°C for 2 hours and is imaged by the backscattered electrons. Micrographs b) through f) have been sintered for 1600 °C for 2 hours.....71

Figure 30 An XRD pattern of BMT doped with 8mol% ZnO and Ga₂O₃ and sintered at 1500°C for 2 hours. The largest superlattice peak has been marked with an arrow.....72

Figure 31 An XRD pattern of BMT doped with 8mol% ZnO and Ga₂O₃ and sintered at 1600°C for 2 hours. This was taken on the top of the pellet; the bottom has the same peaks with the second phase peaks smaller. The zinc gallate peaks have been marked with an asterisk and the largest super lattice peak has been marked with an arrow.....73

Figure 32 A Comparison of the Q*f of 4mol% and 8mol% ZnO and Ga₂O₃ doped BMT. Although the BMT doped with 4mol% had slightly higher densities, the Q-factors were both higher in the BMT doped with 8mol% ZnO and Ga₂O₃.....74

Figure 33 Selected SEM micrographs of BMT doped with 4mol% (a) and b)) and 8mol% (c) and d)) ZnO and Ga₂O₃. Micrographs a) and c) have been sintered at 1400°C for 2 hours and micrographs b) and d) have been sintered at 1500°C for 2 hours. Some of the zinc and gallium rich second phase has been circled and the barium and tantalum rich second phase is indicated by a rectangle.....75

Figure 34 XRD pattern of the top of a sintered pellet of BMT doped with 4mol% ZnO and Ga₂O₃. The barium tantalate second phase peaks have been circled and the largest superlattice peak has been marked with an arrow.....76

Figure 35	An XRD pattern of the bottom of a pellet doped with 4mol% ZnO and Ga ₂ O ₃ and sintered at 1500°C for 2 hours.....	77
Figure 36	An XRD of the top of a pellet of BMT doped with 4mol% ZnO and Ga ₂ O ₃ and sintered at 1500°C for 2 hours with the outer surface removed.....	78
Figure 37	An XRD of the bottom of a pellet of BMT doped with 4mol% ZnO and Ga ₂ O ₃ and sintered at 1500°C for 2 hours with the outer surface removed.....	79
Figure 38	An XRD pattern of a BMT pellet doped with 8mol% ZnO and Ga ₂ O ₃ and sintered at 1400°C for 2 hours.....	80
Figure 39	A Comparison of the Q*f of BMT doped with combinations of ZnO and Ga ₂ O ₃	81
Figure 40	SEM micrograph of BMT doped with 8mol% ZnO and Ga ₂ O ₃ and sintered at 1450°C for 2 hours. Some of the zinc and gallium rich second phase has been circled.....	82
Figure 41	SEM micrograph of BMT doped with 8mol% Ga ₂ O ₃ and sintered at 1450°C for 2 hours. Some of the gallium rich second phase has been circled.....	83
Figure 42	An XRD pattern of a BMT pellet (top) doped with 8mol% Ga ₂ O ₃ and sintered at 1450°C for 2 hours. The largest superlattice peak has been marked with an arrow.	84
Figure 43	An XRD pattern of a BMT pellet (bottom) doped with 8mol% Ga ₂ O ₃ and sintered at 1450°C for 2 hours. The largest superlattice peak has been marked with an arrow.	85
Figure 44	SEM micrograph of BMT doped with 8mol% ZnGa ₂ O ₄ and sintered at 1450°C for 2 hours. Some of the second phase rich in gallium and zinc is circled and some of the second phase rich in barium and tantalum is indicated by a rectangle.....	86
Figure 45	An XRD pattern of BMT doped with 8mol% ZnGa ₂ O ₄ and sintered at 1450°C for 2 hours.....	87
Figure 46	XRD pattern of the bottom of a pellet of BMT doped with 8mol% ZnGa ₂ O ₄ and sintered at 1450°C for 2 hours. The zinc gallate second phase peaks have been marked with an asterisk and the largest superlattice peak has been marked with an arrow.	88
Figure 47	The S ₂₁ spectrum ranging from 1 GHz to 10 GHz.	116
Figure 48	The screen on the Courtney program where the actual data is entered so the program can calculate the dielectric constant.....	117
Figure 49	An example of the results obtained from the Courtney Software.....	118

Figure 50 The resonant coupling circle on the Smith chart for measuring the Q-factor using the single-port reflection technique119

Figure 51 An example of the results obtained from the single-port reflection technique for measuring the Q-factor.....120

1.0 INTRODUCTION

Recently wireless communication systems using microwaves to carry information have become increasingly popular. Microwaves are able to carry more information than radio waves because of their higher frequency. These systems include cellular phones and satellite communications. Wireless communications utilize microwave dielectric components such as dielectric resonators for coupling, selecting and filtering microwaves. Traditional wiring and transistors will not work in these systems due to lead reactance and transit time.

There are three main, very important properties of a dielectric resonator material: relatively high dielectric constant, low dielectric loss, and temperature stability. A relatively high dielectric constant enables the dielectric resonator to be smaller since the dielectric constant is inversely proportional to the size. Low dielectric loss or high quality factor gives a smaller bandwidth at the resonant frequency, a lower degree of noise, and less power loss. Temperature stability is important so that the device can be used in any environment without detrimental effects on the signal.

There are many materials currently used in these applications, many of which are ceramics with a perovskite structure. The two most commonly utilized materials are barium zinc tantalate (BZT) and barium magnesium tantalate (BMT). Although these materials have very good microwave dielectric properties, they can be very expensive to produce. BMT and BZT require high sintering temperatures, often greater than 1600°C, and long annealing times, sometimes for 24 hours or more to obtain the desired properties. This study focused on lowering the sintering temperature of BMT, through the addition of dopants, while maintaining the dielectric properties of the material. BMT was doped with ZnGa_2O_4 (8mol%); Ga_2O_3 (8mol%);

ZnO (8mol%); and Ga₂O₃ along with ZnO (4mol% and 8mol%). The ceramics were synthesized through a solid state reaction and sintered at various temperatures between 1300°C and 1600°C for various times. The dielectric properties of the materials were measured using a network analyzer. The dielectric constant was measured by the Courtney method and the loss was measured by the single port reflection technique. The microstructure analysis was done by x-ray analysis and scanning electron microscopy.

The major technical objective of this research was to investigate the synthesis of BMT using the conventional mixed oxide route, and identify sintering additives that could lower the sintering temperature while maintaining the dielectric properties.

2.0 BACKGROUND

2.1 Microwave Communications

Electromagnetic radiation is a wave of oscillating electric and magnetic influences. The electromagnetic spectrum ranges from 1 MHz to 10^6 GHz and can be broken down into ranges as shown in figure 1. The radio frequency is in the range of 300 KHz to 300 MHz. Radio waves are used to carry information in AM and FM broadcast radio, short wave radio, and VHF television channels. These signals can be carried using traditional transistors, tubes and circuits. Microwaves can also be used to carry information. Microwaves lie in the region from 300 MHz to 300 GHz. The microwave region can be broken down further into the ultra high frequency (UHF) region from 300 MHz to 3 GHz, the super high frequency (SHF) region from 3 GHz to 30 GHz, and the extremely high frequency (EHF) region from 30 GHz to 300 GHz. Microwaves are sometimes more useful in carrying information than radio waves because they have a higher frequency and shorter wavelength. The higher frequency gives a wider bandwidth capacity, enabling it to carry more information. The short wavelength allows the energy to be concentrated into a small area; this is the reason that microwave ovens are so convenient. There are many current applications that use microwaves, including cellular phones (900 MHz) and wireless internet (2.4 GHz). Figure 2 shows the microwave spectrum and many of the current applications. Most microwave systems are located below 30 GHz (between 300 MHz and 30 GHz) because at many frequencies above 30 GHz there is high atmospheric absorption making

them impractical for long-range communication and radar systems. There are some windows above 30 GHz that can be utilized; missile seekers are used at a frequency of about 90 GHz.

Due to lead reactance and transit time microwave systems require special devices to carry and filter the electromagnetic waves; conventional transistors, IC's and wiring will not work. The inductive reactance of the wire increases with frequency and is negligible when the frequencies are low. However, at microwave frequencies, the lead reactance is so high that almost all of the oscillator voltage is dropped across the connecting wire and never gets to the load resistor, meaning that most of the signal (information) is lost.

2.1.1 Dielectric Resonators

A resonator is the most commonly used configuration for filters and oscillators. At high frequencies (>3GHz) the resonator is made from a piece of dielectric rod, called a dielectric resonator. In 1939, Richtmyer⁽¹⁾ showed that unmetallized dielectric objects could function similarly to metallic cavity resonators; he called these dielectric resonators (DR's). A DR, usually a ceramic, is able to resonate at the frequency of the carrier signal to allow that signal to be efficiently separated from other signals in the microwave band; this frequency is called the resonant frequency (f_o). The resonant frequency depends on the dielectric material and the size of the resonator.

It was not until the late 1960's that dielectric resonator ceramics were developed for resonator applications, before this, metallic high Q cavities were utilized. During this time there were many pioneers investigating the behavior of dielectrics at microwave frequencies, including: Rupprecht⁽²⁾, Spitzer⁽³⁾, Haki⁽⁴⁾, Coleman⁽⁴⁾, and Cohn⁽⁵⁾. At this time the

applications were limited due to a lack of suitable materials. Rutile phase (TiO_2) was often used but its large resonant frequency fluctuations with temperature made it impractical for many applications. Single crystal alumina (sapphire) was also used but it is very expensive. By the 1970's, research and development for temperature stable dielectric resonator materials had begun worldwide.

There are many advantages of ceramic dielectric resonators compared to traditional resonators including: size reduction (higher dielectric constant), greater degree of circuit and subsystem integration (due to simpler coupling schemes), better circuit performance (with regard to temperature changes and losses), and a reduction in the overall cost of the systems. Over the years the need for smaller, lighter, faster and cheaper communication devices has driven the industry to explore many new materials and systems. Today microwave dielectric resonators are used to create, filter, and select frequencies in oscillators, amplifiers and tuners.

The most common/advantageous dielectric resonator is a solid, cylinder shape that can sustain an electromagnetic standing wave within its volume because of the reflection at the dielectric-air interface. Several DR's can be assembled into devices to filter microwaves. These devices pass a range of frequencies and reject all others. Since the filter passes only certain frequencies there needs to be large out of band attenuation, low in band insertion loss, and a small bandpass to give greater selectivity. There are two mechanisms of selecting the frequency: absorption and reflection. In absorption, the frequency is selected by absorbing the out of band frequencies. In reflection, the frequency is selected by reflecting out the band frequencies and allowing only in band frequencies. There are three kinds of resonant modes that are often used for dielectric resonant filters: TEM mode, $\text{TE}_{01\alpha}$ and TM_{010} or HE mode. The resonant modes describe the electric field lines around the resonator. The electric field lines of each mode are

shown in figure 3. The TE (transverse electric) has no transverse component of the electric field; the TM (transverse magnetic) has no transverse component of the magnetic field; and the HE (hybrid electro-magnetic) has a transverse component in the electric and magnetic fields.

There are three important properties that need to be considered for materials used for dielectric resonators. The temperature coefficient of resonant frequency, $\hat{\Omega}_f$, describes the temperature stability of the material. This should be as close to zero as possible. The unloaded quality factor, Q_o , is inversely proportional to the losses of the material; therefore this should be as high as possible to get the minimum loss. And the dielectric constant, K' , ultimately determines the resonator dimensions and should also be as high as possible. These qualifications will be discussed separately and in more detail in the following sections.

2.1.2 Microwave Dielectric Properties

2.1.2.1 Dielectric Resonant Frequency. The resonant frequency is the frequency at which the dielectric resonator is utilized. The resonant frequency of a dielectric resonator in the TE_{01δ} mode can be estimated by the following equation:

$$f_o \text{ (GHz)} \approx 8.553 / ((K')^{-2} ((\pi/4)(D^2L^2))^{1/3}) \quad (2-1)$$

f_o is the resonant frequency, K' is the dielectric constant, D is the resonator diameter in inches, and L is the resonator height in inches. This equation gives the resonant frequency within approximately 6%.⁽⁶⁾

The resonant frequency can be changed by altering the dimensions of the DR; from a manufacturing standpoint the height is the easiest dimension to change. It can also be changed

by perturbing the fringing fields outside the dielectric resonator with a metallic or dielectric tuner. A metal tuning stub will pull the frequency up and dielectric-tuning stub will push the frequency down. A draw back to using a tuning stub is that it will slightly decrease the Q-factor and slightly disturb the temperature stability.

2.1.2.2 Dielectric Constant. When a parallel-plate capacitor charged with a voltage has a dielectric between the plates, the dipoles of the material will align with the field. The fields of the dipoles oppose the capacitor field. The result is a reduction in the net electric field between the plates. The dielectric constant is defined as the ratio of capacitance of a capacitor with a dielectric between the plates to that with a vacuum between the plates. This is defined in equation 2-2.

$$K' = C/C_0 = (\epsilon A/d)/(\epsilon_0 A/d) = \epsilon/\epsilon_0 \quad (2-2)$$

K' is the relative dielectric constant, C is the capacitance of the capacitor with the dielectric between the plates, C_0 is the capacitance of the capacitor with a vacuum between the plates, A is the area of the plate of the capacitor, d is the distance between the plates, ϵ is the permittivity of the material, and ϵ_0 is the permittivity of free space. The charged species of the material are displaced in response to the applied field; this increases the ability of the plates to store charge. This orientation of the charged species “ties up” charges on the plates of the condenser and thus neutralizes part of the applied field. The charge that isn’t neutralized (free charge) produces an electric field and voltage towards the outside. Therefore, a smaller external field is required to maintain the same surface charge because some of the charge is held by the polarization in the dielectric. There are four primary mechanisms of polarization: electronic (due to the shift of the electron cloud), atomic (due to the displacement of the positive and negative ions with respect to each other), dipole (due to the molecules containing permanent dipole rotating or rotation of

dipoles between two equivalent equilibrium positions) and interfacial (due to mobile charge carriers that are impeded by a physical barrier). The four primary mechanisms for polarization are shown in figure 4. Each of these involves a short-range motion of charge and contributes to the total polarization of the material.

The dielectric constant of the dielectric resonator material is important because it will ultimately determine the dimensions of the resonator. A cylindrically shaped DR sustains an electromagnetic standing wave within its volume because of the reflection at the dielectric air interface. The wavelength of the standing wave is about equal to the diameter of the cylinder. This is shown in equation 2-3 where D is the diameter of the resonator, C is the capacitance of the resonator, f_o is the resonant frequency and ϵ_r is the permittivity of the resonator.

$$D \approx C / f_o \epsilon_r^{1/2} \quad (2-3)$$

It is therefore important to have the dielectric constant as high as possible in order to reduce the size of the DR.

2.1.2.3 Quality factor. The quality factor or Q-factor is the ability of a dielectric resonator to store microwave energy with minimal signal loss. A perfect dielectric has no losses since its electrical conductivity is zero but real dielectric materials are partially conducting. Therefore the electromagnetic signal loses power as it goes through a dielectric material. The Q-factor is approximately equal to the inverse of the loss tangent; therefore for DR applications it is important for the losses to be minimal and the Q-factor to be as high as possible.

The Q-factor is a measure of the energy loss per cycle as compared to the energy stored in the fields outside the ceramic. The Q-factor is a dimensionless number that can be expressed as a ratio shown in equation 2-4.

$$Q = 2\pi (\text{max. energy stored per cycle}) / (\text{average energy dissipated per cycle}) \quad (2-4)$$

This ratio must be evaluated at the resonant frequency of the material and if the material has more than one resonant frequency, each may have a different Q-factor. When a DR is coupled to a microwave circuit a resonance curve can be produced (a sample curve is shown in figure 5) and by using this curve along with equation 2-5 the Q-factor can be calculated;

$$Q = f_o / \Delta f \quad (2-5)$$

f_o is the resonant frequency and Δf is the half power bandwidth at the resonant frequency. A high Q-factor material has a narrow bandwidth at the resonant frequency. This provides more frequency selections in a frequency range and a better signal to noise ratio. (A more detailed description of measuring Q-factors is given in section 4.4.2 and Appendix C.) This Q-factor is called the unloaded quality factor, Q_u . For cavity resonators there are a number of factors that affect the Q_u including: dielectric loss of the dielectric itself, conduction in the walls of the enclosure, and radiation. These are usually referred to as Q_d , Q_c and Q_r respectively. The losses of the dielectric itself can be broken down further into intrinsic and extrinsic losses. The intrinsic losses are dependant on the composition of the material. The extrinsic losses are determined by the microstructure of the material. The losses arise from interactions of phonons, in ideal crystals, and impurities, vacancies, grain boundaries, porosity and dislocations in real materials. The intrinsic losses are due to decay of the microwave into optical phonons and finally into thermal phonons.⁽⁷⁾ From theory it would seem that the highest Q-factor would be obtained from a single or perfect crystal, since in general, defects and impurities will increase phonon scattering, but there has not been any evidence from research to prove this. The Q-factor is often reported as the Q-factor times the resonant frequency ($Q*f$). Theoretically the Q-factor decreases linearly with increasing frequency; comparing just the Q-factors of different resonators would not be a fair comparison. It is therefore customary to report Q-factors as $Q*f$. If it isn't

clear which value is being reported, the Q-factor is dimensionless and the Q^*f value will have the units of the resonant frequency, usually of GHz.

There are three main mechanisms for microwave absorption: 1) losses in perfect (ideal) crystals because of anharmonic lattice forces which mediate interaction between the crystal and phonons, 2) losses in real but homogenous crystals caused by periodicity defects (isotopes, dopant atoms, vacancies, ect.) and 3) losses in real, inhomogeneous ceramics by extended dislocations, grain boundaries, vacancies, inclusions and second phases. The losses from point 3) are small and can usually be neglected at high frequencies.⁽⁷⁾ Points 1) and 2) can be seen as energy transfers from the excited microwave to transverse optical phonons. These optical phonons can then generate thermal phonons through scattering by impurities and through interaction with other phonons. This leads to dampening of the microwave. The dielectric loss for these scattering effects can be calculated by the following equation:

$$\tan \delta = \omega \sum (\Delta \epsilon / \epsilon(0)) (\gamma \omega^2 / \omega_0) \quad (2-6)$$

where ω is the frequency and γ is the dampening constant. A linear increase of loss with frequency is therefore characteristic for these phonon effects. Therefore, the Q^*f_0 is constant in the absence of extrinsic losses. And when there are extrinsic losses the Q^*f_0 may not increase linearly with frequency.

2.1.2.4 Temperature Coefficient of Resonant Frequency. The temperature coefficient of resonant frequency, τ_f , determines how well a resonator will function when there are fluctuations in temperature. This includes the ambient temperature as well as heating by microwave absorption in the resonator structure. The τ_f is a combination of three independent factors: temperature coefficient of the dielectric constant ($\tau \epsilon$), thermal expansion of the material (α_L) and

the thermal expansion of the environment in which the resonator is mounted. This is shown in equation 2-7⁽⁶⁾.

$$\mathbf{t}_f = 1/2 \tau \epsilon - \alpha_L \quad (2-7)$$

Changes in temperature can cause changes in the dielectric constant, the size of the resonator, and the resonant frequency. In order for materials to be used as oscillators and filters, it is important that the resonant frequency not shift significantly between -20°C and +80°C. If the resonant frequency is too dependent on the temperature, the carrier signal will drift in and out of resonance on hot and cold days. If these fluctuations cannot be avoided, it is preferred that the resonant frequency changes are small and occur linearly because then there are ways to compensate. A material with a small positive variation can often be combined with a material with a small negative variation to make the resonator stable. The equation for calculation is shown in equation 2-8 where \mathbf{t}_k is the temperature coefficient of the dielectric constant and \acute{a} is the thermal expansion coefficient of the dielectric.

$$\mathbf{t}_f = (-1/2) \mathbf{t}_k - \acute{a} \quad (2-8)$$

For DR applications the \mathbf{t}_f should typically be equal to or less than $\pm 3 \text{ppm}/^\circ\text{C}$. The \mathbf{t}_f can also be expressed as a function of frequency as shown in the following equation,

$$\mathbf{t}_f = (\Delta f \text{ (Hz)}) / (f_o \text{ (MHz)}) / (\Delta T) \quad (2-9)$$

where Δf is the resonant frequency at 60°C minus the resonant frequency at 25°C, f_o is the resonant frequency at 25°C and ΔT is 35°C (60-25).

2.1.3 Microwave Dielectric Property Measurements

2.1.3.1 Network Analyzer. A network analyzer is an instrument that is able to measure the reflection and transmission characteristics of devices by applying a known swept signal and measuring the response of the device. The signal that is transmitted or reflected from the device is compared to the incident signal generated by a swept RF source. The signals are applied to a receiver for measurement, signal processing and display.

The network analyzer is able to measure many parameters. Figure 6 shows some of the possible parameters. These describe the signals that the network analyzer is measuring. For example, for a transmission method measurement (S_{21}), the electric field of the microwave signal entering the component input would be compared to the electric field of the microwave signal leaving the component output. Or more simply, the signal entering one side of a cavity would be compared to the signal collected on the other side of the cavity.

2.1.3.2 Measurement of the Quality Factor. There are many ways to measure the Q-factor of dielectric ceramics. A common method and the method used in this study, is the single-port reflection technique. The single port reflection technique was developed by Engineers at Trans-Tech, Inc.⁽⁸⁾ This method uses the TE-01_a mode and the S_{11} parameter. The S_{11} parameter is when the electric field of the microwave signal leaving the component input is divided by the electric field of the microwave signal entering the component input. (The signal is entering and leaving the cavity through the same port.) This technique uses a silver plated cavity that is at least three times the size of the DR. The DR must be separated from the walls of the cavity to reduce conduction loss; therefore the DR is placed on a piece of Styrofoam or other low loss

material. This set up is shown in figure 7. This technique uses the TE-01 \ddot{a} mode, the lowest and most easily coupled mode.

2.1.3.4 Measurement of the Dielectric Constant. The Courtney method is the most common method for measuring the dielectric constant of dielectric ceramics. In 1960, Hakki and Coleman⁽⁴⁾ introduced the parallel-plate dielectric resonator to measure the dielectric constant of ceramics. Courtney⁽⁹⁾ then analyzed the error and investigated the temperature effects of this technique and it is now known as the Courtney method. This is the method that was used to measure the dielectric constant of the materials in this study. The Courtney method is a transmission type measurement that uses a small brass cavity. The sample is placed in the center of the cavity away from the sides. The set up for the Courtney method is shown in figure 8. This technique uses the S_{21} parameter (the electric field of the signal entering the component input is divided by the electric field of the signal leaving the component output) and the TE-011 mode. The resonant frequency at the TE-011 mode, 3dB half power bandwidth, and the insertion loss are obtained from the network analyzer. This data along with the dimensions of the DR are entered into the Courtney software (developed by GDK products, Cazenovia, NY), which calculates the dielectric constant.

2.1.3.5 Measurement the Temperature Coefficient of Resonant Frequency. A simple technique used to measure the temperature coefficient of resonant frequency is to note the shift in frequency with respect to temperature. The DR is placed in the cavity and weakly coupled so that the tuning effects due to expansion are minimized. The set up is heated slowly using a hotplate and the resonant frequency is noted at 25°C and 60°C. Equation 2-8 can then be used to calculate the $\hat{\delta}_f$.

2.2 High Q Perovskite Ceramics

High Q Perovskite ceramics have the general formula $A(B'_{1/3}B''_{2/3})O_3$ where A is a cation with a large ionic radius (Ba^{+2} , Sr^{+2} , etc.), B' is a divalent cation with a smaller ionic radius (Mg^{+2} , Zn^{+2} , etc.) and B'' is a pentavalent cation with a smaller ionic radius (Ta^{+5} , Nb^{+5} , etc.). There are many different compounds with this structure that are utilized or have been investigated for DR applications; the most common are barium magnesium tantalate (BMT) and barium zinc tantalate (BZT). Table 1 shows a list of some common microwave dielectric resonator materials. Recently there has been an increased interest in the niobium compounds especially barium zinc niobate (BZN) because of a price increase in the already expensive tantalum oxide.

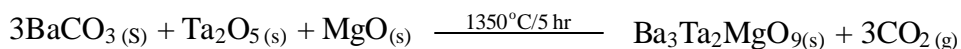
Since there are two different B-site cations, there are two different structures that can exist, the disordered state and the ordered state. The disordered state is a cubic structure; this is the same structure as $BaTiO_3$. The ordered state is a hexagonal perovskite, shown in figure 9. Galasso⁽¹⁰⁻¹³⁾ investigated the structure of many perovskites with a 1:2 mixture of divalent and pentavalent cations in the B-sites. These materials can adopt a structure in which the two cations order onto individual (111) crystallographic planes in a two to one ratio. The extent of this ordering depends on the differences in the ionic radii and the charges of the B-site cations; the greater the differences the greater the ordering. In general, for charge differences ≥ 4 the cations will order, but when the difference is less than 4 it will be disordered unless there is a large difference in the radii.

2.2.1 Barium Magnesium Tantalate (BMT)

As mentioned earlier, BMT is a perovskite ceramic that has been investigated extensively^{(14) (15) (16) (17) (18) (19) (20) (21) (22) (23) (24) (25) (26) (27) (28) (29) (30) (31) (32) (33) (34) (35) (36) (37) (38) (39) (40) (41) (42) (43) (44) (45) (46) (47) (48) (49) (50) (51) (52) (53) (54) (55) (56) (57)} and is utilized for DR applications. BMT has a reported dielectric constant of approximately 25 and a temperature coefficient of resonant frequency of approximately zero; these values have been reported consistently among research groups. There is much less agreement concerning the dielectric loss, reported $Q \cdot f$ values range from 10,400 GHz⁽⁵⁸⁾ to 600,000 GHz even though this is supposed to be a material constant. Some of these variations may be due to different measurement techniques but most are probably due to variations in extrinsic losses due to defects introduced in processing and the purity of the starting materials. Although several factors have been suggested, including B-site cation ordering and point defects, the ranking of the important sources of losses are not clear.

Although BMT has excellent dielectric properties, it can be very expensive to produce. BMT is very refractory and therefore requires very high sintering temperatures (1550°C to 1650°C) and often long annealing times to get the desired properties. Many research groups have investigated solutions to these problems including: chemical synthesis and sintering aids. Unfortunately, these attempts tend to significantly degrade the dielectric properties.

2.2.1.1 Synthesis of BMT. The most common synthesis method for BMT and the method used in this study is through a solid-state reaction. The metal oxides are used as starting materials and mixed homogeneously by ballmilling. The powders are then heated to a high temperature to form BMT according to the following reaction:



This is currently the most common synthesis method because it tends to give ceramics with the best dielectric properties, although they require very high sintering temperatures (1600°C or greater) and sometimes long annealing times (32 hours or longer).^(18, 24, 29, 59, 60)

Another synthesis method is sol-gel synthesis. Chemical synthesis seemed attractive because it tends to produce powders that are more homogeneous with a finer particle size and better control over the particle morphology that often gives improved sinterability. Several research groups were able to produce ceramics with relative densities, over 96%, at temperatures between 1300°C and 1400°C for as little as two hours. Renoult et. al.⁽⁴³⁾ was even able to get complete B-site ordering at 1400°C for 5 hours. (As mentioned earlier, some consider B-site cation ordering to be very important for achieving low loss ceramics.) Despite the high density and ordering parameter the Q-factor was only 6,410 at 7.71GHz ($Q \cdot f = 49,421$ GHz). Even when the sintering temperature of these ceramics was raised to 1600°C, the losses are still relatively high. This may be due to the higher point defect concentrations inherent to low temperature, chemically prepared materials or undetectable second phases.

Maclaren et. al.⁽³⁵⁾ synthesized BMT through hydrothermal synthesis. In hydrothermal synthesis, ceramic sols are created by chemical reactions in an aqueous or organo-aqueous solution under the simultaneous application of heat and pressure. This is usually done in the presence of an alkali or acid that acts as a catalyst. There are some advantages over sol-gel synthesis. Hydrothermal synthesis uses simple salts such as acetates and nitrates instead of expensive alkoxides, the materials are produced directly so there is no need for a calcination step and the particles are produced in a sol form so these sols can be used directly in the production of green bodies without requiring the conversion to a dry powder. This method produced BMT at 200°C. The dielectric properties were not measured but there was evidence of barium carbonate

second phases and particles that were deficient in magnesium, both of which suggest that the dielectric properties would not be acceptable.

Lu et. al⁽³⁷⁾ produced BMT through homogeneous precipitation. This involves the simultaneous precipitation of the ions to give better mixing. One of the problems that occurred was contamination of chlorine ions (from the TaCl₅) that can cause cracking, and the sintering temperature was still 1690°C. None of the dielectric properties were reported.

Another method commonly investigated to reduce the sintering temperature of BMT is the addition of sintering aids. Nomura et. al⁽³⁹⁾ added 1mol% Mn and got a Q of 16,800 at 10.5 GHz ($Q*f = 176,400$) but the ceramics were sintered at 1550°C for 3 hours. Kim et. al⁽³¹⁾ tried 0.083 mol% Ca and got a Q of 9,000 at 10.5 GHz ($Q*f = 94,500$ GHz) by sintering at 1650°C for 2 hours and then annealing at 1500°C for 2 hours. Katayama et.al⁽²⁷⁾ added Co to make Ba(Co_{0.125}Mg_{0.875})_{1/3}Ta_{2/3}O₃, he reported a $Q*f$ of 103,100GHz but sintered the ceramics at 1600°C for 64 hours. Furuya et. al.⁽²³⁾ doped BMT with W to make 0.5mol% Ba(Mg_{1/2}W_{1/2})O₃. He reported a Q of 40,000 at 10 GHz ($Q*f = 400,000$) but he sintered the ceramics between 1500°C and 1600°C for 24 hours. Chen et. al^(21, 22) tried doping with 3.0 wt% NaF and 5% BaO·Nd₂O₃·5TiO₂, these samples were sintered between 1200°C and 1400°C but were reported to have low Q-factors. As mentioned earlier, many researchers have tried several different dopants to try and lower the sintering temperature of BMT while maintaining the microwave dielectric properties, but if the sintering temperatures are lowered, the Q-factor is also significantly lowered.

2.2.1.2 Solid State Sintering. Sintering refers to the process of firing and consolidating a body shaped from powder particles. When powder particles are compacted, they are in contact with each other at many sites with a large amount of pore space between them. The powders that

have been dried and pressed are traditionally called “green products”. These are heated in a furnace to develop the desired structure and properties. This is sufficient to cause significant atomic diffusion for solid-state sintering or significant diffusion and viscous flow when a liquid phase is present or produced by a chemical reaction. The driving force for sintering is the capillary pressure associated with surface curvature where the particles come into contact. In order to reduce the surface area, atoms diffuse to the points of contact, permitting contact flattening. Contact flattening involves the removal of matter between particle centers by volume diffusion, grain boundary diffusion or diffusion through a liquid phase. These mechanisms must be promoted for the pores to shrink and eventually be eliminated. Coarsening mechanisms such as surface diffusion or evaporation-condensation only redistribute matter around surfaces and must be minimized. There are three major stages of sintering. In the initial stage, there is surface smoothing of particles, neck growth, rounding of interconnected open pores. Diffusion of active, segregated dopants can occur and the porosity decreases by <12%. In the intermediate state, there is a formation of continuous pores channels along many three-grain junctions. As densification proceeds, the pore channels form closed pores at densities greater than 92%. In the final stage of sintering, isolated pores are eliminated by mass transport from the grain boundary to the pore. Pores on a grain boundary can be eliminated by grain boundary or lattice diffusion but pores within grains can only be eliminated by lattice diffusion, which can be a problem since volume diffusion often has a higher activation energy. In most ceramics, the lattice diffusivity of the slower rate-limiting constituent is often too slow for effective annihilation of pores that have become trapped in grains. If high density is desired, it is important that the pores remain attached to the grain boundary. In the initial stage there are a number of competing paths for material to be transported to the neck area. Some of these paths will lead to densification, which

is a shrinkage process that requires the centers of the particles to approach. Other paths will lead to coarsening, which is the growth of the neck between the particles leading to a reduction in specific surface area without shrinkage. Generally, densification is desired. These different paths of diffusion are competitive paths of transport; the mechanism that gives the fastest rate of neck growth will dominate and cause either densification or coarsening. Surface diffusion is the general transport mechanism that can produce surface smoothing, particle joining and pore rounding but there is no volume shrinkage. In materials where vapor pressure is high, sublimation and vapor transport to surfaces of lower vapor pressure also produce these effects. In contrast, grain boundary and lattice diffusion produce neck growth and volume shrinkage. At high temperatures, grain boundary diffusion and lattice diffusion tend to dominate and therefore promote densification. Firing at a low temperature can cause coarsening without significant densification and can be useful in making porous materials. Therefore the enhanced solid state sintering of DR's requires dopants that enhance volume and grain boundary diffusion at lower temperatures without significantly enhancing defects responsible for extrinsic defects that effect Q. Solid state sintering of mixed cation oxides such as those used in DR's is an ambipolar diffusion process in which anions and cations must be transported from the source to the sink without kinetic de-mixing. The rate limiting mechanism will be the slowest moving species along the fast path. Therefore, sintering depends a great deal on the diffusivities; and additives which influence diffusion can have an enormous impact on the rate of sintering. Additives can often be beneficial to achieving high densities. Additives can do a number of things including: decrease the rate of coarsening in the earlier stages of sintering, increase the rate of densification, decrease the rate of grain growth or increase pore mobility such that pore-grain boundary separation does not occur.

2.2.1.3 Liquid Phase Sintering. When a wetting liquid is present, bulk viscous flow can cause volume shrinkage. However, commercial ceramics tend to have a small amount of reactive liquid that accelerates the densification rather than facilitate viscous flow. A simple type is a eutectic liquid in which the primary phase is partially soluble is often used in perovskite systems. This can provide a wide variety of results depending on the rate of process, the amount of liquid formed at the sintering temperature, the relative solubility's of the additive and the principle constituents and the wetting behavior of the liquid. In order for the additive to be successful there must be an appreciable solubility for the principle constituent, a reasonably low viscosity for rapid diffusion kinetics and a contact angle that allows it to wet and penetrate between the constituent particles or grains. When the liquid coats each grain, the material can often be sintered to a higher density at a lower temperature with less of a tendency for exaggerated grain growth. Less than 1 vol% liquid phase is sufficient to coat the grains if the liquid is distributed uniformly and the grain size is about 1 μ m. The wetting liquid concentrates at the particle contacts and forms a meniscus; this exerts an effective compressive pressure on the compact. There is a rapid rearrangement of particles into a higher density configuration. This is often where the greatest densification takes place. After the initial rearrangement, further densification takes place as particle contacts flatten under the compressive stress applied to the point contacts by capillary pressure. The contact flattening occurs through dissolution at the particle contacts and transport of the materials towards stress-free interfaces. Since the solubility of the smallest particles is the greatest dissolving grains reprecipitate onto larger grains in a way that leads to flattened boundaries and a more densely packed array of grains. This can lead to appreciable grain growth compared to solid state sintering. In some systems, significant changes can occur during the cooling stage. The solid and liquid compositions change frequently with precipitation

of the principal phase. As the sample cools below the solidus temperature, crystallization of a liquid phase can cause a discontinuous increase in the dihedral angle to a non-wetting configuration, since the solid-solid interfacial tensions are usually greater than the solid-liquid tensions.

2.2.1.4 Point Defects. When there is a decrease or increase in the Q-factor of BMT ceramics many researchers attribute the change to point defects, although very few go into detail about specifics. Kim et.al.⁽³²⁾ looked at defects in BMT doped with BaWO₄. When the W⁶⁺ is assumed to substitute on Ta⁺⁵ position there will be positively charged regions created due to the charge difference between the cations. TEM showed that there was only 1:2 ordering, and therefore compensation did not arise from negative regions created from 1:1 ordering. It is therefore probably compensated by the generation of negatively charged point defects. Kim determined the main defect mechanism in pure BMT was the formation of Ba vacancies by measuring the electrical conductivity as a function of the partial pressure of oxygen and by considering charge neutrality and the mass action law; therefore BMT is a p-type conductor. He also determined that the main defect created by the doping of WO₃ would be the formation of tantalum and oxygen vacancies.

2.2.1.5 B-Site Cation Ordering. Some research groups⁽⁶¹⁻⁶⁴⁾ believe that long range B-site cation ordering can significantly increase the Q-factor of BMT and related ceramics. This conclusion comes from the Q-factors and the ordering parameters both increasing when the ceramics are annealed for long periods of time. This does suggest that there may be some correlation but there have also been many reports that seem to contradict this theory. As mentioned earlier, sol-gel synthesis can produce ceramics that are almost fully ordered and still have a low Q-factor⁽⁴³⁾. Ra et. al⁽⁵⁷⁾ produced BMT through a conventional mixed oxide route and by a columbite route

(to produce ceramics that were more highly ordered). The ceramics produced by the columbite route had an ordering parameter that was 20% higher than the BMT produced by the conventional mixed oxide route but the Q-factor only increased by about 8%. Matsumoto et. al.⁽⁶⁰⁾ doped BMT with BaSnO₃ and found that with increased dopant the Q-factor increased but the ordering parameter decreased. And Yoon et. al.⁽⁵⁰⁾ had similar results with BMT doped with BaWO₃. Therefore although it does seem reasonable that the amount of B-site cation ordering may have some influence on the Q-factor it is probably not the dominant factor. There are many other sources of extrinsic defects.

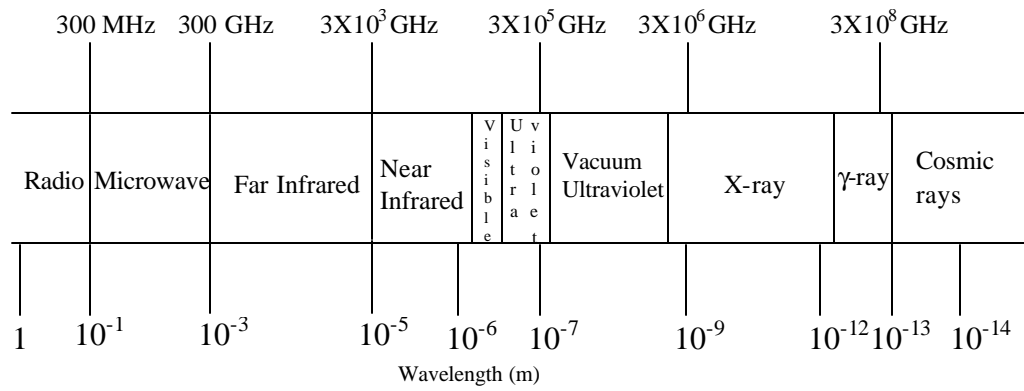


Figure 1 Microwaves are electromagnetic radiation. They lie in the region of 10^{-1} to 10^{-3} m.

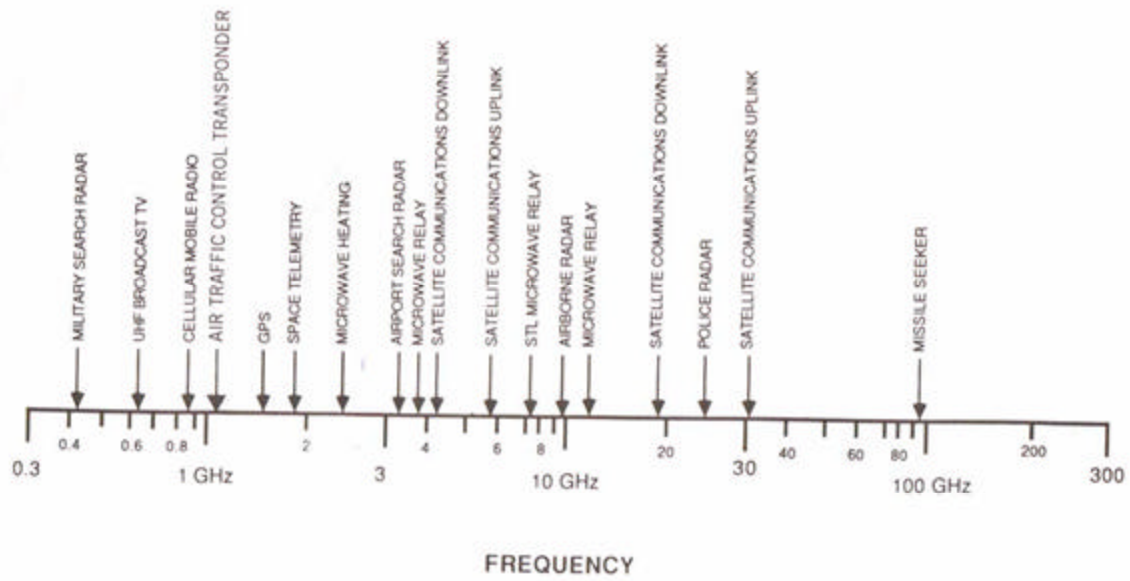


Figure 2 The microwave spectrum and some of the current applications utilizing microwaves.⁽⁶⁵⁾

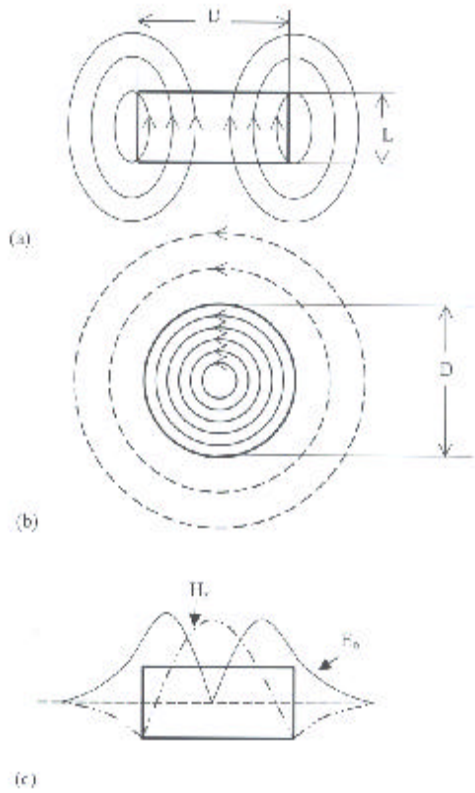


Figure 3 Fields in a microwave dielectric resonator in the simplest standing wave mode (TE_{01d}): (a) magnetic field, H; (b) electric field, E; (c) variation in E_r and H_z with r at $Z=0$ with reference to cylindrical coordinates.

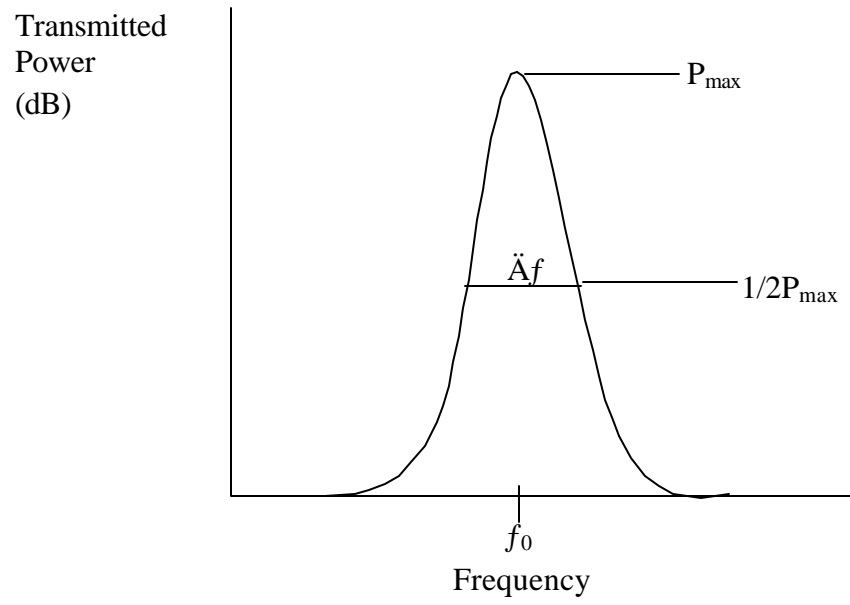
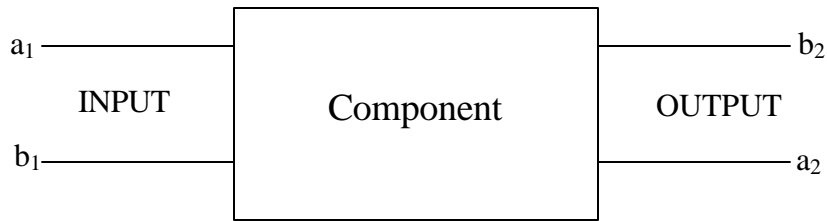


Figure 5 A sample resonance curve that is produced when a DR is coupled to a microwave circuit.



a_1 is the electric field of the microwave signal entering the component input
 a_2 is the electric field of the microwave signal entering the component output
 b_1 is the electric field of the microwave signal leaving the component input
 b_2 is the electric field of the microwave signal leaving the component output

$S_{11} = b_1/a_1$	Return Loss	$S_{21} = b_2/a_1$	Insertion Loss
$S_{12} = b_1/a_2$	Isolation	$S_{22} = b_2/a_2$	Output Return Loss

Figure 6 The parameter used describes the signals that the network analyzer is measuring. The dielectric constant is measured by the S_{21} parameter and the Q-factor is measured using the S_{11} parameter.

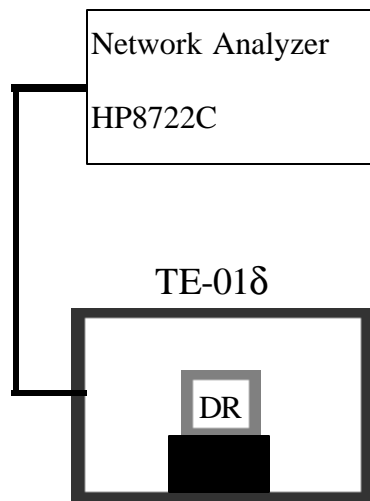


Figure 7 The Q-factor of a microwave ceramic can be measured by using the single port reflection technique. The DR is placed on a piece of Styrofoam in the center of a silver cavity. Microwaves are sent from the network analyzer into the cavity. The signal bounces around the cavity and exits through the same port as it entered.

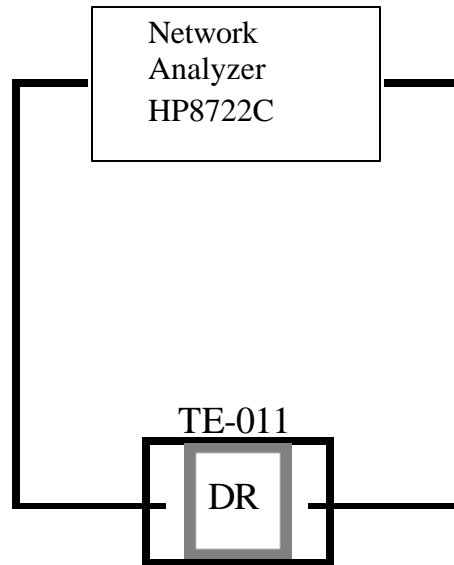


Figure 8 The Courtney method can be used to measure the dielectric constant of a microwave ceramic. The ceramic is placed between two metal plates. The signal comes from the network analyzer into the cavity and leaves the opposite side back into the network analyzer into the cavity and leaves the opposite side back into the network analyzer.

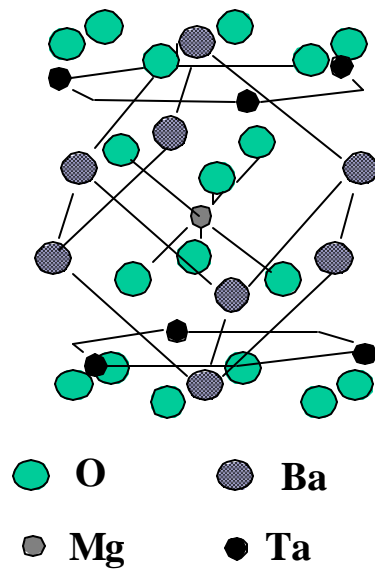


Figure 9 The perovskite structure of BMT. The barium ions occupy the corner positions of the cube. The magnesium and tantalum ions occupy the body-centered positions. And the oxygen anions occupy the face-centered positions.

3.0 OBJECTIVES

The primary objective of this research was to find a dopant(s) that could lower the sintering temperature of barium magnesium tantalate (BMT) while maintaining or improving the microwave dielectric properties. The sub-tasks that were undertaken to achieve this goal were:

- Investigate additive(s) that would form a meta-stable liquid phase that would promote densification while present and then go into solution.
- Investigate additive(s) that would create oxygen vacancies to try and increase the diffusivity of oxygen. Since oxygen is the largest ion it is most likely rate limiting during sintering, therefore adding oxygen vacancies may help to aid sintering. However none of the diffusion coefficients are known.

4.0 EXPERIMENTAL PROCEEDURE

4.1 Synthesis of BMT Powders

High purity (>99+%) BaCO₃ (Aldrich), MgO (Aldrich), Ta₂O₅ (H.C. Stark), ZnO (Aldrich) and Ga₂O₃ (Puratronic) were used as starting materials. The chemical analysis from the manufactures are given in appendix A. The as-received magnesium oxide was calcined in a covered alumina crucible at 1000°C for three hours with a heating and cooling rate of 10°C/min. At 300°C the MgO was removed from the furnace and weighed into plastic bottles. This calcination rids the powder of any carbonate and hydroxide absorbed from the air, assuring, as much as possible, the correct stoichiometry of MgO during mixing. The MgO was difficult to weigh accurately because of the temperature and the rate at which moisture was adsorbed, both caused the weight to fluctuate. Appropriate amounts of starting powders (BaCO₃, calcined MgO, Ta₂O₅, ZnO and Ga₂O₃) were milled in a high-density polyethylene bottle for 24 hours. (The powder amounts are shown in table 1.) The powders were milled using 5-mm yttria-stabilized zirconia (YSZ) balls (YSZ; Union Process Inc., Akron, OH.) and acetone as carrier fluid. The mixed slurry was dried on a hotplate (PMC 730 series, Dataplate; PMC Industries, Inc., San Diego CA.) at 60°C with continuous stirring at 200 RPM to prevent segregation by differential settling. The powder was then kept in a drying oven (OV-18A; Blue M, Hawthorne, CA.) at 108°C for at least 12 hours to ensure complete dryness. The mixed powder was ground with a mortal and pestal and then calcined in a platinum crucible in air at 1300°C for 5 hours with a

10°C per minute heating and cooling rates (Lindberg model 51524; Lindberg, Watertown, WI). The calcined powders were then ball milled again in acetone for 48 hours to break any agglomerates. The mixed slurry was dried on a hotplate at 60°C with continuous stirring at 200 RPM to prevent segregation. The powder was kept in the drying oven at 108°C until further processing. A typical batch produced 30 grams of powder. A schematic of the processing procedure is shown in figure 10 and a detailed processing procedure is given in appendix B.

For the synthesis of the BMT doped with 3% excess MgO; 8mol% ZnO and Ga₂O₃; 4mol% ZnO and Ga₂O₃; 8mol% ZnO; and 8mol% Ga₂O₃, the dopants were added before the first ball milling step. For the BMT doped with ZnGa₂O₄, the dopant was added after the calcination step but before the second ball milling. The ZnGa₂O₄ was prepared similarly to BMT. The appropriate amounts of ZnO and Ga₂O₃ powders were weighed and ball milled in a high-density polyethylene bottle for 24 hours with acetone as the carrier fluid. The powder was dried and kept in the drying oven for 24 hours and then calcined in a platinum crucible with an alumina cover at 1100°C for 24 hours. The powder was then ball milled again for 24 hours in acetone and dried on the hot plate then kept in the drying oven at 108°C until further processing. XRD analysis confirmed ZnGa₂O₄ (3-1155).

4.2 Powder Processing

The BMT powder was ground with a mortar and pestel and made into pellets using single action uniaxial pressing. Portions of approximately 3.92 grams of sample were weighted and pressed into cylindrical pellets with a diameter of 0.5 inches (1.27 cm) and a height of

approximately 0.3 inches (0.76 cm) using 1,000 psi. The pellets were then cold isostatically pressed at 40,000 psi. (R-4-12-60;HIP) The pellets were enclosed in latex (non-lubricated condoms) to keep them from contacting the oil.

The samples were then sintered in a covered platinum crucible and for various temperatures between 1300°C and 1600°C for times between 0 and 24 hours.

Several samples that were doped with 8mol% ZnO and Ga₂O₃ were cut in half and polished to a 1µm finish using diamond paste. The samples were then thermally etched at 1300°C for 12 minutes. This made it possible to examine the microstructure more carefully.

4.3 Microstructural Characterizations

Phase evolution and microstructure characteristics were examined using x-ray diffraction (XRD, Philips X'PERT systems) and scanning electron microscopy (SEM, Philips XL30FEG).

4.3.1 X-ray Diffraction (XRD) Analysis

The calcined powders and sintered surfaces of the ceramics were characterized by XRD. The scans were done on both sides of the sintered pellets to identify any discrepancies. The JCPDS pattern of BMT (18-176) and of zinc gallate (3-1155) are shown in figure 11. The standard Bragg-Brentano geometry pattern was used to characterize the ceramics. The samples were attached to the stage using double-sided tape. The sample and the detector rotate in such a

way that the incident angle and detecting angle are θ and 2θ respectively. The tube voltage was 30 kV and the current was 20 mA. CuK α radiation ($\lambda=1.54\text{\AA}$) was used with a detector slit of $\frac{1}{2}$ degree and a source slit of 0.3. The materials were scanned using a continuous scan from 5 to 80 degrees (2θ) with a scan speed of $0.040^\circ/\text{sec}$.

4.3.2 Scanning Electron Microscopy (SEM) Characterization

Before the SEM analysis, the as-sintered sample surfaces were coated with Pd to reduce charging problems. The SEM was operated at 10-15kV. The surface morphology, grain size, and microstructure were examined using the secondary electron imaging and the backscatter imaging. The backscatter image can be helpful in locating/identifying second phases; phases containing heavier elements appear brighter in the backscatter image. The compositions of the ceramics were analyzed using EDX.

4.3.3 Density Measurements

The density of the sintered ceramics was determined using the dimensions and the weight of the samples. The dimensions were measured using a vernier caliper with a 150 mm scale in 0.05 mm subdivisions. The density was then calculated using equation 4-1.

$$\text{Density} = \text{weight}/((\delta)(\text{radius})^2(\text{height})) \quad 4-1$$

The percent density was then calculated by dividing the calculated density by the theoretical density. It was assumed that the small amount of dopants (ZnGa_2O_4 , MgO , ZnO and Ga_2O_3) did not affect the BMT theoretical density of 7.628g/cm^3 .⁽²⁶⁾

4.4 Microwave Dielectric Property Measurements

The microwave dielectric properties were measured using a network analyzer (Hewlett Packard 8722C). A network analyzer measures the reflection and transmission characteristics of devices by applying a known swept signal and measuring the response of the device. The signal that is transmitted or reflected from the device is compared to the incident signal generated by a swept RF source. The built-in synthesized source generates a continuous wave signal of 40 GHz with a frequency resolution of 100 KHz. The source is generated by a voltage controlled oscillator.

4.4.1 Measurement of the Dielectric Constant

The dielectric constant of a material describes its ability to polarize and store electrical charge. It is simply the ratio of the permittivity of the material to the permittivity of a vacuum. The relative dielectric constant (k') of the sintered ceramics was measured using the Courtney cavity method⁽⁹⁾ and the TE-011 mode. The system set-up is shown in figure 12. This is a transmission type measurement where the signal enters through one side of the cavity and is

collected at the other side. This measurement uses the S_{21} parameter; the S_{21} parameter is equal to the electric field of the microwave signal leaving the component output divided by the electric field of the microwave signal entering the component input. A small brass cavity known as a Courtney cavity is utilized; the sample is secured between the top and bottom of the cavity. The resonance frequency in the TE-011 mode (The mode describes the direction of the magnetic fields used.), 3 dB half power bandwidth, and the insertion loss at the resonant frequency were obtained from the network analyzer. Using this information a software program developed by GDK Products, Cazenovia, NY. was used to calculate the dielectric constant. The accuracy of the Courtney method for measuring the dielectric constant is within 1%.⁽⁹⁾ A detailed procedure is given in appendix C. Measurements were taken from several, randomly selected pellets from each condition.

4.4.2 Measurement of the Quality Factor

The quality factor, Q , is the ability of a dielectric resonator to store microwave energy with minimal signal loss. The Q is inversely proportional to the microwave loss, therefore high Q 's are desirable. The unloaded quality factor (Q_d) of the sintered ceramics were measured using the single port reflection technique (the signal enters and exits through the same port in the cavity) and a silver plated cylindrical aluminum cavity designed originally by engineers at Trans-Tech Inc., Adamstown, MD. The sample was isolated from the cavity walls with a styrofoam support. This is done to reduce conduction. This set-up is shown in figure 13. The sample is placed on the support and centered in the cavity. The network analyzer then sweeps the frequency range and gives a number of resonant modes. This measurement technique uses the

S_{11} parameter; the S_{11} parameter is the electric field of the microwave signal leaving the component input divided by the electric field of the microwave signal entering the component input. The TE-01 (also referred to as the TE_{01δ}) mode is used for this measurement; this is the lowest frequency mode. There are two ways to confirm that the mode is the TE-01 mode. When the lid of the cavity is opened, the TE-01 mode will not disappear. And when a piece of metal is inserted into the cavity, the TE-01 mode will shift up in frequency. This is because the metal has a higher dielectric constant than the ceramic. When the resonant frequency is located, the system is set to span 1GHz (with the resonant frequency near the center). The system is then calibrated for this frequency range using a Hewlett Packard calibration kit. The return loss (S_{11}) is read directly from the network analyzer. The modified return loss (RL') is calculated from the return loss (RL) read from the network analyzer using a program from John Deriso of Trans-Tech, Inc. (This is done to correct for non-perfect coupling.) Even though the RL' can be calculated for any over or under resonant coupling, all the resonant couplings were adjusted to almost critical coupling by moving the probe. Critical coupling is observed when the coupling coefficient is unity. The coupling coefficient is defined as the ratio of the power dissipated in the external circuit to the power dissipated within the shielded cavity. Therefore, if the power dissipated in the external circuit is large in comparison with the power dissipated in the unloaded cavity, the coupling coefficient is large. Coupling is determined using the Smith Chart, a sample smith chart is shown in figure 14. Using the RL' as the half power bandwidth value, the network analyzer calculates the unloaded quality factor. A detailed procedure is given in appendix C. This technique is believed to lead to a Q_d measurement within 2%.⁽⁵⁶⁾

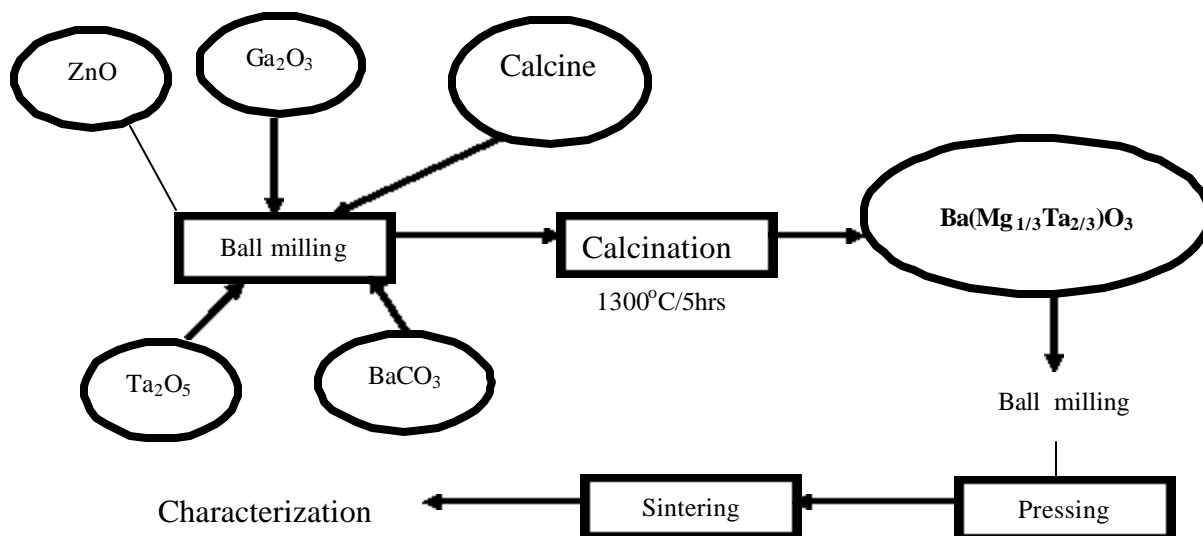


Figure 10 The procedure for the synthesis of BMT. When BMT was doped with ZnO, Ga₂O₃, and MgO, the dopant(s) was added before the first ballmilling. When the BMT was doped with ZnGa₂O₄, the dopant was added before the second ballmilling.

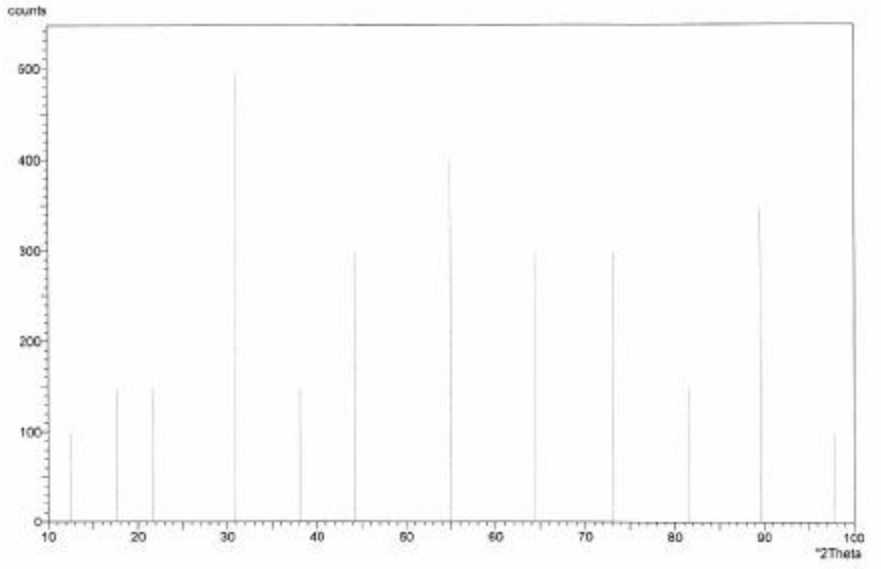


Figure 11 The JCPDS X-ray diffraction pattern for BMT (18-176).

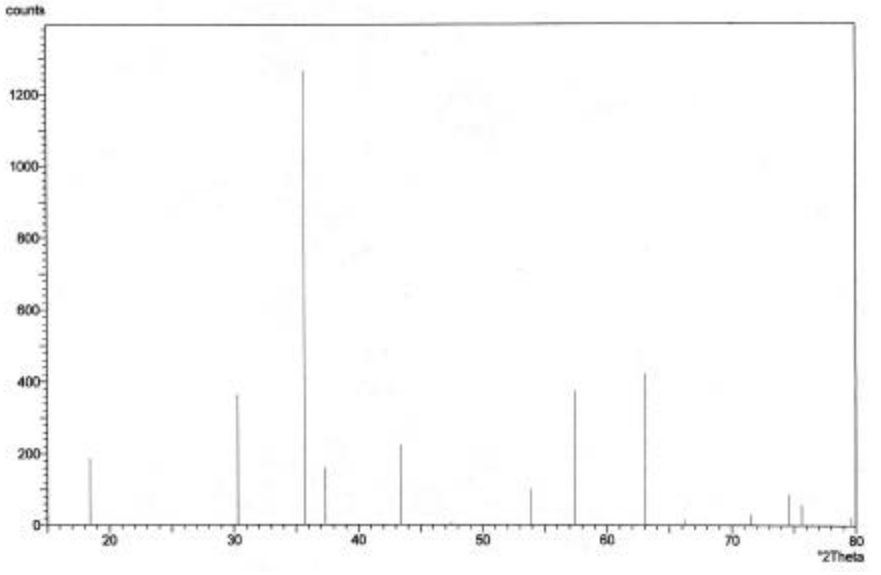


Figure 12 The JCPDS X-ray diffraction pattern for ZnGa_2O_4 (3-1155).



Figure 13 Courtney method set-up for the measurement of the dielectric constant.



Figure 14 Single port reflection technique set-up for the measurement of the quality factor.

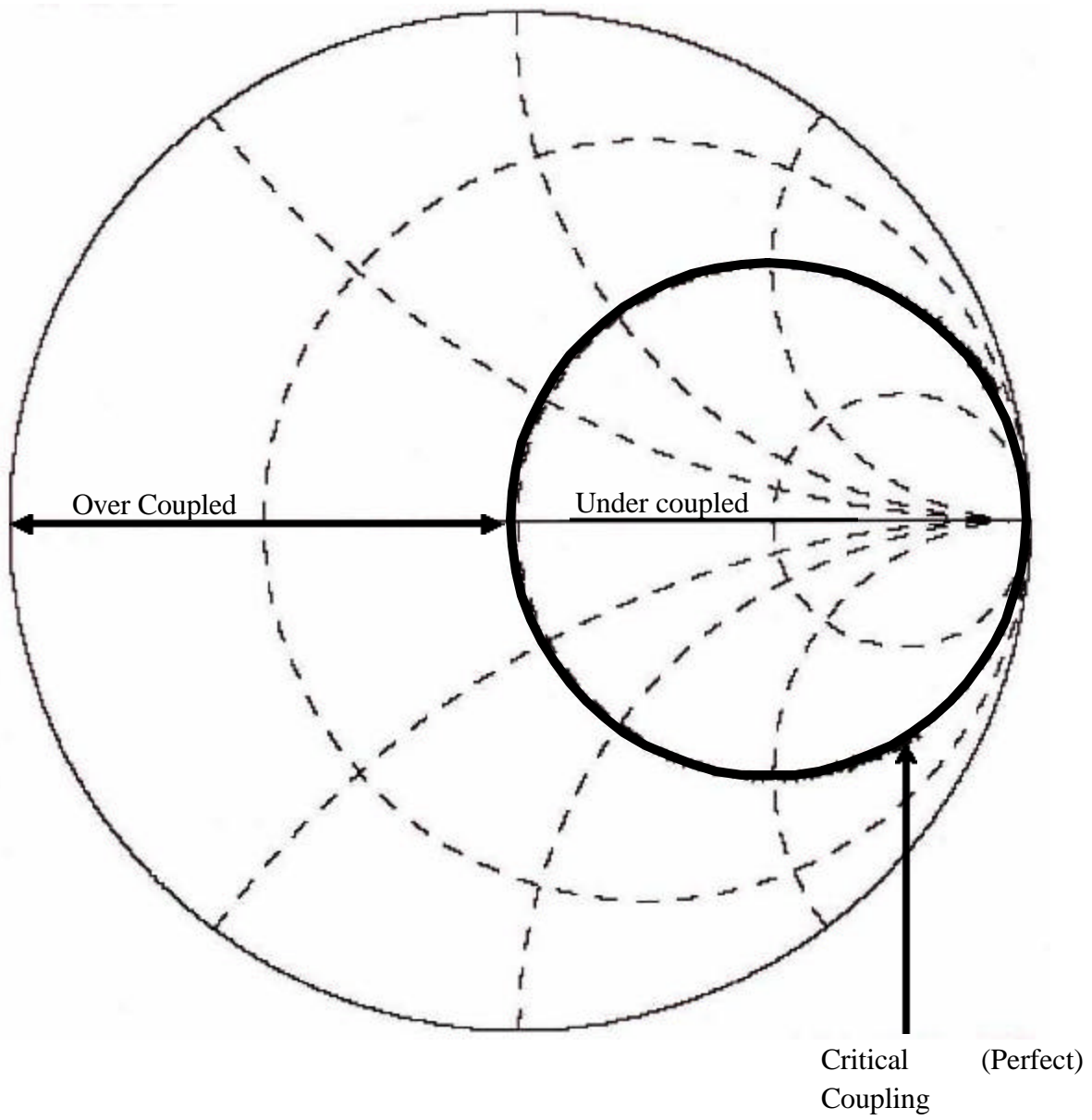


Figure 15 A smith chart showing critical, over and under coupling.

Table 1 Starting Materials for Various Compositions of BMT

Composition of BMT	BaCO₃(g)	Ta₂O₅ (g)	MgO (g)	ZnO (g)	Ga₂O₃ (g)
Undoped	18.8501	14.0703	1.2833	0.0000	0.0000
<i>4mol%ZnO & Ga₂O₃</i>	18.2011	13.5859	1.2391	0.3126	0.7204
<i>8mol%ZnO & Ga₂O₃</i>	17.5445	13.0958	1.1944	0.6288	1.4491
<i>8mol%ZnGa₂O₄</i>	17.5445	13.0958	1.1944	0.6288	1.4491
<i>8mol%Ga₂O₃</i>	17.5445	13.0959	1.1947	0.0000	1.4491
<i>8mol%ZnO</i>	18.4349	13.7608	1.2550	0.6608	0.0000
<i>3% excess MgO</i>	18.8501	14.0703	1.3219	0.0000	0.0000

5.0 RESULTS

5.1 BMT Doped with 8mol% ZnO and Ga₂O₃

5.1.1 Powder Development

The calcined powder of BMT doped with 8mol% ZnO and Ga₂O₃ was examined by x-ray diffraction and scanning electron microscopy. A typical x-ray diffraction pattern is shown in figure 15. All of the powders showed only BMT peaks with no signs of any second phase or any chemically different material by EDS. A typical SEM micrograph is shown in figure 16. This powder showed no signs of second phase. This does not mean that there is no minor crystalline second phase; it may just be below the detection limit of the XRD (≈ 2 vol%)

5.1.2 Ceramics Sintered at a Constant Heating Rate

BMT was co-doped with 8mol% ZnO and Ga₂O₃ before the first ball milling in the synthesis. These ceramics were sintered at a constant heating rate of 10°C/min (heating and cooling) to various temperatures between 1300°C and 1600°C. Figure 17 shows a graph of temperature versus density for these ceramics. The density increases up to 1500°C for 0 hours (density = 94.9 % \pm 1.0), the sample heated to 1600°C for 0 hours showed essentially the same

density (density = $94.7\% \pm 0.3$). As can be seen from the graph, the largest density increase is between the temperatures of 1400°C and 1450°C where the density increases from $79.6\% \pm 3.4$ to $92.9\% \pm 1.3$, suggesting this is a viable temperature range for isothermal sintering without extended sintering times. Figure 18 shows a graph of the same ceramics and conditions with Q^*f verses temperature. The Q-factors start very low ($Q^*f = 24,108 \text{ GHz} \pm 3,014$) and then quickly increase between 1400°C and 1450°C ($37,013 \text{ GHz} \pm 10,404$ to $118,283 \text{ GHz} \pm 5,855$); this is much steeper than the graph of density verses temperature. The large increase in the Q-factor corresponds to the large increase in density from $\approx 80\%$ to over 94% , probably when the pores begin to close off. Therefore, a large increase in the Q-factor seems to correlate with densities above which pore closure is expected. The Q^*f reaches a maximum of $122,247 \text{ GHz} \pm 6,629 \text{ GHz}$ at 1500°C but is only increased slightly from $118,283 \text{ GHz} \pm 5,855$ at 1450°C , so there is no statistical difference.

Selected pellets from each condition were examined using x-ray diffraction and scanning electron microscopy. Several SEM micrographs of the sintered surfaces are shown in figure 19. The microstructure of the sintered surface of ceramics sintered at 1300°C and 1350°C were similar. The grain size was less than $0.5 \mu\text{m}$ and many fine pores were observed, consistent with the measured density. These ceramics showed no signs of any second phase by SEM but it was hard to tell because of the large amount of porosity. When the temperature was increased to 1400°C the microstructure was less porous, the grains were approximately $1 \mu\text{m}$ and there were some signs of second phase. The second phase consisted of small crystals that contain mostly Zn and Ga. These crystals could be imaged in backscatter and were very small ($<0.5 \mu\text{m}$) and difficult to identify. As the temperature was increased to 1450°C and 1500°C the crystals of second phase became much more evident (larger) and there seemed to be an increased number of

them. And when the temperature reached 1600°C the crystals were easily identified and some of them were very large (>20 μm). (There was only one pellet sintered at 1600°C and therefore it was not included on the graphs showing the density and Q-factor.)

The x-ray analysis showed only BMT peaks (82-0371) for most of the ceramics. In some of the patterns there were small second phase peaks or what must be from a second phase. These peaks were identified as either ZnGa₂O₄ (71-0843) or Ba₃Ta₅O₁₅ (83-0713). The ZnGa₂O₄ could have formed from a reaction between the ZnO and Ga₂O₃ therefore the zinc and gallium rich second phase is thought to be zinc gallate. The Ba-Ta phases can form from MgO evaporation. A typical pattern is shown in figure 20 with the second phases marked.

5.1.3 Ceramics Sintered Isothermally at 1350oC

BMT doped with 8mol% ZnO and Ga₂O₃ was isothermally sintered at 1350°C from no dwell time up to 24 hours. This temperature was chosen to allow the kinetics of isothermal sintering to be investigated. Sintering to full density would probably be done above 1400°C. The commonly used semi-log plot is shown in figure 21 and has an R² value of 0.9737. From 0 time to 2 hours the density increases linearly and then begins to level off. Between 2 hours and 6 hours the density is statistically the same at 86.5% ± 5.5 and 90.8 % ± 1.8. For 6, 10 and 24 hours there is little difference in the density (90.8 % ± 1.8, 89.8% ± 1.8, and 93.8 % ± 1.2). The Q*f verses time is shown in figure 22. The Q-factor reaches a maximum at 10 hours with Q*f equal to 142,907 GHz ± 2,770 GHz. The large change in the Q-factor again seems to correlate

with reaching relative densities above 90%. This further supports the hypothesis that isolated porosity is a major requirement for high Q-factors and low dielectric losses.

Selected pellets from each condition were examined using x-ray diffraction and scanning electron microscopy. Several SEM micrographs of the sintered surfaces are shown in figure 23. Micrographs for samples sintered at 0 time and 1 hour were very porous with the average grain size less than $1\mu\text{m}$; there were no signs of any second phases. At 2 hours the microstructure looked less porous with an average grain size of about $1\mu\text{m}$ and there were some second phases of Zn-Ga rich crystals as mentioned in the last section. At sintering times of 6, 10 and 24 hours the micrographs looked very similar. There were more Zn-Ga crystals and they were larger. In samples sintered for 2 hours the Zn-Ga crystals were less than $0.5\ \mu\text{m}$, and in the samples sintered for the longer times the crystals were $2\ \mu\text{m}$ or larger. Figure 24 shows the fracture surface of a pellet sintered at 1350°C for 24 hours. The fracture goes through the BMT grains (intergranular) and around the second phase crystals (transgranular). The second phase crystals appear to be growing out of the BMT solid and there are no pores around crystals. This suggests that the zinc gallate crystals nucleate and grow in the solid-state.

The x-ray analysis showed only BMT peaks for 0 time and 1 hour. In all of the longer times there were some very small second phase peaks. These peaks were identified as either ZnGa_2O_4 or $\text{Ba}_3\text{Ta}_5\text{O}_{15}$. As mentioned earlier, ZnO and Ga_2O_3 can react to form ZnGa_2O_4 and MgO can evaporate to form a Ba-Ta rich phase. The intensities of these peaks varied slightly from pellet to pellet even when sintered at the same condition. A typical pattern is shown in figure 25. The second phase peaks are marked appropriately. The pellet shown was sintered at 1350°C for 24 hours; both the top and bottom of the sintered surfaces of the pellet are similar.

5.1.4 Ceramics Sintered at Various Temperatures for 2 hours

BMT co-doped with 8mol% ZnO and Ga₂O₃ was sintered at various temperatures between 1300°C and 1600°C for 2 hours. Two hours was chosen because it is a desirable sintering time for manufacture. This also allowed the samples to equilibrate more than in the constant heating rate work. The graph of temperature versus density is shown in figure 26. The density increases linearly up to 1400°C to a density of 94.5% ± 0.5 and then drops slightly at 1450°C to 93.9% ± 1.2. As the temperature increases to 1500°C and 1550°C the density remains about constant at 93.2% ± 0.7 and 93.4% ± 0.7. At 1600°C the density drops slightly to 89.6% ± 3.2. Compared to the constant heating rate work the temperature interval in which densification accelerates is shifted to lower temperatures as expected. The plot for Q*f versus temperature is shown in figure 27. The Q-factor increases rapidly from 1300°C to 1350°C (although the error is quite large for the pellets sintered at 1350°C), and then increases much slower between 1350°C and 1500°C. Between 1550°C and 1600°C there is a slight drop in the Q-factor from 139,565 GHz ± 8,762 to 97,737 ± GHz 6,756. Therefore the relationship of temperature with the Q-factor and temperature with density are similar. The results are still consistent with high Q-factors requiring closed pores.

Selected pellets from each condition were examined using x-ray diffraction and scanning electron microscopy. The micrographs from these ceramics are very similar to those that were sintered for 0 time at the same temperatures. The second phase of Ga-Zn rich crystals did appear at 1400°C instead of 1450° where they first became evident in the samples sintered at 0 time. This is consistent with what would be expected if the system is equilibrating during the sintering process and Ga-Zn crystals are nucleating and growing. Another difference was in the samples

sintered at 1600°C. The sintered surface of these ceramics varied from one part to another and also between the different sides of the pellet. Several of these micrographs are shown in figure 28. Some micrographs showed very dense BMT with no second phases (b), some showed very large (some >10µm) second phase crystals (Zn-Ga) (f), and some showed much the same microstructure as was seen previously (e). There was no evidence of any Ba-Ta phases in these samples. There also seemed to be some cracking in the parts of the microstructure with large amounts of the crystals.

XRD analysis showed similar results to those obtained when the sintering time was 0 hours. The small second phase peaks did occur earlier, at 1350°C. A typical pattern is shown in figure 29. The samples sintered at 1600°C for 2 hours were different than the one sintered for 0 time at the same temperature. The pattern showed very large second phase peaks of ZnGa₂O₄ on the bottom and very small peaks on the top. A sample pattern is shown in figure 30. This suggests that the Zn-Ga rich crystals grow and may segregate to certain surfaces, due to non-wetting behavior. This will be discussed later.

5.2 Comparing the Concentration of ZnO and Ga₂O₃ on the Sintering and Microwave Dielectric Properties of BMT

BMT was co-doped with 4mol% and 8mol% ZnO and Ga₂O₃. Both were added before the first ball milling step in the synthesis. These ceramics were sintered at 1400°C for 2 hours and 1500°C for 2 hours. At both of these temperatures the densities were slightly higher in the BMT doped with 4mol% ZnO and Ga₂O₃. At a sintering temperature of 1400°C for 2 hours the

densities were $94.5\% \pm 0.5$ and $95.2\% \pm 0.9$; and at a sintering temperature of 1500°C for 2 hours the densities were $93.2\% \pm 0.73$ and $96.1\% \pm 0.7$. Although the density was higher in the BMT doped with 4mol% ZnO and Ga_2O_3 the Q^*f values were higher for the BMT doped with 8mol% ZnO and Ga_2O_3 at both sintering temperatures. The Q^*f values at a sintering temperature of 1400°C for 2 hours were $129,041 \text{ GHz} \pm 4,614 \text{ GHz}$ and $126,102 \text{ GHz} \pm 5,141 \text{ GHz}$; and at a sintering temperature of 1500°C for 2 hours the Q^*f 's were $151,595 \text{ GHz} \pm 1,918 \text{ GHz}$ and $130,936 \text{ GHz} \pm 4,526 \text{ GHz}$. A graph comparing the Q-factors at both concentrations and sintering temperatures are shown in figure 31. This shows that the difference at 1400°C was not significant but at 1500°C the difference is more pronounced.

Selected pellets from each of these conditions were examined using x-ray diffraction and scanning electron microscopy. SEM micrographs showed second phases of crystals that were rich in Zn and Ga for both compositions and sintering conditions. These crystals are the same as the Zn-Ga rich crystals discussed earlier. Typical SEM micrographs from each condition are shown in figure 32. The Zn-Ga rich crystals appear darker than the “normal” BMT grains in the images obtained from the backscattered electrons. The BMT doped with 4mol% ZnO and Ga_2O_3 and sintered at 1500°C for 2 hours also showed long, cylindrical second phases that are rich in barium and tantalum. These second phases are only seen on the top of the pellets. The XRD confirms these findings showing large second phase peaks on the tops of these pellets. A typical XRD pattern is shown in figure 33. These second phase peaks also appear on the bottom of the pellets but are very small. These peaks were identified as $\text{Ba}_3\text{Ta}_5\text{O}_{15}$ (83-0713), which would be consistent with MgO evaporation. Not all of the intensities match exactly with the JCPDS patterns but this can happen when the grains/crystals are not randomly oriented when they grow on the surface. The surfaces of a pellet sintered at 1500°C for 2 hours were removed to try and

remove the Ba-Ta phases. These XRD patterns are shown in figure 34; the second phase peaks disappeared almost completely. The removal of these phases lowered the Q-factor from 27,834 to 25,917, although this could be due to surface grinding. The XRD patterns for the pellets sintered at 1400°C for 2 hours showed small second phase peaks similar to the bottom of the pellets sintered at 1500°C for 2 hours. A typical XRD pattern for BMT doped with 8mol% ZnO and Ga₂O₃ is shown in figure 35. The patterns for both conditions are the same along with both sides of the pellets. The patterns showed all of the BMT peaks and some small second phase peaks. These peaks correspond to Ba₃Ta₅O₁₅ (83-0713), which can form from MgO evaporation and ZnGa₂O₄ (71-0843), which can form through the reaction of ZnO and Ga₂O₃. The intensities of the small second phase peaks varied slightly from batch to batch, almost disappearing in some cases. The results are consistent with more MgO evaporation and barium tantalate formation on the surface of 4mol% ZnO and Ga₂O₃. The effect of the sintering additive on this is unclear but could be due to Zn dissolution.

5.3 Comparing the Effect of Several Similar Dopants (ZnO and Ga₂O₃; Ga₂O₃; ZnO and ZnGa₂O₄) on BMT Sintered at 1450°C for 2 hours

BMT was doped with several variations of zinc oxide and gallium oxide to determine the effect of each dopant. BMT was doped with 8mol% of each of the following: ZnO and Ga₂O₃; Ga₂O₃; ZnO; and ZnGa₂O₄. The ZnO and Ga₂O₃ were added before the first ball milling of the BMT; the ZnGa₂O₄ was added after the BMT calcination step in the synthesis. Figure 36 shows a graph comparing the Q*f values and the densities. It is clear that the BMT doped with ZnO

and Ga_2O_3 has the highest Q^*f at $135,164 \text{ GHz} \pm 17,825 \text{ GHz}$ although it also had the lowest density at $93.9\% \pm 1.2$. The BMT doped with Ga_2O_3 and with ZnGa_2O_4 had Q^*f 's of $84,391 \text{ GHz} \pm 4,313 \text{ GHz}$ and $93,743 \pm 33,520 \text{ GHz}$ even though they both had average densities over 95%. (BMT doped with Ga_2O_3 had a density of $95.2\% \pm 0.6$ and BMT doped with ZnGa_2O_4 had a density of 95.2 ± 0.6 .)

SEM micrographs of the BMT doped with 8mol% ZnO and Ga_2O_3 and sintered at 1450°C for 2 hours showed Zn-Ga rich second phase crystals as described before. This is shown in figure 37. These crystals appear to be zinc gallate that can form from a reaction between the ZnO and Ga_2O_3 . As mentioned earlier, when the fracture surface is examined, the fracture goes through the BMT grains and around the Zn-Ga rich crystals. Another important finding was that there are no pores around the second phase crystals. As would be expected given the density results the microstructures show more porosity than the ceramics with the other dopants sintered at the same conditions. The XRD patterns looked similar to samples sintered at 1500°C for 2 hours and shown in figure 29. The patterns show all of the BMT peaks and small second phase peaks which are indicated. The small second phase peaks correspond to zinc gallate (38-1240).

SEM micrographs of BMT doped with 8mol% Ga_2O_3 showed plate-like second phase crystals. These appear darker in the backscatter image and can be seen clearly in figure 38. When a fracture surface was examined using SEM, the fracture went around the Ga-rich second phase and through the BMT grain; there was no surrounding porosity. According to EDS, these are rich in gallium. The XRD of both sides of the pellets are shown in figure 39. The patterns show all of the BMT peaks and a few very small second phase peaks. These peaks are slightly larger on the top of the pellets. These small second phase peaks correspond to gallium oxide (38-1240).

SEM micrographs of BMT doped with 8mol% ZnGa_2O_4 and sintered at 1450°C for 2 hours is shown in figure 40. This micrograph shows two different second phases: long, cylindrical second phases that are rich in Ba and Ta; and groups of crystals that are rich in Zn and Ga. These crystals appear darker when viewing the backscatter image. The Zn-Ga rich crystals appear to be the same crystals that are seen on BMT doped with ZnO and Ga_2O_3 . When the fracture surface was examined it looked like the fracture surface of the BMT doped with 8mol% ZnO and Ga_2O_3 . The fracture went through the BMT grains and around the Zn-Ga rich second phases; there was no surrounding porosity. There were also no signs of any Ba-Ta rich phases on the interior surfaces, confirming that these phases were formed by the evaporation MgO. The XRD patterns of both sides are shown in figure 41. All of the BMT peaks are present and both sides show large second phase peaks; the peaks on the top are larger. The second phase peaks seem correspond to two different second phases, zinc gallate and barium tantalate ($\text{Ba}_3\text{Ta}_5\text{O}_{15}$). The peak intensities do not match exactly but this can be caused when the crystal are not oriented randomly when they grow on the surface.

5.4 Overall Effect of Density on the Q-factor

Figure 42 shows a plot of $Q \cdot f_0$ verses density for all of the pellets produced. With the exception of series four there is a clear increase in the Q-factor when the density is above about 90% of the theoretical density. This is most likely when the pores of the ceramics are all closed off preventing water moisture from getting into the samples. Water strongly absorbs microwaves, which can significantly increase the losses.

5.5 Effect of Additives and Process Condition on Ordering

In all the XRD patterns, the largest superlattice peak has been marked with an asterisk. These peaks are very small compared with the largest BMT peak indicating that there is very little ordering occurring in the samples or that the antiphase domains are too small to be detected by XRD.

5.6 The Effect of Additives and Processing Condition on the Dielectric Constant

The dielectric constant was measured on a couple of pellets from each condition to be sure that it was not being adversely affected. None of the dopants severely (<24) decreased the dielectric constant of BMT; BMT normally has a dielectric constant of approximately 25.

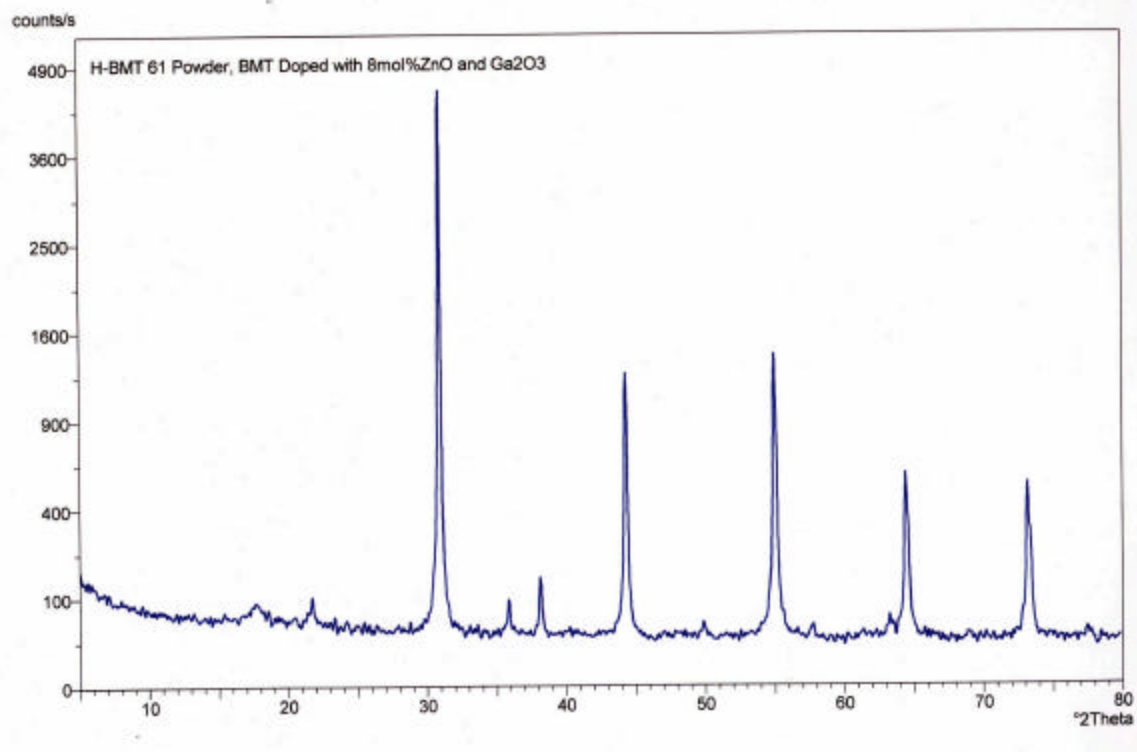


Figure 16 X-ray diffraction pattern of calcined BMT powder doped with 8mol% ZnO and Ga₂O₃. This pattern shows only BMT peaks and no superlattice peaks.

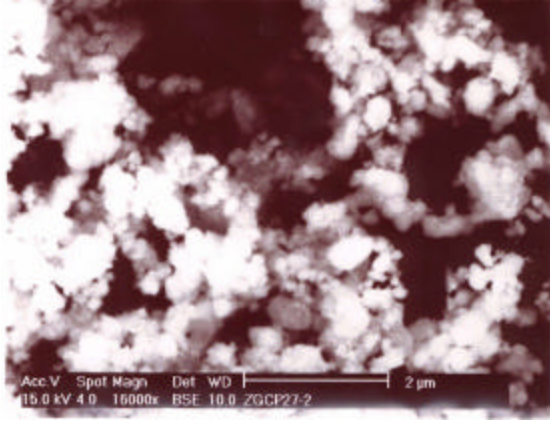


Figure 17 SEM micrograph of calcined BMT powder doped with 8mol% ZnO and Ga₂O₃. There is no evidence of any second phases.

Constant Heating Rate for BMT Doped with 8mol% ZnO and Ga₂O₃

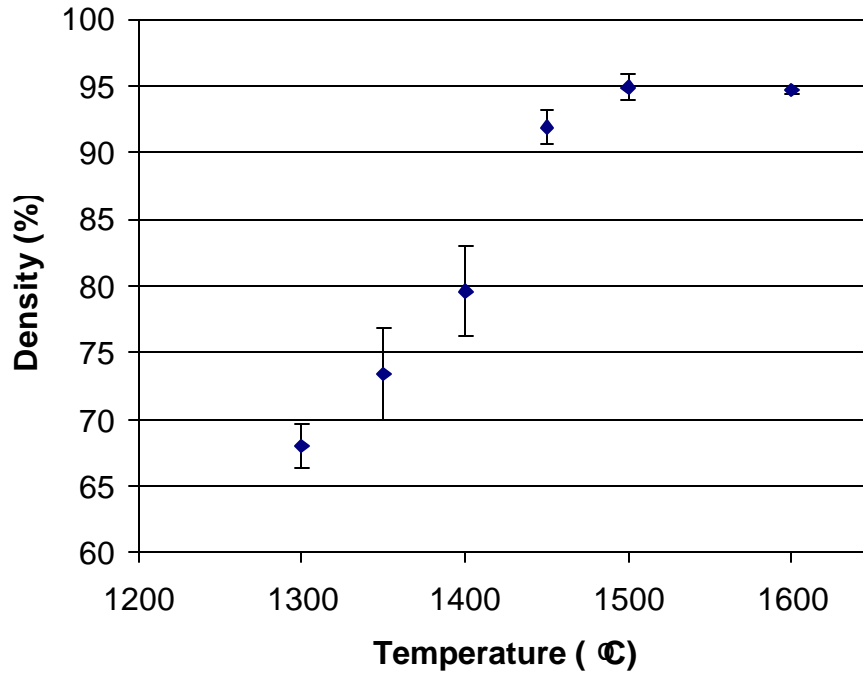


Figure 18 The density Vs sintering temperature for BMT co-doped with 8mol% ZnO and Ga₂O₃ and sintered at a constant heating rate of 10°C/min.

**Constant Heating Rate of 10 C/ min. of BMT Doped
with 8mol% ZnO and Ga₂O₃**

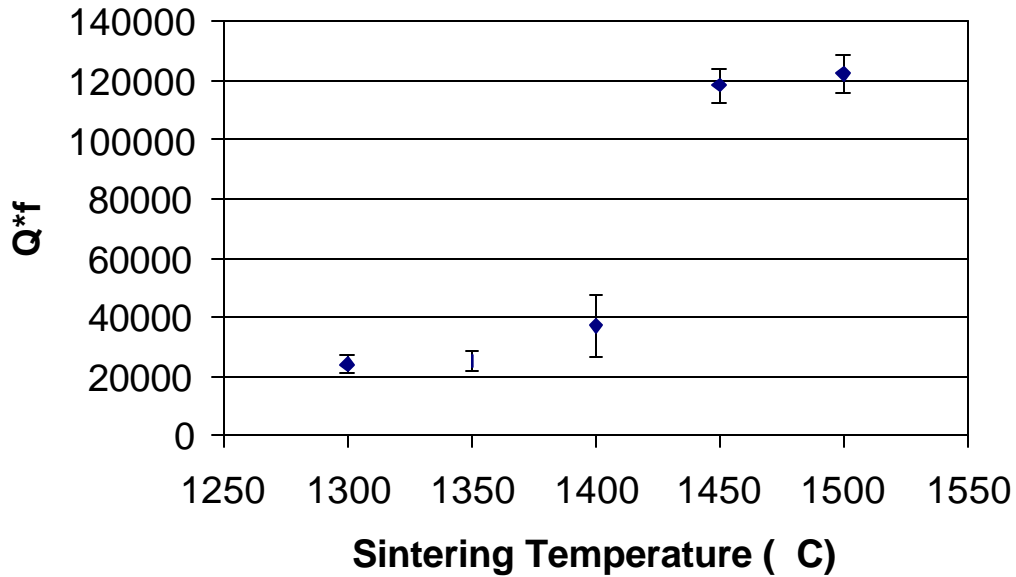


Figure 19 The $Q \cdot f$ vs sintering temperature for BMT doped with 8mol% ZnO and Ga₂O₃ and sintered at a constant heating rate of 10°C/min. The largest increase in Q-factor was between the temperatures of 1400°C and 1450°C; this corresponds to densities where the pores would be closing off. (The resonant frequency for these pellets was approximately 4.9 GHz.)

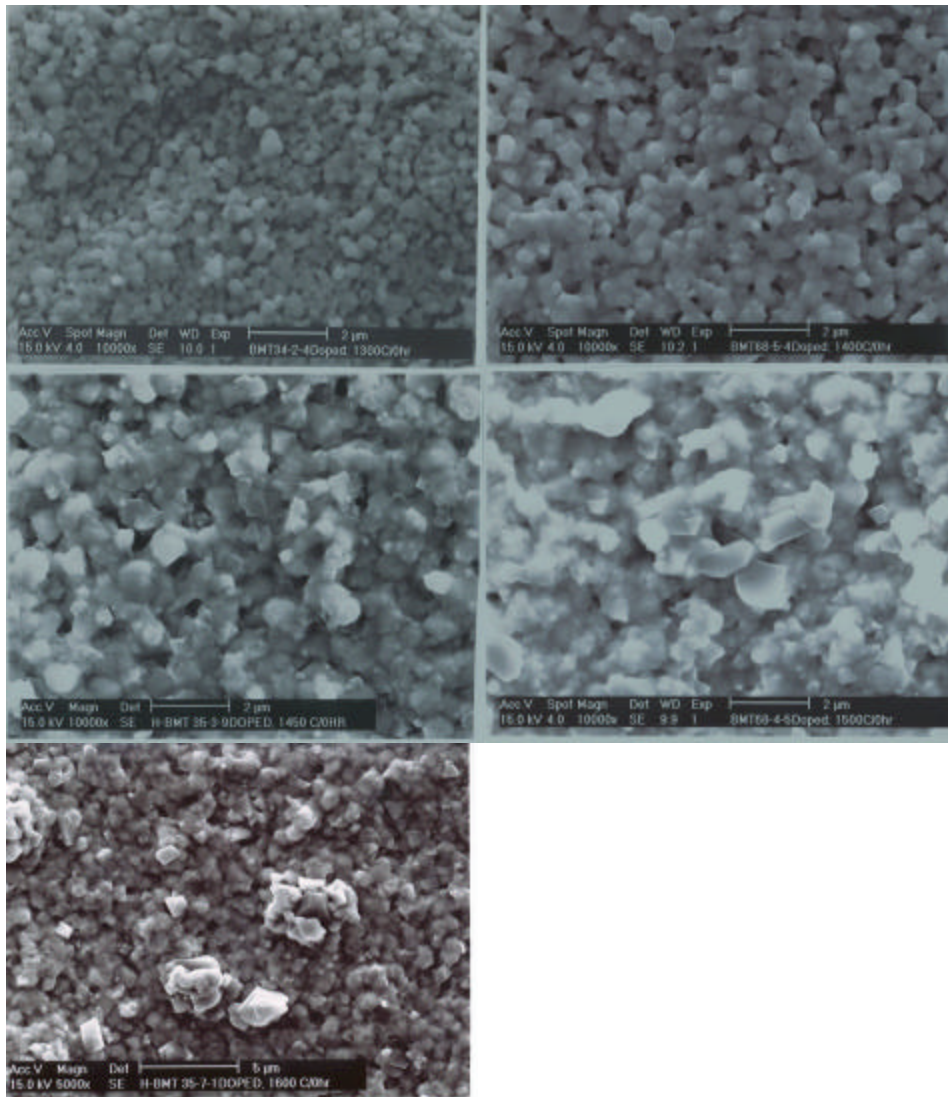


Figure 20 Selected SEM micrographs of BMT doped with 8mol% ZnO and Ga₂O₃ and sintered at a constant heating rate of 10^oC/min. Some of the zinc and gallium rich second phase has been circled. The only pellet shown that did not show any evidence of Zn and Ga rich second phase is shown in figure (a) and was sintered at 1300^oC for 0 hours. The pellets were also sintered at 1400^oC for 0 hours (b), 1450^oC for 0 hours (c), 1500^oC for 0 hours (d), and 1600^oC for 0 hours(e).

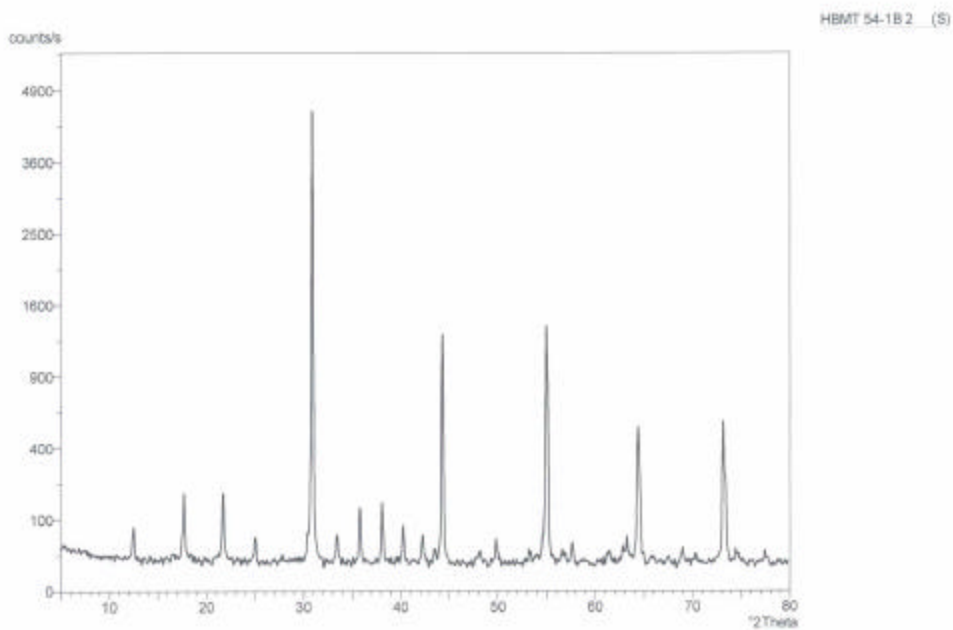


Figure 21 An XRD pattern of BMT doped with 8mol% ZnO and Ga₂O₃ and sintered at a constant heating rate of 10°C per minute increasing to 1500oC and then immediately decreasing at 10° per minute to room temperature.

Figure 6 Density Vs. Sintering Time for BMT Doped iwth 8mol% ZnO and Ga2O3 and Sintered at 1350C

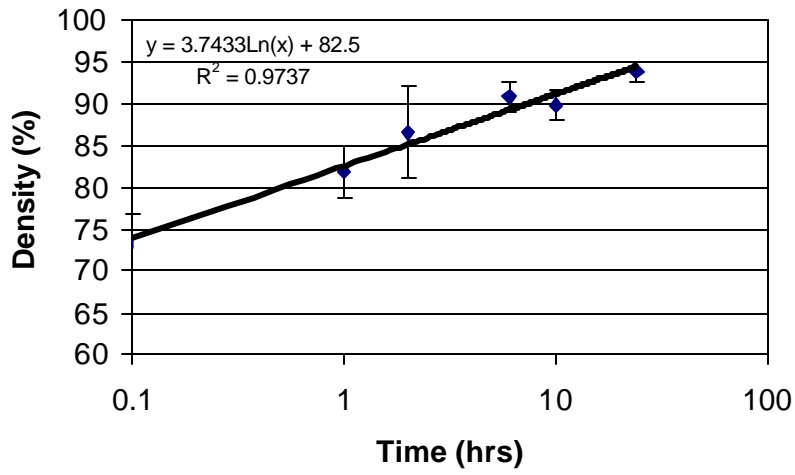


Figure 22 The density vs. sintering time for BMT doped with 8mol% ZnO and Ga₂O₃ and sintered at 1350°C

Isothermal Sintering at 1350 C for BMT Doped with 8mol% ZnO and Ga₂O₃

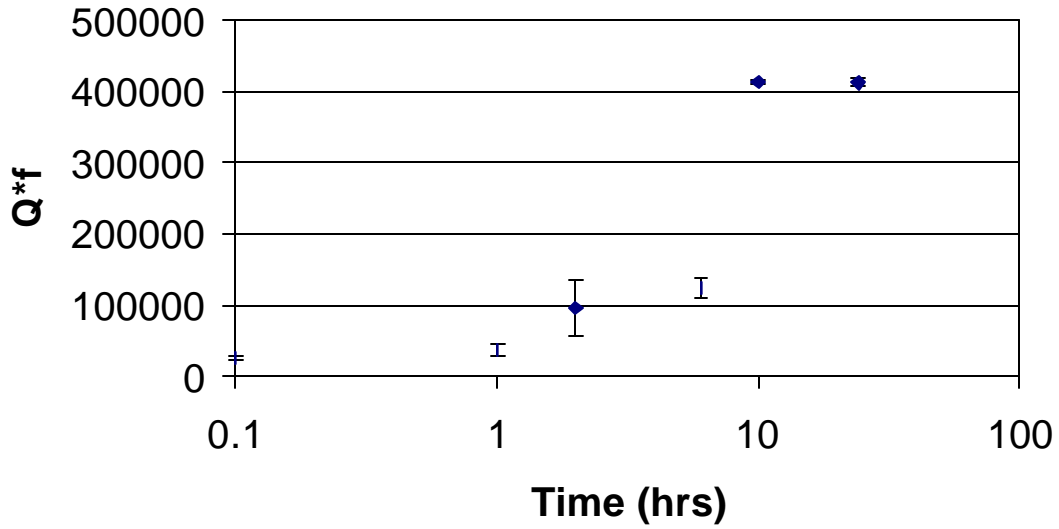


Figure 23 The $Q \cdot f$ vs. sintering time for BMT doped with 8mol% ZnO and Ga₂O₃ and sintered at 1350°C (The resonant frequency for these pellets was approximately 4.9 GHz.)

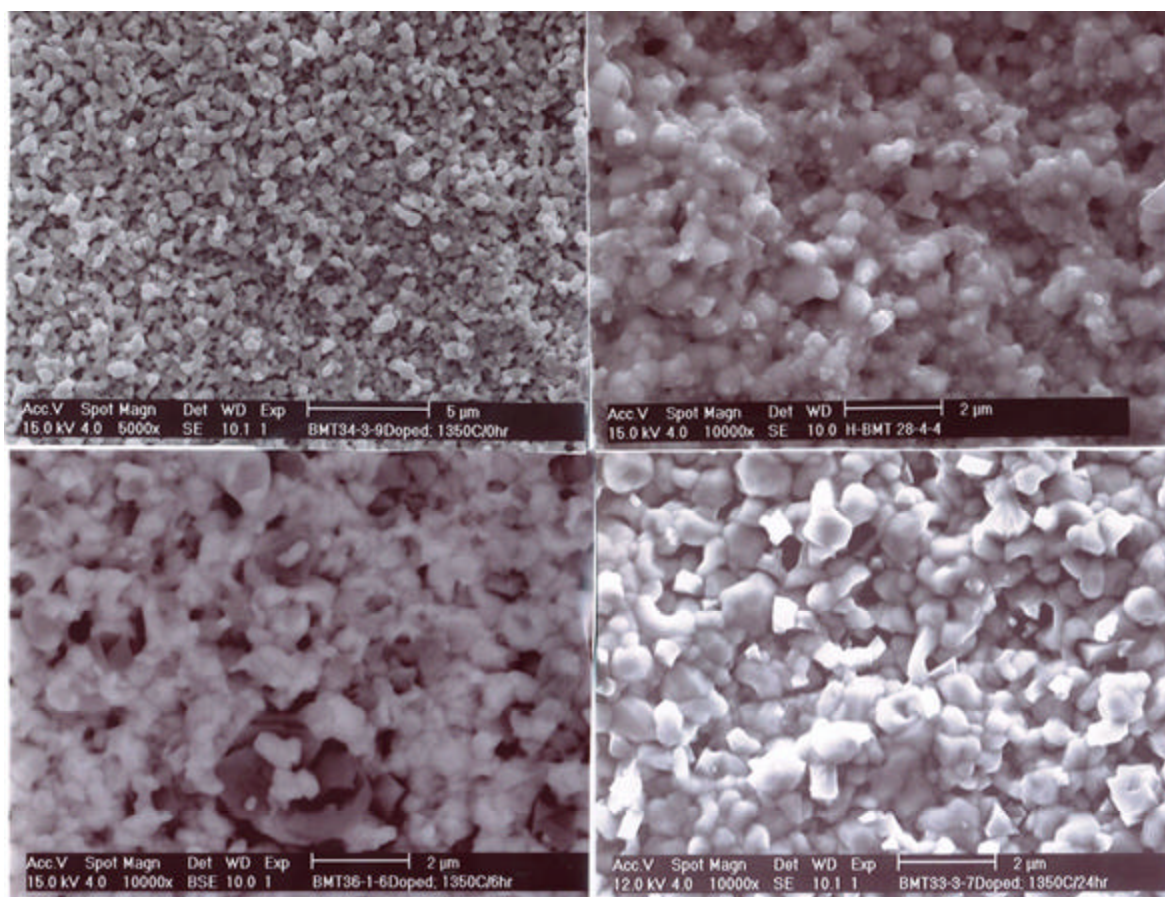


Figure 24 Selected SEM micrographs of sintered surfaces of BMT doped with 8mol% ZnO and Ga₂O₃ and sintered isothermally at 1350°C. Some of the zinc and gallium rich second phase has been circled. The pellet shown in micrograph (a) has been sintered at 1350°C for 0 hours and shows no evidence of any Zn and Ga rich second phase. The pellet shown in micrograph (b) has been sintered at 1350°C for 2 hours, (c) has been sintered at 1350°C for 6 hours. Micrograph (c) was taken using the backscattered electrons and therefore the Zn and Ga rich crystals appear darker than the BMT grains. And the pellet shown in micrograph (d) has been sintered at 1350°C for 24 hours.

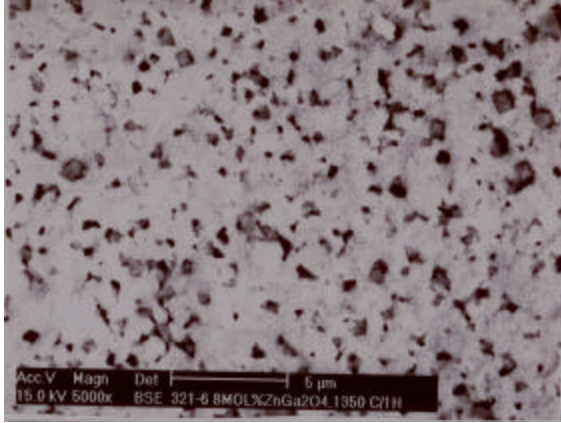


Figure 25 A SEM micrograph of a fracture surface of BMT doped with 8mol% ZnO and Ga₂O₃ and sintered at 1350°C for 1 hour. Some of the Zn and Ga rich second phase has been circled.

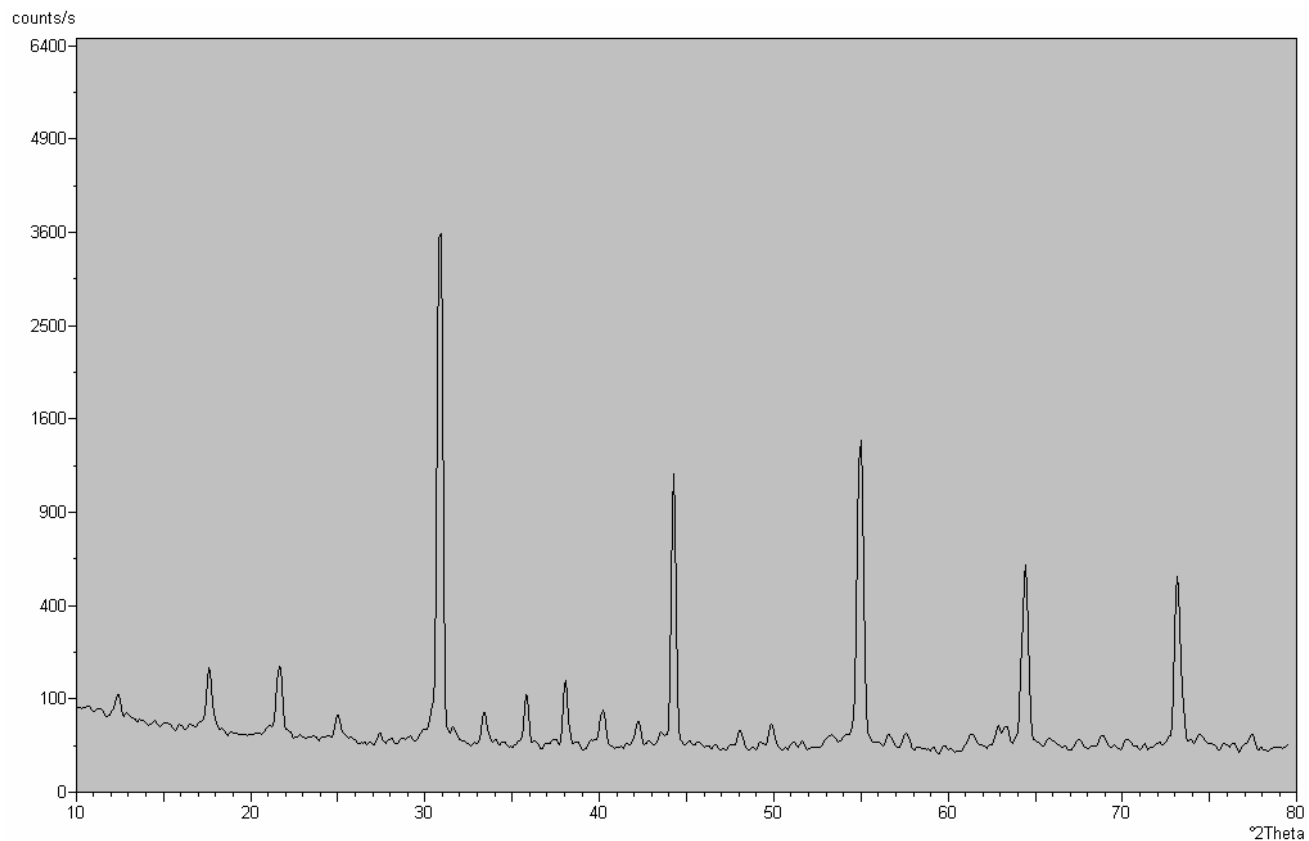


Figure 26 A typical pattern from BMT doped with 8mol% ZnO and Ga₂O₃. This particular pattern came from a sample sintered at 1350°C/24hr. The circles peak has been identified as the start of barium tantalite. All other peaks have been identified as BMT peaks.

BMT Doped

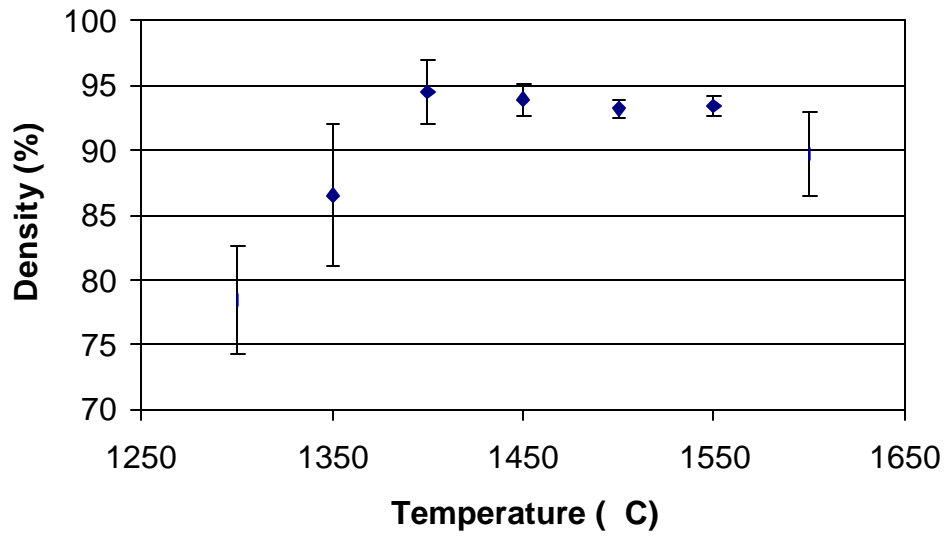


Figure 27 A graph of Density vs. Sintering Temperature (time=2 hrs) for BMT Doped with 8mol% ZnO and Ga₂O₃.

BMT Doped with 8mol% ZnO and Ga₂O₃ Sintered at Various Temperatures for 2 hours

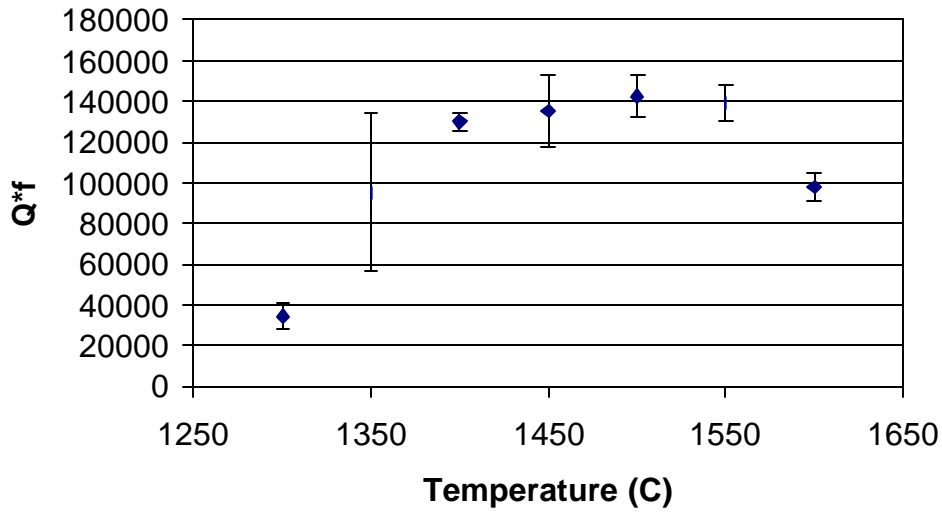


Figure 28 The $Q \cdot f$ vs. sintering temperature (time=2 hrs) for BMT doped with 8mol% ZnO and Ga₂O₃. (The resonant frequency was approximately 4.9 GHz.)

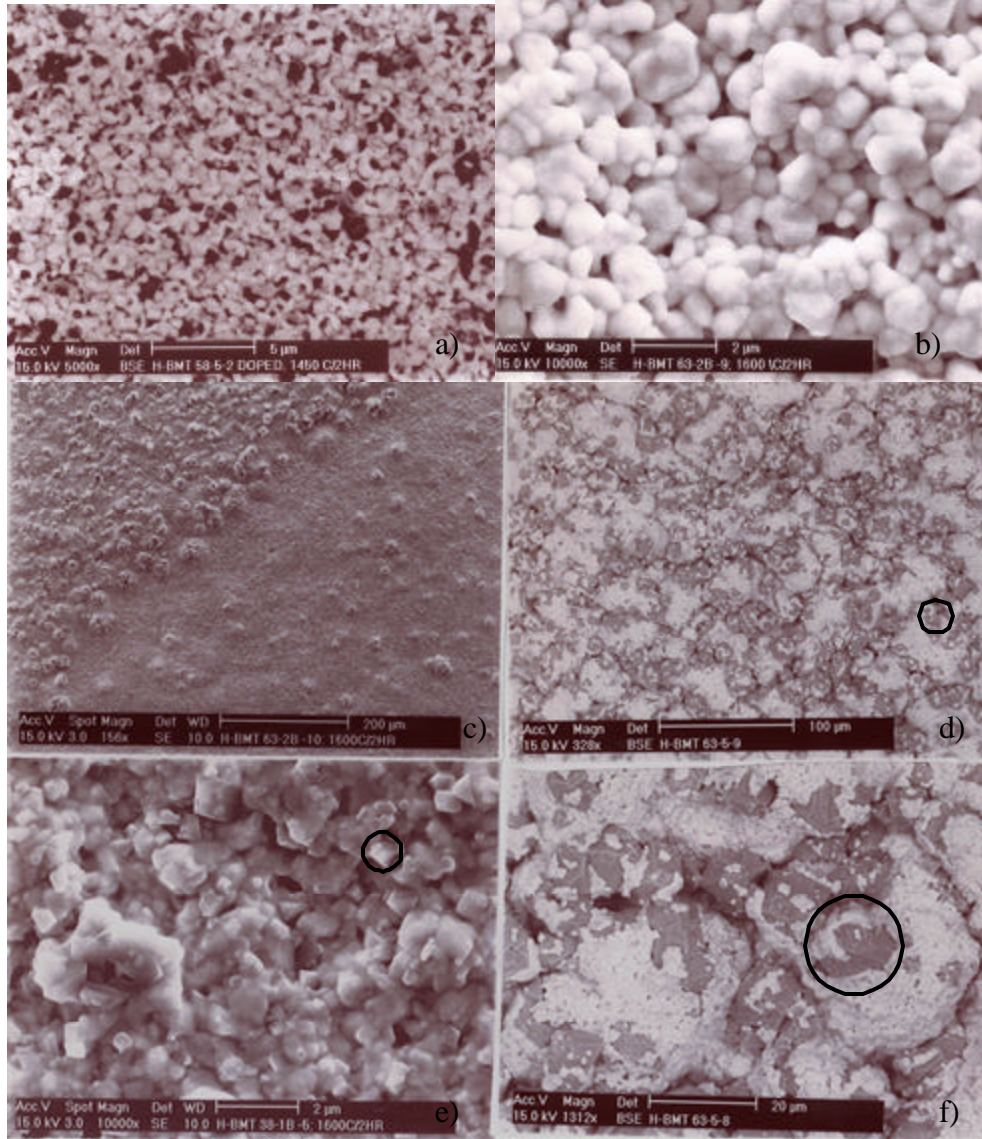


Figure 29 Selected SEM micrographs of BMT doped with 8mol% ZnO and Ga₂O₃ and sintered at various temperatures for 2 hours. Some of the zinc and gallium rich second phase has been circled. Micrograph a) has been sintered for 1450°C for 2 hours and is imaged by the backscattered electrons. Micrographs b) through f) have been sintered for 1600 °C for 2 hours.

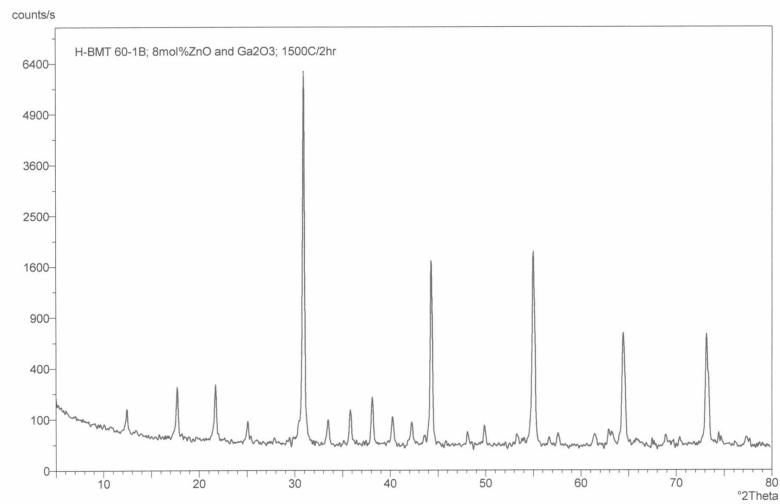


Figure 30 An XRD pattern of BMT doped with 8mol% ZnO and Ga₂O₃ and sintered at 1500°C for 2 hours. The largest superlattice peak has been marked with an arrow.

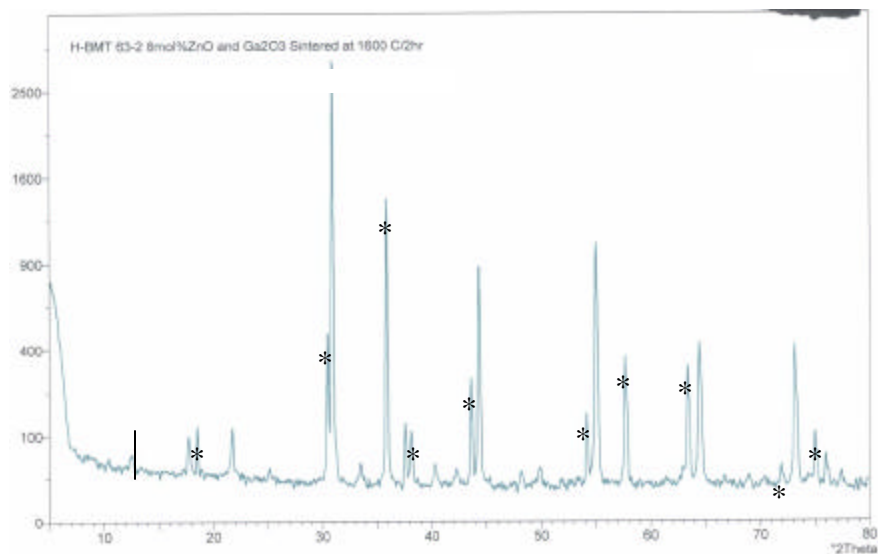


Figure 31 An XRD pattern of BMT doped with 8mol% ZnO and Ga₂O₃ and sintered at 1600°C for 2 hours. This was taken on the top of the pellet; the bottom has the same peaks with the second phase peaks smaller. The zinc gallate peaks have been marked with an asterisk and the largest super lattice peak has been marked with an arrow.

Comparing the Concentration of ZnO and Ga₂O₃ Doped BMT

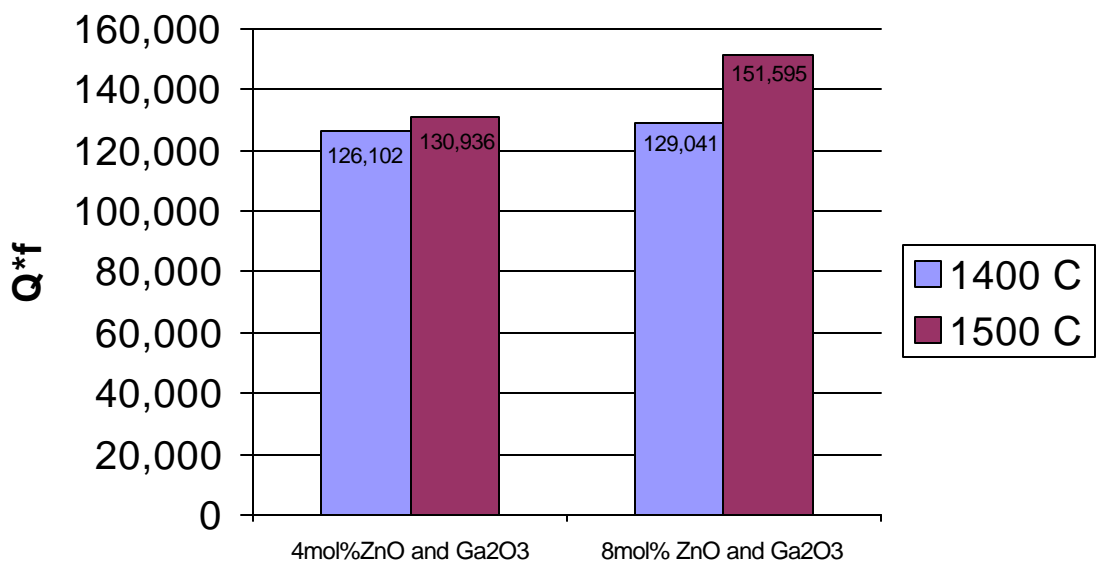


Figure 32 A Comparison of the Q*f of 4mol% and 8mol% ZnO and Ga₂O₃ doped BMT. Although the BMT doped with 4mol% had slightly higher densities, the Q-factors were both higher in the BMT doped with 8mol% ZnO and Ga₂O₃.

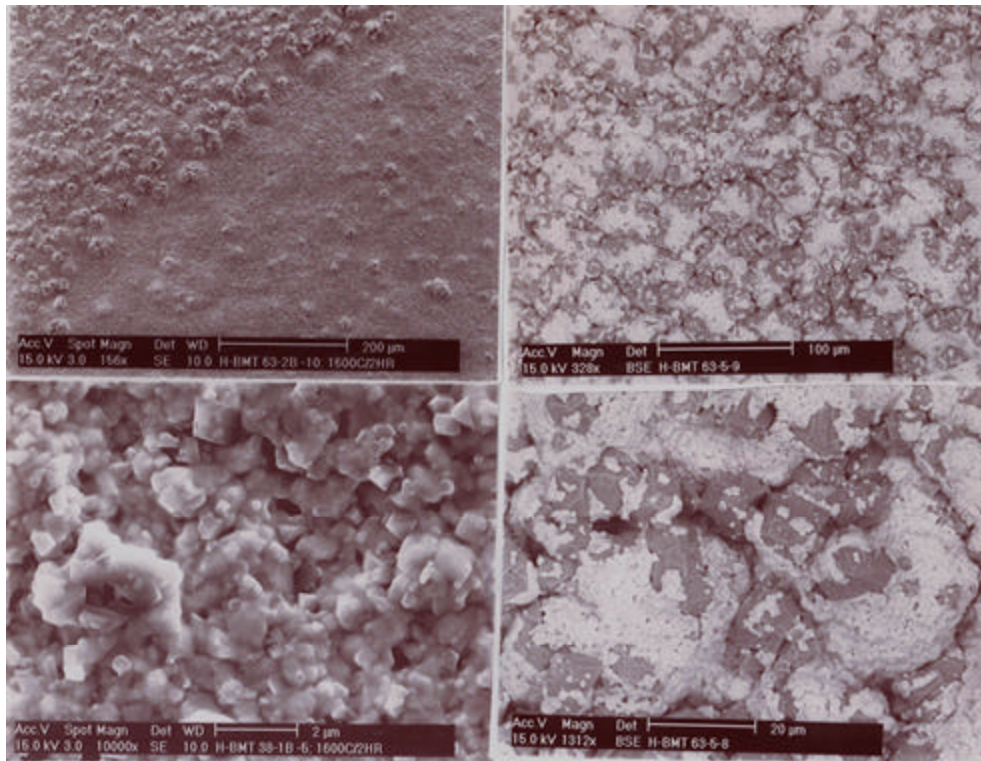


Figure 33 Selected SEM micrographs of BMT doped with 4mol% (a) and b)) and 8mol% (c) and d)) ZnO and Ga₂O₃. Micrographs a) and c) have been sintered at 1400°C for 2 hours and micrographs b) and d) have been sintered at 1500°C for 2 hours. Some of the zinc and gallium rich second phase has been circled and the barium and tantalum rich second phase is indicated by a rectangle.

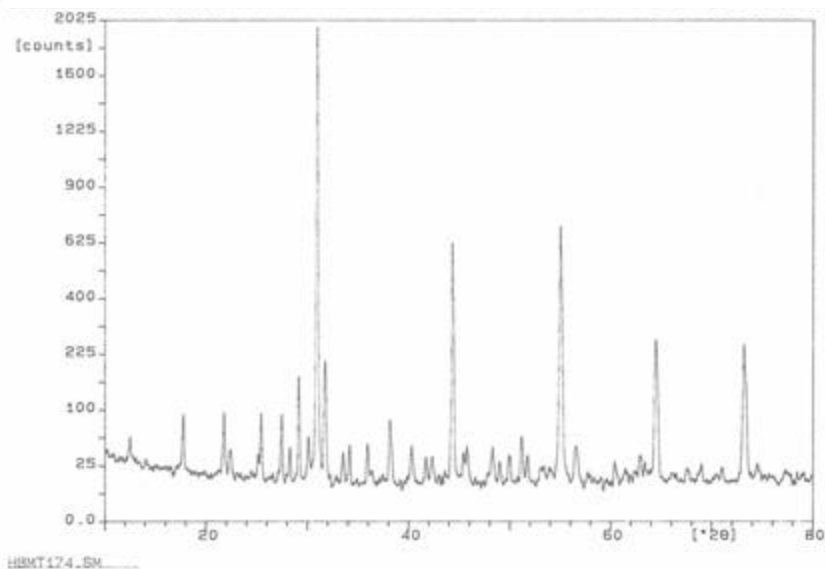


Figure 34 XRD pattern of the top of a sintered pellet of BMT doped with 4mol% ZnO and Ga₂O₃. The barium tantalate second phase peaks have been circled and the largest superlattice peak has been marked with an arrow.

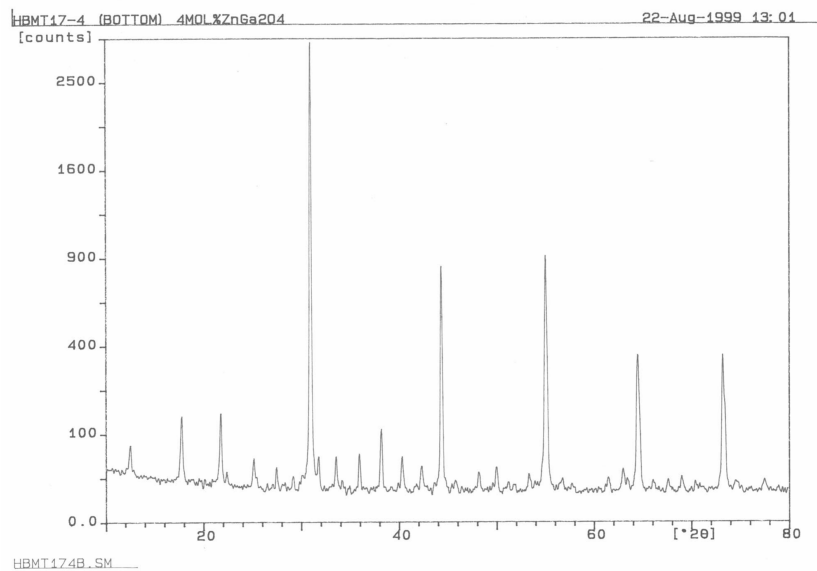


Figure 35 An XRD pattern of the bottom of a pellet doped with 4mol% ZnO and Ga₂O₃ and sintered at 1500°C for 2 hours.

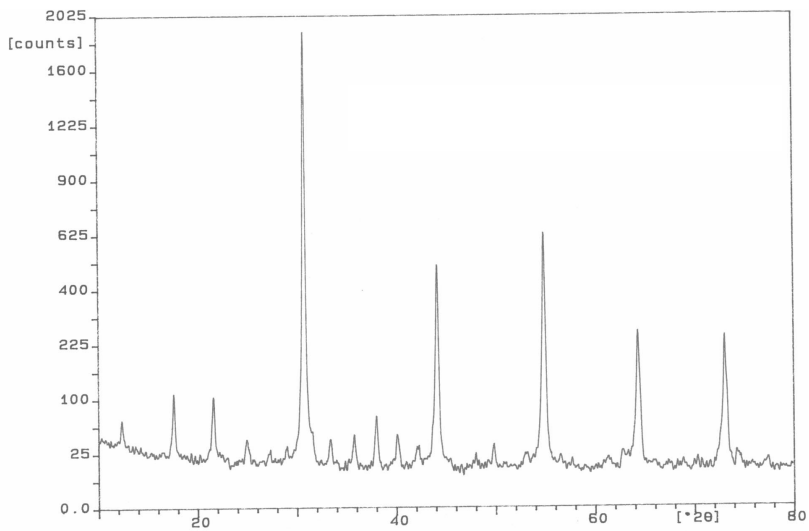


Figure 36 An XRD of the top of a pellet of BMT doped with 4mol% ZnO and Ga₂O₃ and sintered at 1500°C for 2 hours with the outer surface removed.

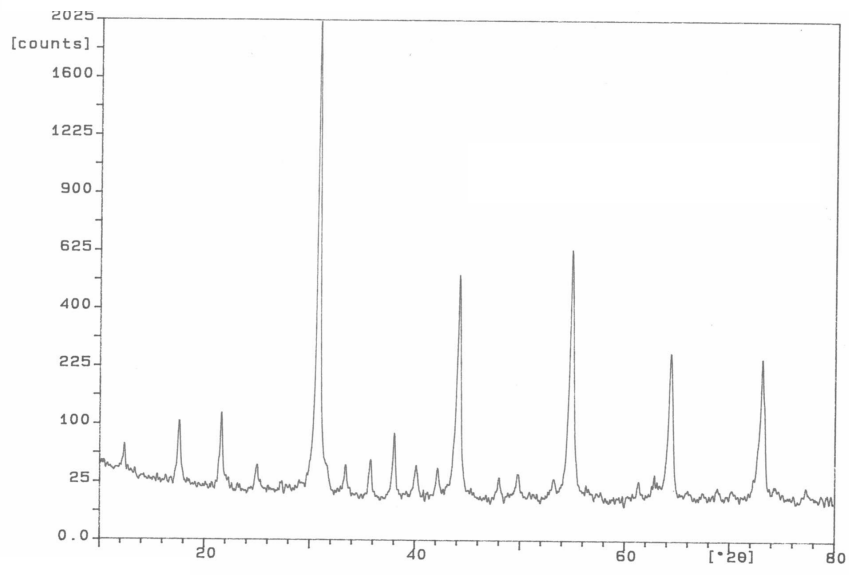


Figure 37 An XRD of the bottom of a pellet of BMT doped with 4mol% ZnO and Ga₂O₃ and sintered at 1500°C for 2 hours with the outer surface removed.

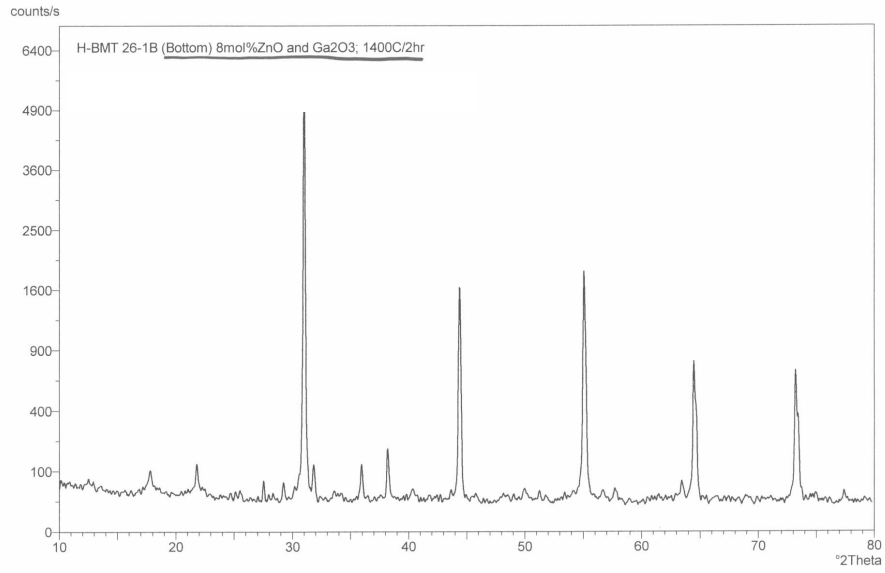


Figure 38 An XRD pattern of a BMT pellet doped with 8mol% ZnO and Ga₂O₃ and sintered at 1400°C for 2 hours.

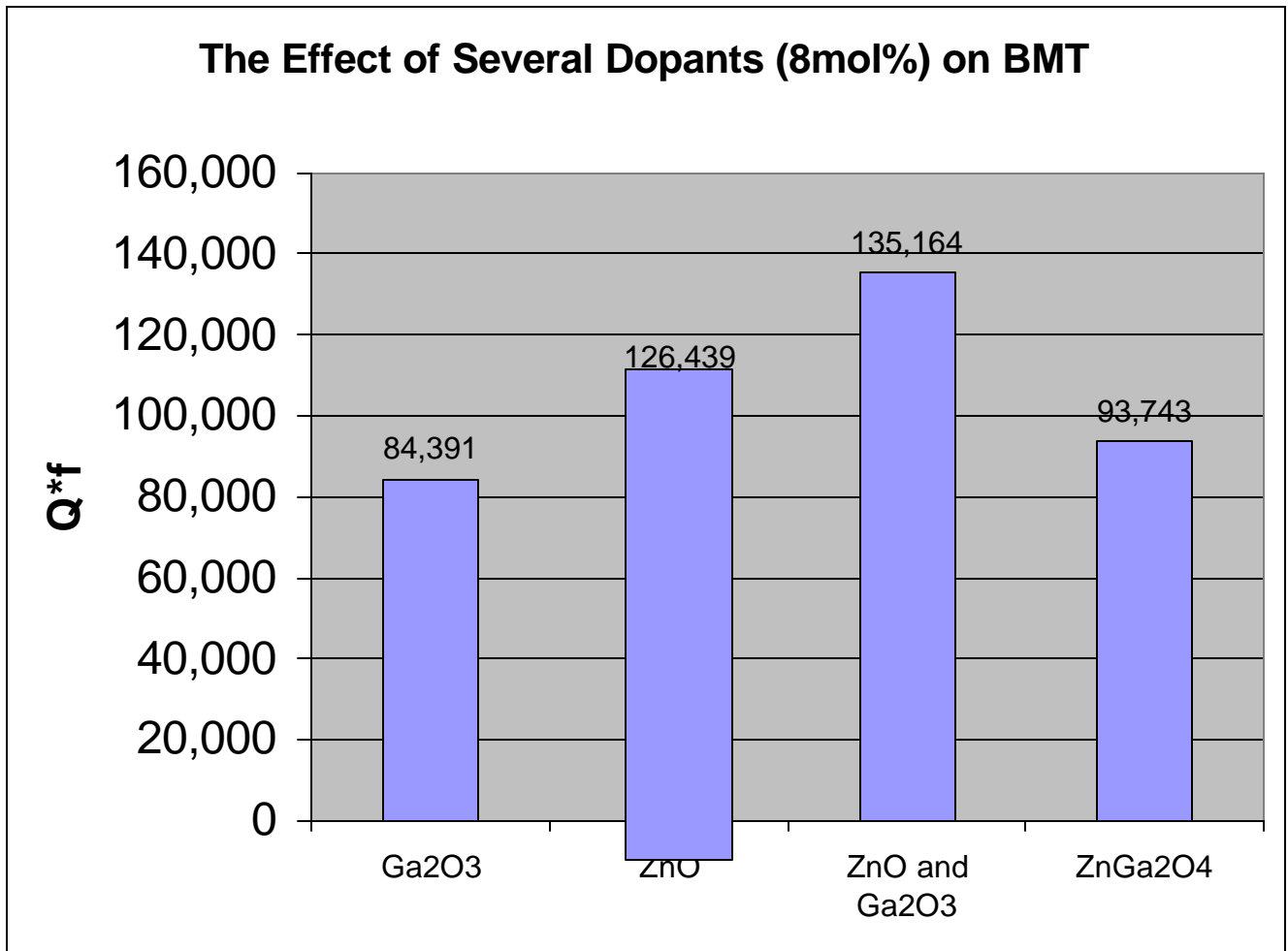


Figure 39 A Comparison of the Q^*f of BMT doped with combinations of ZnO and Ga₂O₃.

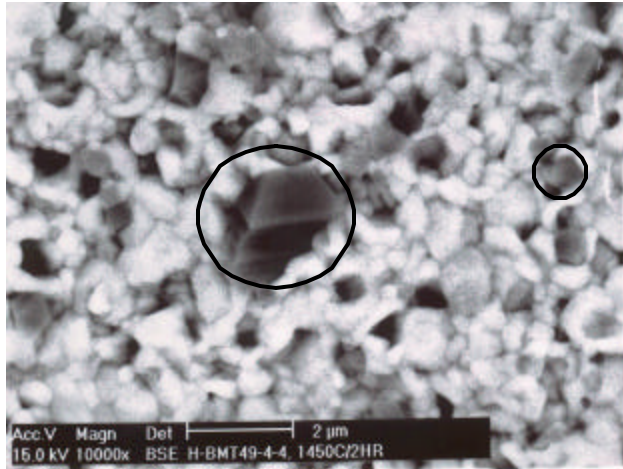


Figure 40 SEM micrograph of BMT doped with 8mol% ZnO and Ga₂O₃ and sintered at 1450°C for 2 hours. Some of the zinc and gallium rich second phase has been circled

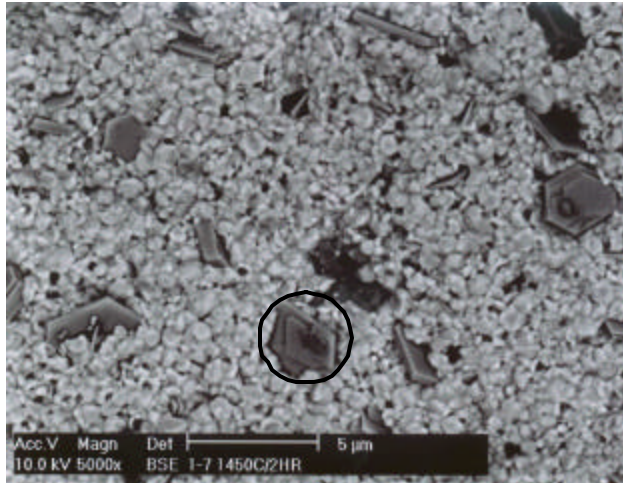


Figure 41 SEM micrograph of BMT doped with 8mol% Ga_2O_3 and sintered at 1450°C for 2 hours. Some of the gallium rich second phase has been circled.

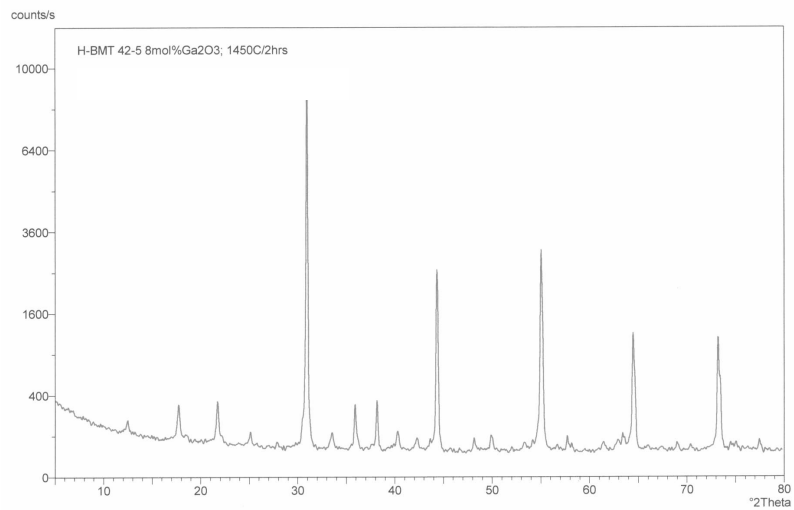


Figure 42 An XRD pattern of a BMT pellet (top) doped with 8mol% Ga_2O_3 and sintered at 1450°C for 2 hours. The largest superlattice peak has been marked with an arrow.

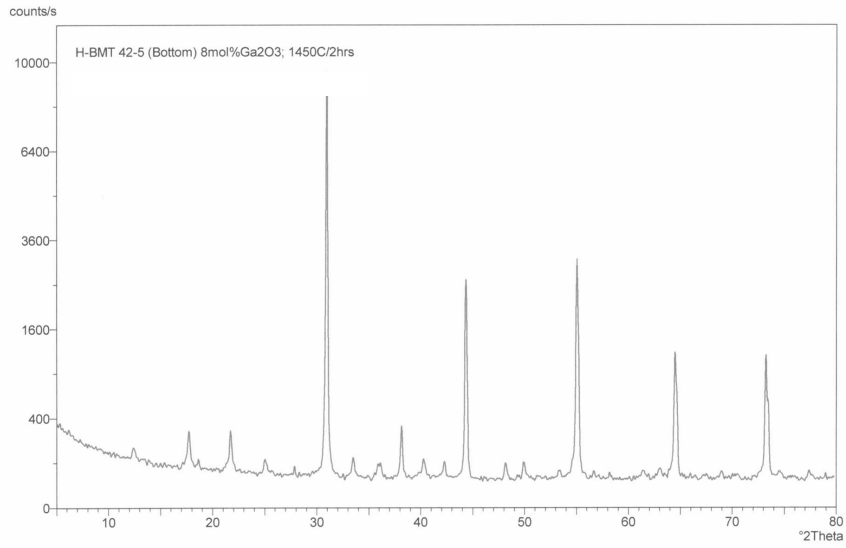


Figure 43 An XRD pattern of a BMT pellet (bottom) doped with 8mol% Ga_2O_3 and sintered at 1450°C for 2 hours. The largest superlattice peak has been marked with an arrow.

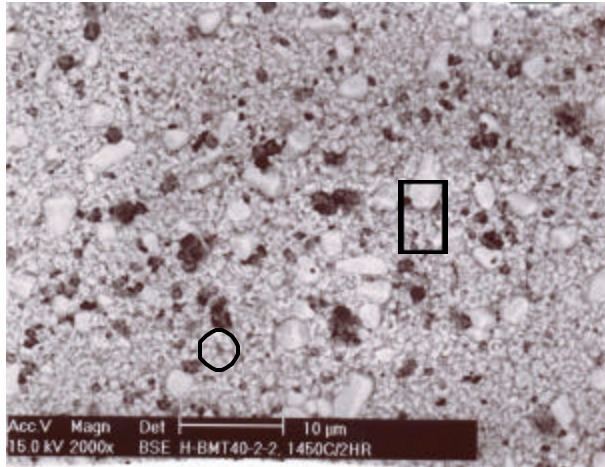


Figure 44 SEM micrograph of BMT doped with 8mol% ZnGa₂O₄ and sintered at 1450°C for 2 hours. Some of the second phase rich in gallium and zinc is circled and some of the second phase rich in barium and tantalum is indicated by a rectangle.

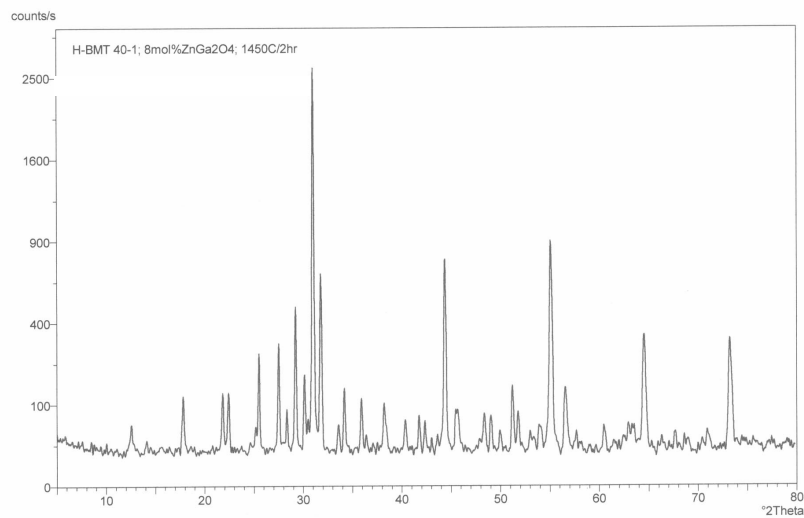


Figure 45 An XRD pattern of BMT doped with 8mol% ZnGa_2O_4 and sintered at 1450°C for 2 hours.

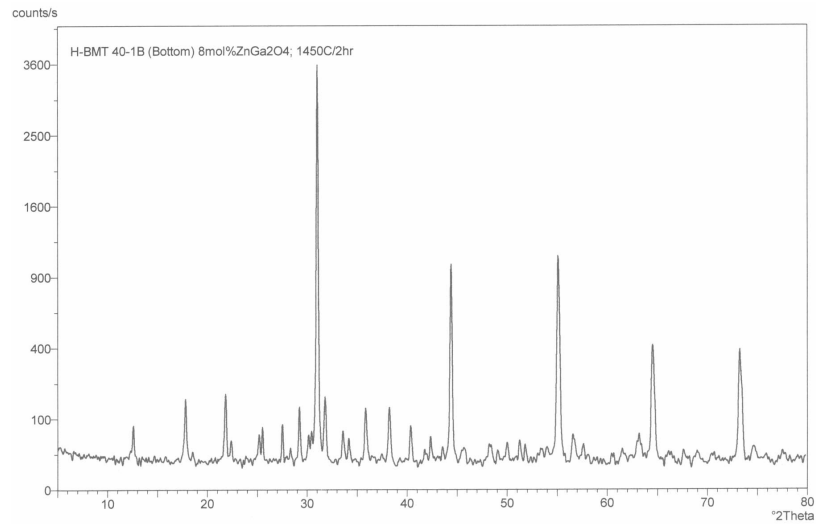


Figure 46 XRD pattern of the bottom of a pellet of BMT doped with 8mol% ZnGa_2O_4 and sintered at 1450°C for 2 hours. The zinc gallate second phase peaks have been marked with an asterisk and the largest superlattice peak has been marked with an arrow.

6.0 DISCUSSION

6.1 Phase Evolution

6.1.1 BMT Doped with ZnO & Ga₂O₃ and ZnGa₂O₄

When the micrographs and XRD patterns of the BMT co-doped with ZnO and Ga₂O₃ and ZnGa₂O₄ are compared, the co-doped additives appear to react to form ZnGa₂O₄ (zinc gallate). This is evident when the second phase crystals are compared. The second phase peaks on the XRD patterns confirm zinc gallate crystals in both instances. This suggests that there is no reason to react the zinc gallate before it is added to the BMT as a sintering aid; and the BMT doped with ZnO and Ga₂O₃ actually had slightly lower losses. The only difference is the Ba-Ta rich second phases that appear in some of the BMT samples doped with pre-made zinc gallate. This can be caused by the evaporation of MgO during sintering. In the BMT doped with zinc and gallium, the zinc may react with the Ba-Ta rich phases to form BZT. There were no signs of any BZT on any micrographs or XRD patterns but it may be below the detection limit of the instrumentation. The XRD patterns and the SEM micrographs of the samples doped with 4mol% and 8mol% ZnO and Ga₂O₃ were similar. The micrographs of the samples doped with 8mol% seem to have more second phase crystals but since a quantitative study was not done it cannot be said for certain.

When BMT is doped with zinc and gallium they react during the heating to form zinc gallate. Therefore, after the heating we are assuming that the BMT doped with zinc oxide and gallium oxide and the BMT doped with zinc gallate will react similarly. There was no evidence of any zinc gallate in any micrographs or x-ray diffraction patterns of the calcined powder. There is probably some present it is just too small to be detected. The pre-made zinc gallate was calcined and formed at 1100°C for 24 hours and the BMT doped with gallium and zinc was calcined at 1300°C for 5 hours suggesting that at least some zinc gallate was already formed. There were zinc gallate second phase crystals in most of the micrographs and x-ray diffraction patterns of the sintered surfaces. These second phases grew and became more evident as the temperature and time was increased. On the samples sintered at 1300°C and 1350°C over the first hour there were no signs of any of this second phase on the sintered surface. However, when the fracture surface of a pellet sintered at 1350°C for 1 hour was examined, there were small amounts of second phase present on the interior of the pellet. When the fracture surface of this and others were examined, the fracture went through the BMT grains and around the zinc gallate crystals. Another important observation was that there were no pores around the second phases. This suggests that the phase was formed in the solid state, and that the reaction by which zinc gallate is formed is slow compared with sintering.

6.1.2 BMT Doped with Ga₂O₃, ZnO and MgO

When BMT was doped with Ga₂O₃ (8mol%), ZnO (8mol%), and MgO (3% excess), the solubility of each was exceeded. Therefore, each had large second phase peaks on the XRD patterns and evident second phases on the SEM micrographs. These dopants were added to try

and increase the amount of oxygen vacancies, which is thought to increase mass transport because it is the largest ion and therefore the slowest moving. However it is unclear how much of the dopant actually went into solid solution.

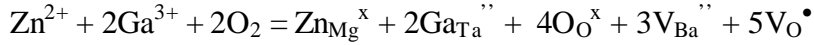
6.2 Densification Behavior

6.2.1 BMT Doped with ZnO & Ga₂O₃ and ZnGa₂O₄

Densification is significantly enhanced by the addition of zinc oxide & gallium oxide and the addition of zinc gallate. The zinc oxide and gallium oxide probably form zinc gallate at the calcination or sintering temperature and then it is coarsening during the sintering. The enhanced sintering could be due to a meta-stable liquid phase that is rich in zinc and gallium. When the system approaches equilibrium, the liquid then forms zinc gallate crystals and there was no residual liquid detected. The materials will have reached equilibrium when the volume fraction of zinc gallate remains constant

Another possible explanation for the increase in sinterability is that some of the zinc and/or gallium go into solid solution to create barium, tantalum and/or oxygen vacancies. Kim⁽³²⁾ determined that the main defect mechanism in pure BMT was the formation of Ba vacancies and when BMT is doped with WO₃, the main defect mechanism is the formation of tantalum and oxygen vacancies. However, there is no evidence presented to support these statements. The creation of these vacancies may help to increase diffusivity of the barium and

oxygen ions (the largest ions) and therefore increase the sinterability. It is assumed that no interstitials will be formed and due to the size of the ions it is assumed that the gallium will go onto tantalium sites and the zinc will go onto magnesium sites. Table 6.1 shows the ionic radii of the ions. There are many possible defect equations. Given the charge and ionic radii a tentative equation is given below. This creates barium and oxygen vacancies.



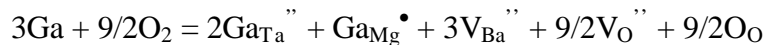
As will be discussed in the following sections, this is probably not the primary mechanism for the increase in sinterability.

6.2.2 BMT Doped with Ga₂O₃, ZnO and MgO

The BMT doped with 8mol% Ga₂O₃ could be sintered to ≈95% density at 1450°C for 2 hours. It is not clear what is increasing the sinterability. Some of the gallium could be going into solid solution and creating barium and/or oxygen vacancies. The following defect equation is assuming that there are no interstitials are formed; it is also assuming that the gallium will go onto tantalium sites and the oxygen will go onto to oxygen sites.

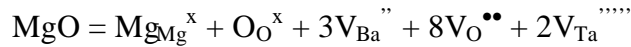
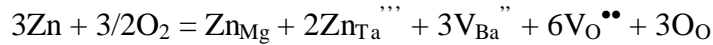
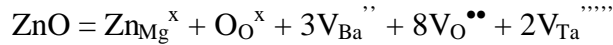


Other possible substitutions include,



all create oxygen vacancies. Alternatively, an unstable gallium rich liquid could form and enhance sintered and then precipitate Ga₂O₃ as equilibrium is approached.

The BMT doped with 8mol% ZnO and the 3% excess MgO did not sinter at 1600°C for 2 hours. If some of the zinc and/or magnesium could have gone into solid solution it would have created oxygen and barium vacancies, which would be expected to increase the sinterability. It is assumed that there will be no interstitials formed and that the magnesium and zinc will go onto magnesium sites due to the size of the ions.



Again the oxygen vacancies are only created. The extent to which this is possible will depend on the limit of stability which is presently not known. The sinterability of BMT was not increased by the addition of ZnO or MgO. Since these additives would also create O and Ba vacancies but would not be expected to form a liquid phase it is thought that a meta-stable liquid phase is the most likely the cause of the enhanced sintering in the gallium containing materials. As equilibrium is established after sintering is complete, zinc gallate or gallium oxide would continue to form by nucleation and growth in dense material. Therefore, porosity is not preferentially located around the second phases. This study did not positively identify the presence of a meta-stable phase and the explanation of the sintering behavior emails a hypothesis requiring a more detailed microstructure study.

6.3 Q-factors

6.3.1 BMT Doped with ZnO & Ga₂O₃ and ZnGa₂O₄

For the case of BMT samples doped with ZnO & Ga₂O₃, and ZnGa₂O₄, as long as the ceramics got to densities where the pores are closed, the Q-factors were good. This suggests that the second phase crystals do not significantly increase the losses; the losses are measured at relatively high frequency where the interfacial relaxation mechanisms may not significantly contribute to the losses.⁽⁷⁾ This argument would suggest that Q may decrease at lower frequencies when interfacial effects become important.

6.3.2 BMT Doped with each of the following Ga₂O₃, ZnO and MgO

Although the BMT samples doped with Ga₂O₃ had high densities the Q-factors were not as high as the samples doped with zinc gallate. As was mentioned earlier, interfacial relaxation does not usually contribute significantly to the losses at these relatively high frequencies. This suggests that the second phases that are formed may strongly absorb microwaves, which could significantly increase the losses. It is not known how strongly gallium oxide absorbs microwaves.

The BMT samples doped with ZnO and MgO did not get dense enough for the pores of the sample to close. As discussed earlier, in order to achieve a high Q-factor the sample must have closed pores. Before the pores are closed off, water moisture is able to get into the sample.

Since water moisture is a strong absorber of microwaves, this significantly increases the losses of the ceramic.

The implication of this study is that multiphase DR ceramics can be manufactured with high Q values. The processing of high purity materials by high temperature sintering and prolonged annealing may not be necessary for all microwave ceramics. Therefore sintering aids and conventional sintering practice are a viable way of lowering processing temperatures even if they create second phases, as long as these phases do not strongly absorb microwaves. At present there is not way of predicting the effects of sintering aid on Q.

Table 2 **Ionic Radii of BMT and Other Relevant Ions**

Ion	Ionic Radius in Å with a coordination number of 6
Ba ²⁺	1.35
Mg ²⁺	0.72
O ²⁻	1.40
Ta ⁵⁺	0.64
Ga ³⁺	0.62
Zn ²⁺	0.74

7.0 CONCLUSION

- BMT can be sintered to high densities at 1450°C or lower for 2 hours by the addition of zinc gallate with out significantly lowering the Q-factor. The dopant can be added as zinc gallate or as zinc oxide and gallium oxide.
- Zinc gallate may lower the sintering temperature of BMT through a meta-stable transient liquid phase.
- When BMT is doped with zinc gallate or zinc oxide and gallium oxide, second phase crystals are formed at either the calcination temperature or the sintering temperature and then coarsen during continued sintering.
- Multiphase materials can have high Q-factors or low losses at a frequency of around 5 GHz.
- BMT doped with 8mol% ZnO and sintered at 1450°C for 2 hours only had a density of approximately 85% but it had a relatively high $Q \cdot f$ of 126,439 GHz . Only one batch of this composition was made so it is not clear if this is significant.
- BMT can be sintered to high densities at 1450°C for 2 hours by the addition of gallium oxide, but this significantly lowers the Q-factor of the materials.

8.0 SUGGESTIONS FOR FUTURE WORK

1. A measure the Q-factor of doped BMT ceramics at lower frequencies could determine the effect of the second phases on the loss.
2. A detailed microstructure evaluation needs to be done to determine when the systems reaches equilibrium and if there are any signs of liquid phases sintering. In particular TEM investigation of the chemical composition of second phases collected at triple points must be performed.
3. The temperature coefficient of resonant frequency should be measured to determine if it is severely degraded by the dopants.

APPENDICES

APPENDIX A

Chemical Analysis of Starting Materials

Barium Carbonate (BaCO₃)

Purchased from Aldrich

Product Number: 23710-8

Formula Weight: 197.35

Appearance: White Powder

Impurities:

Calcium	0.003%
Chloride	0.0007%
Iron	0.0003%
Heavy Metals	<0.001%
Sodium	0.001%

Gallium (III) Oxide (Ga₂O₃)

Purchased from Puratronic

Product Number: 11151

Formula Weight: 187.44

Appearance: White Powder

Impurities: (ppm)

Al	0.13	As	<0.20	Au	<0.50
B	0.08	Ca	0.18	Cd	<0.10
Co	<0.01	Cr	0.03	Cu	<0.05
Fe	0.04	Ge	<0.05	Hg	<0.10
In	Binder	Mg	0.19	Mn	<0.01
Na	0.97	Ni	0.04	P	0.04
Pb	<0.05	S	0.89	Si	4.60
Sn	0.56	Te	<0.05	Zn	<0.10

Magnesium Oxide (MgO)

Purchased from Aldrich

Product Number: 20371-8

Formula Weight: 40.31

Appearance: White Powder

Impurities: (ppm)

Zn	25	Ba	0.6
Al	20	Zr	0.8
Na	20	Li	1.8
Mn	15	Mo	3.0
Ca	7.7	Ti	0.4
Pb	7.4	Ni	0.2
Cu	4.0	B	0.1

Tantalum Pentoxide (Ta₂O₅)

Purchased from H.C. Starck

Product Number: 99/45904

Formula Weight: 441.89

Appearance: White Powder

Impurities: (ppm)

Fe	<10
Nb	33
Ni	<10
Si	<10
Ti	<2
W	<5
Zr	<2
Alkali	<30

Zinc Oxide (ZnO)

Purchased from Aldrich

Product Number: 20553-2

Formula Weight: 81.37

Appearance: White Powder

Impurities: (ppm)

Cd	5
Al	3
Na	3
Ca	2
Fe	2
Pb	1
Ba	0.3
Mg	0.3

APPENDIX B

Procedure for the Synthesis of BMT Ceramics

Sample Preparation

1. Calcine MgO in an alumina crucible with cover at 1000°C for 3 hours. Use a heating and cooling rate of 10°C/min, terminating at 300°C.
2. At 300°C remove the MgO from the furnace.
3. Weigh the MgO immediately and place in clean milling bottles with a few mL of acetone – be sure to write the weight of the MgO on bottle
4. Weigh stoichiometric amounts of Ta₂O₅, BaCO₃ and any dopant, being sure wiping spatula and inside of balance with acetone and kim-wipes between each chemical.
5. Place powders in milling bottle with MgO.
6. Add the grinding media labeled “BMT mix” and fill with acetone, ball mill for 24 hours.
7. Clean strainer in ultrasonic cleaner and rinse it with D.I. water and then acetone, then place it over a clean beaker
8. Carefully pour powder slurry into a clean beaker and clean the grinding media over the strainer using acetone.
9. Be sure the media is clean before storing, rinsing with dilute HNO₃ if necessary (not over the slurry beaker)
10. Dry sample on the hot plate using a magnetic stir bar to prevent settling (60°C & 200 RPM)
11. When all of the acetone is evaporated, place the beaker in drying oven for at least 24 hours.
12. Grind the powder with agate mortar and pestle as finely as possible.
13. Weigh platinum crucible empty, add powders and weigh again, record weights.
14. Calcine powders in an uncovered platinum crucible at 1300°C for 5 hours with a heating and cooling rate of 10°C/min.
15. Record the weight of the powder and crucible; calculate the weight loss.
16. Ball mill the powder with acetone in grinding media label “BMT Calcined” for 48 hours
17. Remove ball media and dry sample as before.
18. When all acetone has evaporated, place beaker in drying oven for at least 24 hours.
19. Grind the powder with agate mortar and pestle as finely as possible.

Uniaxial Pressing

1. Clean ½" diameter die with isopropyl alcohol and kim-wipes
2. Apply lubricant with swab to the contact surfaces of the die and top punch, but never on the face of the punch.
3. Weigh out 3.92 g of sample powder.
4. Place bottom punch in die, pour in powder, shake to settle it.
5. Slowly insert top punch.
6. Slide into press, being sure to hold bottom punch in place.
7. Close valve.
8. Increase pressure to 1,000 lbs, hold 5-10 secs, open valve slowly.
9. Remove bottom punch.
10. Invert die (with top punch in place) and set with foam under sides.
11. Push die down to force pellet up.
12. Remove pellet with tweezers.
13. Apply lubricant to die with new swab as needed (i.e. every other time).
14. Repeat steps 3-14 with rest of sample powder.
15. Clean die and punches with isopropyl alcohol.

Cold Isostatic Pressing

1. Open and rip rim off of non-lubricated condoms (# condoms = ½ # pellets).
2. Place pellet in bottom, remove all air with vacuum and knot.
3. Use 2 pellets for each condom; tie in separate compartments.
4. Put filled condoms in metal tube near press.
5. Put tube into oil in reactor (watch out for splash).
6. Settle back-up ring (oil should be ¼ inch below this level).
7. Open cover vent valve (allows excess oil to drain, use dish to catch).
8. Rotate cover by hand, holding center up with bar so it does not drop.
9. Tighten cover last few turns with bar, allowing time for oil to drain, and further tightening as this happens (don't use too much force).
10. Once cover is snug, back it off 10-15 degrees to ease removal.
11. Close vent on cover when draining oil slows or stops.
12. Close vent valve on pump.
13. Open air inlet valve on pump.
14. Wait for gauge to read 40,000 psi.
15. Close inlet valve on pump.
16. Open vent valve on pump *very slowly*.
17. Open lid, remove tube and drain oil from tube.
18. Remove condoms from tube and squeeze off excess oil.
19. Over newspaper cut condoms open and remove pellets with tweezers, being careful to keep oil off pellets.

Sintering

1. Clean Pt crucible with acetone
2. Weigh each pellet and record weight.
3. It is possible to sinter 4 pellets in a Pt crucible.
4. Note the location of each pellet using a reference point.

5. Cover pellets with smaller Pt crucible.
6. Sinter for specific amount of time and temperature.
7. Weigh and record weight of each pellet.

APPENDIX C

Procedure for the Network Analyzer

C.1 Network analyzer preparation

- A frequency sweep is a plot in the log magnitude format. This is indicated on the upper left of the network analyzer screen. To change the format to log mag, press **FORMAT*** on the panel then choose **LOG MAG** on the screen. There are two channels to observe the measurement. For convenience choose channel 1 for S_{11} (for Q factor) and S_{21} (for dielectric constant) measurements and channel 2 for the Smith chart. The channel shown on the screen can be changed using **CH1** or **CH2** buttons on the panel.
- Change the number of the data points to 1601: for maximum resolution.
 - Press **MENU** on the panel.
 - Choose **NUMBER OF POINTS** on the screen: When this is not 1601, change it to 1601 using the arrow keys on the panel.
- Press **USER PRESET** on the panel when something is strange or you don't know what happened. Then start over.
- Refer "Operating manual for HP8722C Network Analyzer" for more detailed information about the network analyzer.
- Wear the wrist strap when you use the network analyzer for static free work.

* Buttons on the network analyzer are highlighted.

C.2 Procedure for the Courtney method

The Courtney method is used for measuring the dielectric constant using the Courtney cavity (smaller brass cavity) and Courtney program. This is a transmission method and therefore uses 2 cables. Adaptors (one end is male and the other end is female (Wiltron) always attached to cavity) should be connected between the cavity and both cables. Thus the connection should be, from port 1, cable, gold connector (HP), adapter (wiltron), cavity, adapter (wiltron), gold connector (HP), and cable to port 2.

- Check channel and format of the screen. If they are not log magnitude format with channel 1 go to network analyzer preparation step (section C.1).
- Prepare network analyzer for the dielectric constant measurement.
 - Press **MEAS** on the panel.
 - Choose **S₂₁** on the screen.
- Set scale of screen as 5dB.
 - Press **SCALE REF** on the panel.
 - Choose **SCALE/DIV** on the screen.
 - Hit **5** and **x1** on the keypad.
- Set reference value as -15 dB.
 - Press **SCALE REF** on the panel.
 - Choose **REFERENCE VALUE** on the screen.
 - Enter - **1 5** and **x1** on the keypad.
 - Choose **REFERENCE POSITION** on the screen.
 - Move reference line using arrow keys on the panel.
 - Move small arrow on left side to the middle of the screen.
- Choose adequate frequency range (usually 1 to 10 GHz).
 - Press **START** on the panel and enter **1** then **G/n** on the keypad for setting a start frequency.
 - Press **STOP** on the panel and enter **1 0** on keypad then press **G/n** for setting a start frequency.
- Load the calibration from disk or manually calibrate the network analyzer. Before starting the calibration, make sure everything such as data points, span range, channel, and etc. is set up. You can recall it from the disk when you have a stored calibration for same frequency range (section C.6).
 - Disconnect cables from the cavity: Wiltron adaptor should be connected to cable.
 - Press **CAL** on the panel: Calibration menu will show up the screen.
 - Be sure that the CAL KIT is 2.92 mm: if it is not set up for 2.92 mm change it.
 - Choose **CAL KIT** on the screen.
 - Choose **SELECT CAL KIT** on the screen.
 - Choose **2.92 mm** on the screen.
 - Choose **RETURN** on the screen: Calibration menu will show up the screen.
 - Choose **CALIBRATION MENU** on the screen.
 - Choose **RESPONSE** on the screen.

- Connect standard (Wiltron) (Both ends are male, kept in a plastic box in front of a network analyzer) to both cables with adaptors that were mentioned in C.2. The connections are now cable, from Port 1, gold connector (HP), adapter (wiltron), standard, adapter (wiltron), gold connector (HP), and cable to Port 2.
- Choose **THRU** on screen: THRU screen will be underlined after a sweep.
- Choose **DONE** on screen: Options for store calibration either on a disk or on a network analyzer will show up on the screen.
- Save calibration on a disk. (see Section C.4)
- Put a sample into the Courtney cavity.
 - Sample should be in center of the cavity.
 - Close lid and gently tighten three screws evenly.
 - Make sure that the lid is not tilted.
 - Screen now shows frequency spectrum. (Figure 42)
- Mark TE-011 mode peak.
 - Below 15 dB is not considered a peak. The first peak (above 15 dB) is the HE14 mode. Typical S_{21} spectrum of the ceramic sample is shown in Figure C-1. It shows several resonant peaks. The TE-011 mode is the second lowest peak. Consider the one that is above the reference line (red line on the screen), -15dB, as a peak.
 - Press **MKR** on the panel: Another menu will be shown.
 - Choose **all OFF** on the screen: all markers will be erased.
 - Choose **MODE MENU** on the screen: another menu will be shown.
 - Choose **REF=1** on the screen.
 - Point marker on the second lowest peak using the knob.
- Center TE-011 mode peak on the screen.
 - Press **MKR FCTN** on the panel: another menu will be shown.
 - Choose **MARKER MENU** on the screen.
 - Choose **MARKER CENTER** on the screen: Ignore the caution message.
- Reduce sweep span to 100 MHz
 - Press **SPAN**: “span” will be shown on the left upper screen.
 - Press **1 0 0** and **M/m** on keypad: Spectrum with 0.1 GHz span will be shown.
- Calibration (Repeat Cal step).
 - Calibrate a network analyzer again for this frequency span (0.1 GHz span), although a larger frequency span can be used if necessary.
- Save calibration.
- Connect cables to the cavity: Do not forget to connect Wiltron adaptor between cable and cavity. Connection should be cable, from Port 1., gold connector (HP), adapter (wiltron), cavity, adapter (wiltron), gold connector (HP), and cable to Port 2.
- Measure S_{21} (insertion loss)
 - Press **MKR FCTN** on the panel: Another menu will be shown.
 - Choose **MAX** on the screen.
 - Choose **BANDWIDTH MENU** on the screen.
 - Choose **BW MEASURE** on the screen.
 - Choose **BANDWIDTH VALUE** on the screen.
 - Press **- 3** and **x1** on the keypad: This sets the BW value as -3dB.

- Read values for BW, loss (S_{21}), and cent (resonant frequency) from the screen, or see optional step following.
 - Press **DISPLAY** on the panel
 - Choose **DATA→MEMORY** on the screen.
 - Choose **MEMORY** on the screen: Now sweep stop.
 - Press **MKR FCTN** on the panel: Another menu will be shown.
 - Choose **MAX** on the screen.
 - Read values.
- (OPTIONAL) Print the values from screen.
 - Press **COPY**
 - Choose **PRINT (66)**
- Use Courtney program for calculating the dielectric constant.
- Change display mode to actual data.
 - Press **DISPLAY** on the panel.
 - Choose **DISPLAY:DATA** on the screen.

C.3 Courtney program

Use computer on the wooden desk (386 with windows 3.1).

- Change directory to C:/COURTNEY/COURTNEY/ on DOS mode.
- Run COURTNEY program.
 - Type COURTNEY then ENTER.
 - Hit ENTER again to continue the program: screen will be changed.
- Enter the values for program.
 - Enter values for pressure, temperature, humidity, and ambient dielectric constant as shown in figure 43. For diameter, height, resonance frequency, 3dB bandwidth, and insertion loss use the actual data for sample that you want to measure.
- Calculate the dielectric constant
 - Hit “Esc” key: Result will be shown as figure 44.
 - Hit “F9” key to return to previous display.

C.4 Save calibration

The calibration can be saved on a floppy disk or on the network analyzer. After finishing the calibration, options for save will be shown on a screen.

- Choose **STORE TO DISK** on the screen.
- Another menu will be shown.
- Initialize a disk: This is only for a new disk. When you are using initialized disk skip this step.
 - Insert a new disk into drive 0.
 - Choose **DEFINE, INIT, PURGE** on the screen.
 - Choose **INITIALIZE DISK** on the screen.
 - Choose **YES**: wait until the drive stops.
 - Choose **RETURN**: Another menu will be shown.
- Label file name
 - Choose **STORE TO DISK** on the screen.
 - Choose **TITLE FILE** on the screen.
 - Choose one of **TITLEs** on the screen.
 - Choose **ERASE TITLE** on the screen.
 - Point to the letter using the knob and press **SELECT LETTER** on the screen:
Repeat until the name is finished.
 - Choose **DONE** on the screen: Menu will be changed.
 - Choose **RETURN** twice on the screen.
 - Choose **STORE** (what you named it): Wait until the drive stops. When disk does not have enough space to store, caution message will pop up. Then insert a new disk and initialize first, then store the calibration.

C.5 Procedure for Q factor measurement

This method is called single port reflection technique. Only one cable port (port 1) is required. It uses a silver plated aluminum cavity. For this method, only one cable and HP connector are used, i.e. no Wiltron adaptors were used with single cable. Thus connection should be, from Port 1, cable, yellow connector (HP), and cavity.

- Check channel and format of the screen. If they are not log magnitude format with channel 1 go to network analyzer preparation step (chapter C.1).
- Prepare network analyzer for the Q factor measurement.
 - Press **MEAS** on the panel.
 - Choose **S₁₁** on the screen.
- Set scale of screen as 2dB.
 - Press **SCALE REF** on the panel.
 - Choose **SCALE/DIV** on the screen.
 - Enter **2** and **x1** on the keypad.
- Set reference value as 0 dB.
 - Press **SCALE REF** on the panel.
 - Choose **REFERENCE VALUE** on the screen.
 - Enter **0** and **x1** on the keypad.
 - Choose **REFERENCE POSITION** on the screen.
 - Move reference line using arrow key on the panel to (2) two lines from the top.
- Place a sample into a cavity.
 - It should be on the center of a styrofoam support.
 - Close lid gently.
- Choose adequate frequency range: It depends on the size of the ceramic sample and its dielectric constant. For the sample prepared in this lab, it starts from 1GHz.
 - Press **START** and enter **1** and **G/n** on the keypad. This changes the starting frequency to 1 GHz.
 - Set span as 100 MHz.
 - Press **0.1**, and **G/n** on the keypad: Spectrum with 0.1 GHz span will be shown.
- Sweep the sample with 100 MHz span from 1GHz until you find the peak.
 - Keep the same span.
 - Press **CENTER** and enter **1** and **G/n** on the keypad. This changes the center frequency to 1 GHz.
 - After one sweep and no peaks are observed, increase the center frequency by 100 MHz.
 - Press **CENTER** and enter new value using keypad then press **G/n** for a new center frequency.
 - Check TE-01 δ mode.
 - Whenever you find the peak, open the lid of the cavity a little bit. If the peak disappears, keep increasing the center frequency by 100MHz until you find the peak that stays at the same position with the lid open. When a piece of metal is inserted through a hole into the cavity the peak should

shift slightly up in frequency. This confirms that this peak is TE-01 δ mode.

- Mark the TE-01 δ mode peak.
 - Press **MKR** on the panel: Another menu will be shown.
 - Choose **all OFF** on the screen: All markers will be erased.
 - Choose **MARKER=1** on the screen
 - Point marker to the resonant peak identified in last step.
- Center TE-01 δ mode peak on the screen.
 - Press **MKR FCTN** on the panel: Another menu will be shown.
 - Choose **MARKER MENU** on the screen.
 - Choose **MARKER CENTER** on the screen: Ignore the caution message.
- Reduce span to 1 MHz.
 - Press **SPAN**: “span” will be shown on the left upper screen.
 - Press **1** and **M/m** on keypad: Spectrum with 1 MHz span will show up (entire peak must be on the screen). If the range is too small to include the whole peak, keep increasing the span by 1 MHz increments until it fits.
- Calibration.
 - If you have a stored calibration for the frequency then recall it from the disk. (See section C.6)
 - If you don't have a stored calibration you must calibrate. Disconnect the cable from the cavity: Yellow HP connector should be with a cable.
 - Press **CAL**.
 - Choose **CALIBRATION MENU** on screen.
 - Choose **S₁₁ 1-PORT** on the screen.
 - Connect the three standards (yellow HP, kept in a plastic box in front of a network analyzer) to cable the one by one. There are three standards (OPEN, CLOSE, and LOAD). They may be done any order.
 - Connect the CLOSE standard to the cable. (The close and short standards are labeled, the load is the smaller thinner standard that isn't labeled.)
 - Choose **CLOSE** on the screen: **CLOSE** will be underlined after a sweep.
 - Connect the OPEN standard to the cable.
 - Choose **OPEN** on the screen: **OPEN** will be underlined after a sweep.
 - Connect the LOAD standard to cable.
 - Choose **LOAD** on the screen: a different menu will show up.
 - Choose **BROADBAND** on the screen: Broadband will be underlined after a sweep.
 - Choose **DONE** on the screen for returning to Cal menu.
 - Choose **DONE 1-PORT CAL** on the screen: the analyzer will calculate the calibration. The save menu will show up.
- Save calibration on a disk. (section C.4)
- Adjust the coupling probe inside of the cavity.

- Press **CH2**: Smith chart (channel 2) will show up instead of the log magnitude format. The coupling loop will show up on the Smith chart. The coupling loop should be touching the big circle of the Smith chart at a point where resistance is infinite (Figure 44), i.e. the edge.
- If a loop is out of the center of the Smith chart move it into center.
 - Press **SCALE REF**.
 - Choose **PHASE OFFSET** on the screen.
- Move the coupling loop using the knob to center circle.
- Move the probe a little bit with extra caution.
- Close the lid after adjusting the probe.
- Observe the coupling loop on the screen of the network analyzer.
- Adjust the coupling probe until the coupling loop of on the Smith chart overlaps the 50 ohms circle (Figure C-4).
- Display both channels simultaneous
 - Press **DISPLAY**
 - Choose **DUAL CHAN** on the screen: Log magnitude format (channel 1) will be above the Smith chart (channel 2). (Figure 45)
- Measure S_{11} (return loss)
 - Press **CH1** to control the log magnitude format.
 - Press **MKR FCTN** on the panel: Another menu will be shown.
 - Choose **MIN** on the screen as soon as one sweep is done. From this step to choosing “data→memory” step should be done within one full sweep. Otherwise minimum point on channel 1 may be different value from channel 2, since the return losses are slightly different from each sweep.
 - At the same time read the resistance on the channel 2: It is highlighted in the Figure A-5.
 - Press **DISPLAY**
 - Choose **DATA→MEMORY** on the screen.
 - Choose **MEMORY** on the screen: Now sweep stops.
 - Determine under/over coupling.
 - If the resistance at the minimum point of the resonant peak is less than 50 ohms, it is an overcoupling.
 - If the resistance at the minimum point of the resonant peak is larger than 50 ohms, it is an undercoupling.
- Measure the unloaded Q factor from the network analyzer.
 - Press **MKR FCTN** on the panel.
 - Choose **BANDWIDTH MENU** on the screen.
 - Choose **BW MEASURE** on the screen.
 - Read return loss (RL) from the screen.
- Calculate modified return loss (RL’).
 - Use a computer sit on right hand side (Pentium with Windows 98).
 - Double click “Couple” from the desktop menu: Icon is on the screen.
 - Enter value of RL into spreadsheet (Figure 46).
 - Hit ENTER.
 - Modified return loss (RL’) will be calculated.
- Measure the unloaded Q factor from the network analyzer.

- Press **MKR FCTN** on the panel.
- Choose **BANDWIDTH MENU** on the screen.
- Choose **BANDWIDTH VALUE** on the screen.
- Enter the RL' value using the keypad then press **x1**.
- Read Q value.
- Print out the result.
 - Press **COPY** on the panel.
 - Choose **PRINT** on the screen.
- Reset for next measurement
 - Display log magnitude format on the screen.
 - Press **CH1** on the panel.
 - Press **DISPLAY** on the panel.
 - Choose **DUAL CHAN** on the screen (off).
 - Change display mode to actual data.
 - Press **DISPLAY** on the panel
 - Choose **DISPLAY:DATA** on the screen.

A.6 Recall the calibration file from a disk.

- Insert a disk into the drive 0.
- Press **RECALL**: Menu will show up the screen.
- Choose **LOAD FROM DISK** on the screen: Another menu will show up on the screen.
- Choose **LOAD FILE TITLES** on the screen: It will show 5 titles at a time from the disk. Repeat until you see the filename that you want to load on the network analyzer.
- Choose filename that you want on the screen.

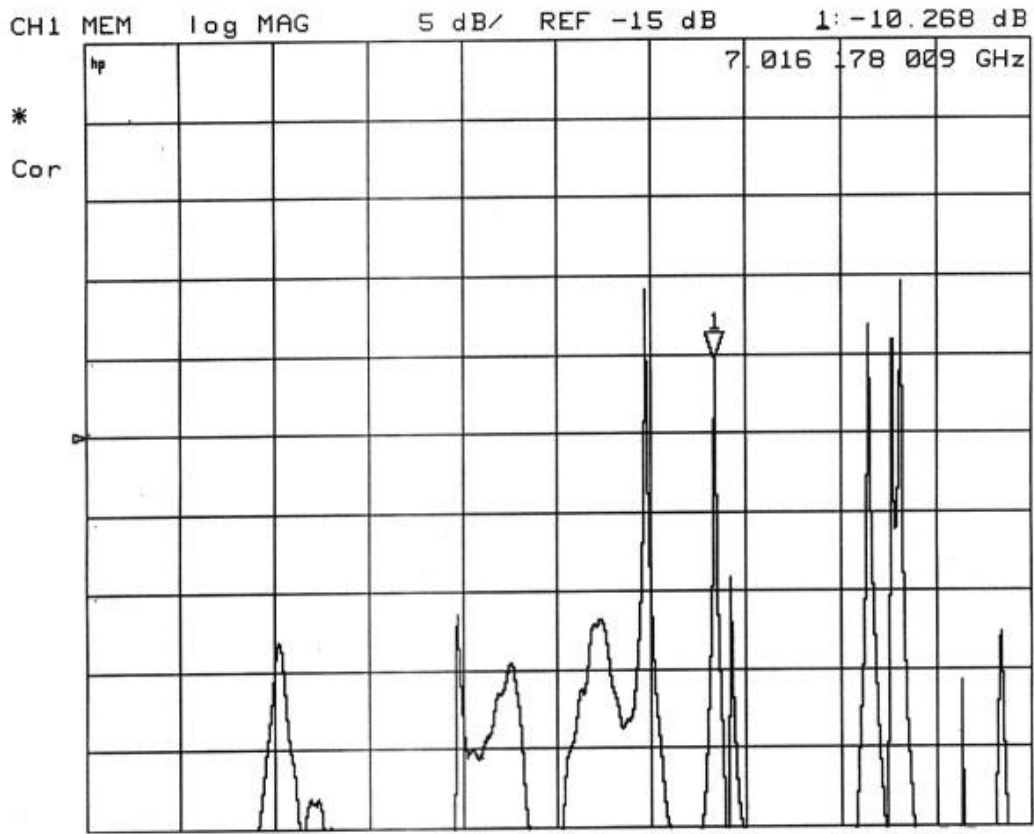


Figure 47 The S_{21} spectrum ranging from 1 GHz to 10 GHz.

```

                                The Courtney Problem

Enter Data and press Esc to see results.  Press F9 to quit.
Test Specimen Identification: Defaults

    760 :pressure (mm)
    25  :temperature (C)
    0   :humidity (%)
    1   :ambient dielectric constant
actual :specimen diameter (cm)
actual :specimen height (cm)
    0  :specimen thermal exp. coeff. (ppm/K), No entry=0

actual :resonance frequency (GHz)
actual :3 dB bandwidth (GHz)
actual :Insertion loss (dB positive or negative)
    0  :mode index: 0=TE-011, 1=TM-010, 2=TM-020

Solves the Courtney problem for the TE-011, TM-010, or TM-020 mode.
The order of resonance frequencies (increasing) is TM-010, TM-020,
HEM-111, and TE-011.  The HEM-111 mode is not computed.
```

Figure 48 The screen on the Courtney program where the actual data is entered so the program can calculate the dielectric constant.

The test specimen identification is Defaults.

Specimen diameter (cm):	1.000
Specimen height (cm):	.500
Coeff. thermal exp. (ppm):	0
Ambient temperature (C):	25.0
Ambient dielectric const.:	1.00053

The input data and results for the TE-011 mode are:

Resonance frequency (GHz):	7.0000
3dB bandwidth (GHz):	.00400
Insertion loss (dB):	25.0
Loss tangent (ppm):	400
Dielectric constant:	35.65

The maximum frequency for this mode is 29.97 GHz.

Figure 49 An example of the results obtained from the Courtney Software.

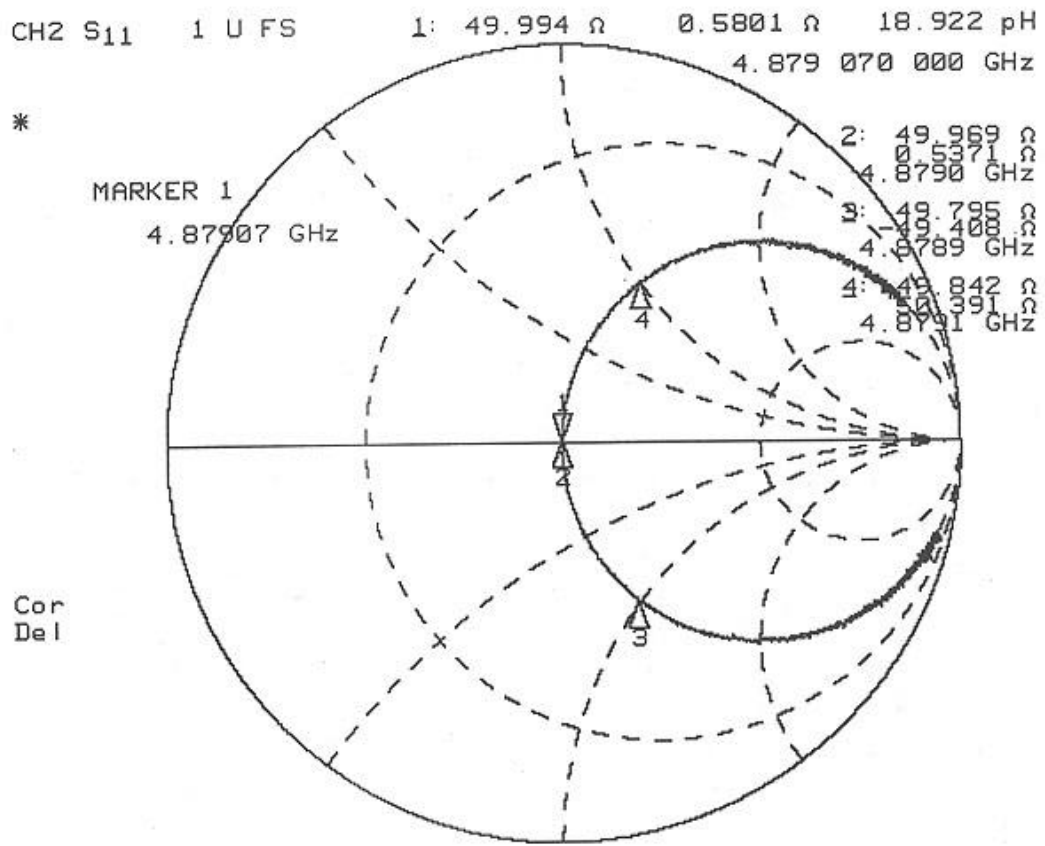


Figure 50 The resonant coupling circle on the Smith chart for measuring the Q-factor using the single-port reflection technique

BIBLIOGRAPHY

BIBLIOGRAPHY

1. Richtmyer RD. 1939. *J. Applied Physics*. 10: 391
2. Ruprecht G, Bell RO. 1962. *Physics Review* 125: 1915-20
3. Spitzer WG, Miller RC, Kleinman DA, Howarth LE. 1962. *Phys. Rev.* 126: 1710-21
4. Hakki BW, Coleman PD. 1960. *IRE Trans. on MTT* MTT-8: 402-10
5. Cohn SB, Kelly KC. 1966. *IEEE Trans. Microwave Theory Tech.* MTT-14: 406--10
6. Inc. T-T. <http://www.trans-techinc.com>.
7. Wersing W. 1991. *High Frequency Ceramics and their Applications for Microwave Components*. London: Elsevier. 67-115 pp.
8. Deriso J. 1996. Single Port Reflection Technique.
9. Courtney WE. 1970. *IEEE Trans. on MTT* MTT-18: 476-85
10. Galasso F, Pyle J. 1963. *Inorganic Chemistry* 2: 482-4
11. Galasso FS. 1969. *Structure, Properties and Preparation of Perovskite - type Compounds*. New York: Pergamon Press
12. Galasso FS. 1970. *Structure and Properties of Inorganic Solids*. New York: Pergamon Press
13. Galasso F, Pyle J. 1963. *J. Physics Chemistry* 67: 1561-2
14. Barber DJ, Moulding KM, Zhou J, Li M. 1997. *Journal of Materials Science* 32: 1531-44
15. Bian J, Zhao M, Yin Z. 1998. *Mater. Lett.* 34: 275-9
16. Akbas MA, Davies PK. 1998. *J. Am. Ceram. Soc.* 81: 2205-8

17. Byun JD, Ko SW, Choi IK, Lee DS, Kim YS. 2000. *Materials Research Bulletin* submitted
18. Chai L, Akbas MA, Davies PK, Parise JB. 1997. *Materials Research Bulletin* 32: 1261-9
19. Chen XM, Suzuki Y, Sato N. 1994. *Materials in Electronics* 5: 244-7
20. Chen XM. 1995. *Journal of Materials Science Letters* 14: 1041 - 2
21. Chen XM, Wu YJ. 1996. *J Mat. Sci.: Materials in Electronics* 7: 369-71
22. Chen XM, Wu YJ. 1996. *J. Mat. Sci: Materials in Electronics* 7: 427-31
23. Furuya M. 1999. *J. Appl. Phys.* 85: 1084-8
24. Guo R, Bhalla AS, Cross LE. 1994. *J. Appl. Phys.* 75: 4704-8
25. Kakegawa K, Wakabayashi T, Sasaki Y. 1986. *J. Am. Ceram. Soc.* 69: C82-C3
26. Katayama S, Sekine M. 1992. *J. Mater. Chem.* 2: 889-90
27. Katayama S, Yoshinaga I, Yamada N, Nagai T. 1996. *J. Am. Ceram. Soc.* 79: 2059-64
28. Katayama S, Yoshinaga I, Nagai T, Sugiyama M. 1998. *Key Eng. Mater.* 150 (Sol-Gel Production): 89-95
29. Kim ES, Yoon KH. 1994. *Journal of Materials Science* 29: 830 - 4
30. Kim ES, Yoon KH. 1992. *Ferroelectrics* 133: 187-92
31. Kim ES, Yoon KH. 1994. *Ferroelectrics* 154: 343-8
32. Kim YK, Lee KM, Jang HM. 1998. *J. Korean Phys. Soc.* 32: S292-S5
33. Lee MK, Chung JH, Ryu KW, Lee YH. 1998. *Microwave Dielectric Properties of Ba(Mg,Ta)O₃-Ba(Co,Nb)O₃ Ceramics*. Presented at International Symposium on Electrical Insulating Materials, in conjunction with 1998 Asian International Conference on Dielectrics and Electrical Insulation and 30th Symposium on Electrical Insulating Materials, Toyohashi, Japan
34. Li M. 1997. *Ferroelectrics* 195: 87-91
35. Maclaren I, Ponton CB. 1998. *J. Mater. Sci* 33: 17-22

36. MacLaren I, Ponton CB. 1997. *TEM investigation of hydrothermally synthesised Ba(Mg_{1/3}Ta_{2/3})O₃ powders*. Presented at Electron Microscopy and Analysis Group Conference, Cambridge
37. Lu C-H, Tsai C-C. 1998. *Materials Science and Engineering B* 55: 95-101
38. Lu CH, Tsai CC. 1998. *Mater. Sci. Eng. B* 55: 95-101
39. Nomura S, Toyama K, Kaneta K. 1982. *Japanese Journal of Applied Physics* 21: L624-L6
40. Ravichandran D, Jin B, Roy R, Bhalla AS. 1995. *Materials Letters* 25: 257-9
41. Ratheesh R, Sebastian MT, Tobar ME, Hartnett J, Blair DG. 1998.
42. Ravichandran D, Jr. RM, Roy R, Guo R, Bhalla AS, Cross LE. 1996. *Materials Research Bulletin* 31: 817-25
43. Renoult O, Boilot JP, Chaput F, Papiernik R, Hubert-Pfalzgraf LG. 1992. *J. Am. Ceram. Soc.* 75: 3337-40
44. Sagala DA, Koyasu S. 1993. *J. Am. Ceram. Soc* 76: 2433-36
45. Sawada A, Kuwabara T. 1989. *Ferroelectrics* 95: 205-8
46. Srinivas J, Dias ED, Murthy GS. 1997. *Bull. Mater. Sci.* 20: 23-5
47. Sugiyama M, Inusuka T, Kubo H. 1989. *Ceramic Transactions: Materials and Processes for Microelectronic Systems* 15: 153-66
48. Tien L-C, Chou C-C, Tsai D-S. 2000. *Ceramics International* 26: 57-62
49. Tochi K. 1992. *Journal of the Ceramic Society of Japan* 100: 1441-3
50. Yoon KH, Kim DP, Kim ES. 1994. *J. Am. Ceram. Soc.* 77: 1062-6
51. Yoon KH, Kim DP, Kim ES. 1994. *Ferroelectrics* 154: 337-42
52. Youn HJ, Kim HY, Kim H. 1996. *Japanese Journal of Applied Physics* 35: 3947-53
53. Zhou J, Su Q-X, Moulding KM, Barber DJ. 1996.
54. Zhou J, Su Q, Noulding KM, Barber DJ. 1997. *J. Mater. Res.* 12: 596-9

55. Zhou J, Barber DJ. 1997. *J. Mater. Sci. Lett.* 16: 1426-9
56. Ra S. 1998. *Synthesis, Processing and Microwave Dielectric Properties of Barium Magnesium Tantalate and Other Ceramics for Wireless Communications*. M.S. thesis. University of Pittsburgh, Pittsburgh
57. Ra SH, Phulé PP. 1999. *J. Mat. Res.* 14: 4259-65
58. Schnoeller M, Wersing W. 1991. *Sol-Gel Synthesis of Advanced Microwave Ceramics and their Dielectric Properties*. Presented at Proceedings of the Second European Conference on Sol-Gel Technology, Saarbrucken, Germany
59. Lu C-H, Tsai C-C. 1996. *Journal of Materials Research* 11: 1219 - 27
60. Matsumoto H, Tamura H, Wakino K. 1991. *Japanese J. Appl. Phys.* 30: 2347-9
61. Davies PK. 1995. *Influence of Structural Defects on the Dielectric Properties of Ceramic Microwave Resonators*. Presented at Symposium on Materials and Processes for Wireless Communication, Boston, MA
62. Davies PK, Tong J. 1997. *J. Am. Ceram. Soc.* 80: 1727-40
63. Kawashima S, Nishida M, Ueda I, Ouchi H. 1983. *J. Am. Ceram. Soc.* 66: 421-3
64. Matsumoto K, Hiuga, T., Takada, K., Ichimura, H. 1986. *Ba(Mg_{1/3}Ta_{2/3})O₃ Ceramics with Ultra - Low Loss at Microwave Frequencies*. Presented at Proceedings of the 6th IEEE International Symposium on Application of Ferroelectrics
65. Scott AW. 1993. *Understanding Microwaves*. New York: John Wiley & Sons, Inc.
66. 1984. *Standard Test Method for Water Absorption, Bulk Density, Apparent Specific Gravity of Fired Whiteware Products*. Philadelphia: American Society for Testing and Materials. C372-3 pp.